

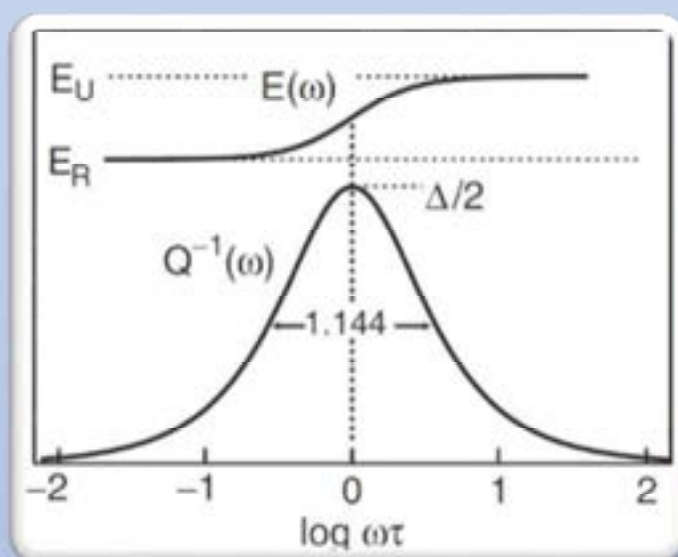
## Abstracts

*19th International Conference on*

# **INTERNAL FRICTION AND MECHANICAL SPECTROSCOPY**

Rome, 27.06 - 01.07.2022

<https://icifms19.ism.cnr.it>



Dear Colleagues,

On behalf of the organizing committee, it is our pleasure to invite you to the 19th International Conference on Internal Friction and Mechanical Spectroscopy (ICIFMS-19). The ICIFMS-19 event was initially supposed to take place during 29/6-3/7/2020 at the National University of Science and Technology “MISIS”, Moscow, Russia, with Igor S. Golovin (NUST MISiS) and Francesco Cordero (CNR-ISM, Rome) as co-chairmen (<http://icifms19.ru>). The conference has been postponed of two years due to the Covid-19 pandemic and the new international situation forced us to move the organization to Rome (<https://icifms19.ism.cnr.it>), maintaining the established dates 27/06-01/07/2022.

The conference is the 19th in a series that began in Providence (USA) in 1956 and continued in Ithaca (USA, 1961), Manchester (England, 1965), Providence (USA, 1969), Aachen (Germany, 1973), Tokyo (Japan, 1977), Lausanne (Switzerland 1981), Urbana (USA, 1985), Beijing (China, 1989), Rome (Italy, 1993), Poitiers (France, 1996), Buenos Aires (Argentina, 1999), Bilbao (Spain, 2002), Kyoto (Japan, 2005), Perugia (Italy, 2008), Lausanne (Switzerland 2011), Hefei (China, 2014) and Foz do Iguaçu (Brazil, 2017).

The ICIFMS-19 is a great opportunity for the exchange of experiences and ideas in research focused on theory, advances and applications of anelasticity in materials physics, high and low damping materials and on internal friction, mechanical spectroscopy, dynamic-mechanical analysis and related techniques. We also encourage and invite scientists from neighbouring research fields to share their expertise, which will make ICIFMS-19 a stimulating event. The Conference program consists of plenary, invited (27 min + 3 min discussion), long (17 + 3 min) and short (8 + 2 min) talks.

To minimize the damage from the pandemic we organized, with the support from Journal of Alloys and Compounds (impact factor 5.316 in 2020), the publication of the Special IFMS-19 issue in order to collect topic-related papers both in printed and in virtual book (<https://www.sciencedirect.com/journal/journal-of-alloys-and-compounds/special-issue/10MHG1DWWC1>).

It is our pleasure to thank not only the researchers who have contributed to this Issue but also our reviewers for their hard work. The Special IFMS-19 issue or Proceedings of ICIFMS-19 Conference already includes more than 52 original topical papers (13 June 2022) by authors from seventeen countries and continues the excellent series of proceedings of the previous eighteen Conferences.

In order to spread the interest in the field of anelasticity, the virtual participation without presentation is free of charge, while the fee for participating with presentation of a contribution is 60 €.

On behalf of the Organizing Committee, we look forward to meeting you virtually or in presence!

*Igor S. Golovin and Francesco Cordero*

# Abstracts

## Plenary talks

- |   |                            |  |       |
|---|----------------------------|--|-------|
| 1 | E.K.H. Salje               | Internal friction in complex ferroelastic twin patterns                            | p. 7  |
| 2 | J. M. Pelletier, J.C. Qiao | Mechanical spectroscopy in amorphous materials: case of bulk metallic glasses      | p. 8  |
| 3 | S. Kustov                  | 80 years after: new categories of magnetomechanical damping                        | p. 9  |
| 4 | Jose M. San Juan           | Internal friction at nano-scale and size-effects on damping in shape memory alloys | p. 10 |

## Amorphous materials

- |   |                            |   |       |
|---|----------------------------|---|-------|
| 1 | J. M. Pelletier, J.C. Qiao | Mechanical spectroscopy in amorphous materials: case of bulk metallic glasses   | p. 8  |
| 2 | T. Ichitsubo               | Spatial elastic inhomogeneity of metallic glasses before and after structural relaxation using inelastic x-ray scattering and ultrasound techniques | p. 13 |
| 3 | L.V. Panina                | Magnetomechanical effects in ferromagnetic microwires of Co-rich compositions   | p. 15 |
| 4 | A. Berezner                | Relaxation behavior of an Al-Y-Ni-Co metallic glass in as-prepared and cold-rolled state  | p. 17 |
| 5 | R.A. Sergiienko            | DYNAMIC MECHANICAL ANALYSIS OF $Zr_{65}Cu_{17.5}Ni_{10}Al_{7.5}$ METALLIC GLASS   | p. 19 |

## Fe-based alloys

- |   |                |  |       |
|---|----------------|--|-------|
| 1 | Q.F. Fang      | Internal friction phenomena in a wide temperature range up to 1073K in stable Fe-(0-30 at.%) Ga Alloys                           | p. 22 |
| 2 | V.V. Palacheva | Mechanical spectroscopy of atomic ordering in Fe-(16-21) Ga-RE alloys  | p. 23 |
| 3 | A.K. Mohamed   | Mechanical spectroscopy of phase transitions in Fe-(23-38)Ga-RE alloys   | p. 25 |
| 4 | L. Li          | Effect of phase composition on the internal friction and magnetostriction in the $L1_2/DO_3$ biphasic Fe <sub>27</sub> Ga alloys | p.28  |

## Metallic alloys

- |   |                     |  |       |
|---|---------------------|--|-------|
| 1 | A.V. Mikhaylovskaya | Mechanical spectroscopy of Al-based alloys with $L1_2$ precipitates                  | p. 30 |
| 2 | R. Montanari        | Mechanical spectroscopy study of as-cast and additive manufactured AlSi10Mg          | p. 32 |
| 3 | M. Tane             | Kinetics of diffusionless isothermal and athermal omega transformations in Ti alloys | p. 33 |

4	M.L. No	Influence of Nb on the Ti diffusion in $\gamma$ -TiAl intermetallics studied by mechanical spectroscopy	p. 35
5	P. P. Pal-Val	Effect of annealing on low-temperature acoustic properties of nanocomposites Cu-Fe obtained by batch hydroextrusion techniques	p. 37

### Low damping materials

1	X. Liu	Comparing amorphous silicon prepared by e-beam evaporation and sputtering toward eliminating atomic tunneling states	p. 41
2	T. H. Metcalf	Internal friction measurements of low energy excitations in amorphous germanium thin films	p. 42
3	D. Lumaca	Stability of samples in coating research: from edge effect to ageing	p. 43

### Domain Walls

1	E. Salje	Internal friction in complex ferroelastic twin patterns	p. 7
2	W. Schranz	Local properties of domain walls	p. 47
3	L.N. Korotkov	Attenuation of low-frequency sound in the $\text{Na}_{0.875}\text{Li}_{0.125}\text{NbO}_3$ solid solution	p. 49

### Ceramics and ferroelectrics

1	D. Kajewski	Lattice dynamics in niobium doped $\text{PbZrO}_3$ single crystal	p. 51
2	O. Aktas	Depolarization of ferroelectrics measured by their piezoelectric and elastic response	p. 52
3	I.I. Popov	Low-frequency internal friction in ferroelectric $\text{Ba}_{0.8}\text{Sr}_{0.2}\text{TiO}_3$ and $\text{Ba}_{0.8}\text{Sr}_{0.2}\text{TiO}_3 + 0.2$ mass % La ceramics	p. 54
4	P. S. da Silva Jr	Ferroc glass behavior in $(\text{Bi},\text{Na})\text{TiO}_3$ - based lead-free electroceramics	p. 55
5	F. Trequattrini	Cation reorientation and octahedral tilting in the metal-organic perovskites MAPI and FAPI	p. 58

### Point defects

1	H. Numakura	Interaction between interstitial-substitutional solute atoms and formation of their clusters in bcc iron	p. 62
2	C.R. Grandini	Stress-induced ordering due to oxygen present in Ti-15Mo alloy	p. 63

3	F. Cordero	Hopping and clustering of oxygen vacancies in BaTiO <sub>3-δ</sub> and the influence of the off-centred Ti atoms	p. 65
4	D.R.N. Correa	The role of Ag on the stress-induced ordering of oxygen in the Ti-15Zr-15Mo alloy	p. 67
5	P. Maugis	Thermo-kinetic modelling of the giant Snoek effect in carbon-supersaturated iron	p. 69
6	L.Z. Huang	Atomistic investigation on the impact of substitutional Al and Si atoms on the carbon kinetics in ferrite	p. 71

## Theory

1	V.G. Gavriljuk	Mobility of dislocations in the iron-based C-, N-, H-solid solutions measured using i.f.: effect of electron structure	p. 74
2	V.V. Dezhin	On Internal Friction due to Elastic Waves Radiation during Dislocation Bendin Vibration in the Peierls Relief	p. 76
3	L.V. Elnikova	Electrical, elastic properties and defect structures in isotactic polypropylene oped with nanografite and graphene nanoparticles	p. 78

## Magnetic materials

1	S. Kustov	80 years after: new categories of magnetomechanical damping	p. 9
2	H.W. Chang	Enhancement of the magneto-mechanical properties in directional solidified Fe <sub>80</sub> Al <sub>20</sub> alloys by doping Tb	p. 81
3	H. Tanimoto	Anelasticity Study of Antiferromagnetic FeMnMo Alloy	p. 82
4	I. Tkalcec Vâju	Magneto-mechanical damping and phase transformations in iron-based alloys	p. 84
5	M. Comas Muntaner	Remanent magnetization of antiferromagnetic Dy through domain wall freezing: an acoustic study	p. 87
6	F.G. Bonifacich	Magnetic behavior in commercial iron-silicon alloys controlled by the dislocation dynamics at temperatures below 420K	p. 88
7	M.L. Corró	Villari points in single crystalline Dy as an example of "horizontal hysteresis" in ferroic materials	p. 90

## Grain boundaries

1	L. Degeneve	Relaxation time shift of cobalt related internal friction peak in wc-co cemened carbide	p. 92
2	L. Favre	Analysis of the recrystallization peak of Ti 5553 using torsion pendulum	p. 95
3	B. Weidenfeller	Analysis of the damping capacity in a weltklang saxophone manufactured in 1969	p. 97

4	L. Weidenfeller	Study of the damping behaviour on iron-electrodeposited copper samples from an ionic liquid	p.99
5	C.C. Duan	Mechanical relaxation due to grain boundary diffusion and grain boundary viscous flow	p101

### **Shape memory alloys and phase transition**

1	M. Pérez-Cerrato	Determination of the Clausius-Clapeyron coefficient in SMA through mechanical spectroscopy	p104
2	J.F. Gómez-Cortés	Superelastic damping in Cu-based shape memory alloys by nano-compression test	p106
3	L. Del-Río	Internal friction associated with martensite in shape memory steels	p108
4	A. Ojeda Sánchez	Effect of stabilization and destabilization by prestrain on acoustic properties and resistivity of Ni-Ti-Nb shape memory alloy	p110
5	A. Sabareesh	Effect of Ni and Mn additions on the damping characteristics of Cu-Al-Fe base high temperature	p111
6	M. Sun	Defect relaxation and phase transition behavior in manganese-containing microalloyed steels	p112

### **Composites and inhomogeneous materials**

1	G. Nithyanandh	Comparison of Internal friction measurements on Ni-Ti reinforced smart composite prepared by additive manufacturing	p114
2	M. Weidenfeller	Evaluation of the diagenesis degree in archaeological bones through the Havriliak-Negami expression	p115
3	V. Zadorozhnyy	Mechanical properties of the metal/polymer composites membranes for hydrogen separation	p118
4	A. Paolone	Mechanical spectroscopy study of quaternary cation ionic liquids: effects of different conformational flexibility	p119
5	J. Göken	Temperature-dependent damping of the tonewood spruce	p121
6	A.S. Voznesenskii	Temperature dependence of internal mechanical losses of gypsum stone with composition and structure	p122

# Plenary talks

## Internal friction in complex ferroelastic twin patterns

Ekhard K.H. Salje <sup>1\*</sup>

<sup>1</sup> *University of Cambridge, Cambridge, UK*

\* [es10002@cam.ac.uk](mailto:es10002@cam.ac.uk)

The internal friction (IF) of complex ferroelastic twin patterns was derived by atomistic molecular dynamics simulations [1]. Linear and non-linear IF regimes were found at different stress amplitudes and separated by a pinning/depinning threshold. The IF is directly related to the motion of ferroelastic needle twins.

A low linear IF background is nearly independent of temperature and the configuration of the twin patterns at external stresses below the pinning/depinning threshold. With increasing stresses, twin boundary motions generate non-linear anelasticity where the stress dependent IF increases to a maximum and then decays. This IF maximum is lowered and shifted to higher stresses by extrinsic pinning effects and decreases further with increasing temperature. The non-linear IF depends by power law on the strain with exponents near 2 below the IF maximum and -1 at strains higher than the maximum. Vacancies destroy the power law and break the scale invariance of the domain boundary movements.

Bent domain walls lead to weak piezoelectricity even when the bulk material is non-piezoelectric. In some cases, the bending leads to the formation of kinks in walls which enhance the piezoelectricity [2,3].

[1] X. He, S. Li, X. Ding, J. Sun, S. Kustov, E.K.H. Salje, Internal friction in complex ferroelastic twin patterns 2022, *Acta Materialia* 228, 117787.

[2] O. Aktas, M. Kanhama, G. Linyu, G. Catalan, X. Ding, A. Zunger, E.K.H. Salje, Piezoelectricity in nominally centrosymmetric phases. 2021, *Phys. Rev. Research* 3, 043221.

[3] G. Lu, S. Li, X.D. Ding, J. Sun, E.K.H. Salje, Electrically driven ferroelastic domain walls, domain wall interactions, and moving needle domains. 2019, *Phys. Rev. Materials* 3, 114405.

# Mechanical spectroscopy in amorphous materials: case of bulk metallic glasses

J. M. Pelletier<sup>1</sup>, J.C. Qiao<sup>2</sup>

<sup>1</sup>*MATEIS, INSA-Lyon, Université de Lyon, France*

<sup>2</sup>*NPWU, Xi'an, China.*

Amorphous materials exhibit a specific mechanical behavior due to the absence of long range order. Therefore, the concepts of point defects, dislocations or grain boundaries are no longer available. Amorphous materials may concern either polymers, oxide glasses or amorphous metals and thus either covalent, Van des Waals, ionic or metallic bonding are involved. Atomic mobility in these materials can be investigated using mechanical spectroscopy. Various relaxations can be observed either as a function of frequency or temperature. This point will be addressed in the presentation. A more detailed insight will be done in bulk metallic glasses. These materials are the topic of many researches because they possess excellent mechanical properties, in particular their yield strength. We will briefly review the main results obtained in various bulk metallic glasses. A physical analysis of the mechanical response will be presented. Similarities and differences with the other amorphous materials will be discussed.

## **80 years after: new categories of magnetomechanical damping**

Sergey Kustov

*Departament de Física, Universitat de les Illes Balears, Palma de Mallorca, Spain*

Magnetomechanical damping (MMD) in ferromagnets includes three canonical contributions - microeddy and macroeddy linear non-thermally activated relaxations and non-linear hysteretic damping. The first and the last of these three categories are due to the oscillatory motion of magnetic domain walls (DW), whereas the macroeddy component is derived from the net macroscopic magnetization of a sample. The concepts of these MMD components date back to 1930-1950-1960 and no fundamentally new observations have been done since then.

During the last few years, using resonant technique, operating around  $10^5$  Hz - the frequency range of the maximum sensitivity to DW related magnetomechanical effects - two new MMD categories have been uncovered:

low-temperature “freezing” of DWs, resulting in an intense thermally-activated relaxation and concomitant  $\Delta E$ -effect;

frequency-independent magnetic transitory damping term, associated with temperature/structural transition/magnetic field related rearrangement of DW structure.

The number of MMD categories thus increases from three to five. The disclosed MMD components offer new interpretations for a number of physical phenomena still being intensively discussed, like spin and re-entrant spin glass transitions, formation of tweed in ferromagnetic materials, etc.

# Internal friction at nano-scale and size-effects on damping in shape memory alloys

J. M. San Juan<sup>1\*</sup>, J.F. Gómez-Cortés<sup>1</sup>, M.L. Nó<sup>2</sup>

<sup>1</sup> Dpt. Physics of Condensed Matter, Faculty of Science and Technology, University of the Basque Country, UPV/EHU, Apdo. 644, 48080-Bilbao, Spain

<sup>2</sup> Dpt. of Applied Physics II, Faculty of Science and Technology, University of the Basque Country, UPV/EHU, Apdo. 644, 48080-Bilbao, Spain

\*e-mail jose.sanjuan@ehu.es

The short life of the present millennium is characterized by the emergence of a new paradigm of science, Nanotechnology, which spread across all branches of science, including Physics and Materials Science. Obviously, nanotechnology constitutes a challenge to approach the characterization of the material's properties at small scale, and new experimental techniques were required or improved to successfully face such challenge. This is also the case of mechanical spectroscopy, which nowadays is being required to give new insights on the mechanisms controlling the mechanical properties at very small scale.

In the present talk I will describe the endeavor to measure internal friction at nano-scale. First, I will remember the capabilities of the new techniques of instrumented nano indentation that were used to test and measure the damping at nano-scale in shape memory alloys [1,2]. Then, I will describe the observed size-effects on the mechanical behavior and in particular on damping [2-5], which will be analyzed in terms of the physics underlying behind such size-effects.

Indeed, damping can be measured at small scale in a broad range of experimental conditions, for instance in the case of shape memory alloys (SMA) can be measured not only during the stress-induced transformation by superelastic effect [2-5], but also in martensitic state [6], and follow the evolution on cycling [7], as in Figure 1 where an example of square pillars and the measure of damping as a function of the number of cycles is presented.

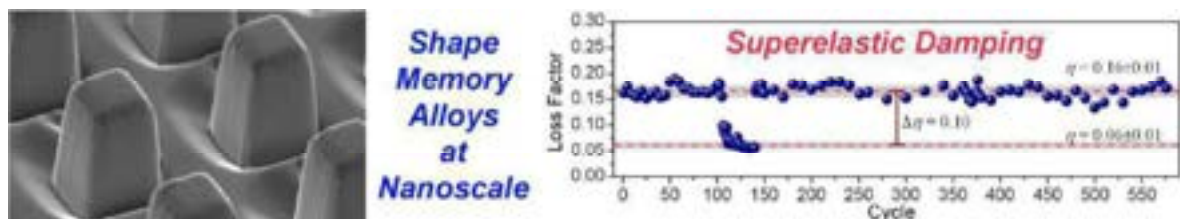


Fig.1 Example of square pillars of 1.6 micrometer side, milled by FIB, and damping measured during the stress-induced transformation by superelastic effect, as a function of the number of cycles performed at 0.2 Hz. Between the cycles 100 and 150 it can be seen a drop of the damping, which is associated to the unexpected stabilization of the martensite, which spontaneously reverted to austenite along cycling.

This new methodology opens the way to measure internal friction at very small scale, using the instrumented nano-indenters available in the scientific market, as well as the ones designed to perform in-situ experiments at the Scanning and Transmission Electron Microscopes (SEM & TEM). In the last part of my talk I will present how these techniques were used to measure the long-term evolution of

damping [7,8], in order to develop nano-dampers for technological applications in Micro Electro Mechanical Systems.

The door is open to develop Mechanical Spectroscopy at nano-scale, and to close my talk I will emphasize that still remain many challenges to be faced, in order to fully pave the road allowing to spread it across the Materials Science Community. This will be the role of new gamers, the new generation of young researchers.

- [1] J. San Juan, M.L. Nó, C.A. Schuh, *Advanced Materials* 20 (2008) 272-278.
- [2] J. San Juan, M.L. Nó, C.A. Schuh, *Nature Nanotechnology* 4 (2009) 415-419.
- [3] J. San Juan, M.L. Nó, *J. Alloys & Compounds* 577S (2013) S25-S29.
- [4] J.F. Gómez-Cortés, M.L. Nó, I. López-Ferreño, J. Hernández-Saz, S.I. Molina, A. Chuvilin, J. San Juan, *Nature Nanotechnology* 12 (2017) 790-796.
- [5] V. Fuster, J.F. Gomez-Cortes, M.L. Nó, J. San Juan, *Advanced Electronic Materials* 6 (2020) 1900741 (1-7).
- [6] J. San Juan, J.F. Gómez-Cortés, G.A. López, C. Jiao, M.L. Nó, *Applied Physics Letters* 104 (2014) 011901 (1-5).
- [7] J.F. Gomez-Cortes, M.L. Nó, I. Ruiz-Larrea, T. Breczewski, A. Lopez-Echarri, C.A. Schuh, J. San Juan, *Acta Materialia* 166 (2019) 346-356.

# **Amorphous materials**

## Spatial elastic inhomogeneity of metallic glasses before and after structural relaxation using inelastic x-ray scattering and ultrasound techniques

T. Hayashi<sup>1</sup>, M. Luckabauer<sup>2</sup>, M. Wakeda<sup>3</sup>, H. Tanimura<sup>1</sup>, T. Kawaguchi<sup>1</sup>,  
S. Tsutsui<sup>4</sup>, S. Hosoakwa<sup>5</sup>, J. Saida<sup>6</sup>, H. Kato<sup>1</sup>, T. Ichitsubo<sup>1\*</sup>

<sup>1</sup>*Institute for Materials Research, Tohoku University, Sendai, Japan*

<sup>2</sup>*Faculty of Engineering Technology, University of Twente, Enschede, The Netherlands*

<sup>3</sup>*Research Center for Structural Materials, National Institute for Materials Science, Tsukuba, Japan*

<sup>4</sup>*Japan Synchrotron Radiation Research Institute (JASRI), Hyogo, Japan*

<sup>5</sup>*Institute of Industrial Nanomaterials, Kumamoto University, Kumamoto, Japan*

<sup>6</sup>*Frontier Research Institute for Interdisciplinary Sciences, Tohoku University, Sendai, Japan*

\*tichi@tohoku.ac.jp

Glassy materials are non-crystalline solids with frozen supercooled structures in which the constituent atoms are (semi)randomly arranged in a metastable or unstable thermodynamic state. In particular, metallic glasses, which are composed mainly of metallic elements, have both excellent mechanical properties and electrical and thermal conductivity.[1] Unlike crystalline materials, glass materials do not have periodic atomic arrangements, making it difficult to determine their structures by X-ray diffraction measurement, which is a powerful tool for crystalline materials. Thus, we have been using the inelastic X-ray scattering (IXS) to elucidate the microscopic structure of glass from an acoustic point of view. This technique enables us to measure the interaction between X-rays and phonons reflecting the microscopic structure of the material and has revealed that the structure of glass is spatially inhomogeneous in terms of local elasticity.[2] This elastic inhomogeneity has been suggested by many experiments and simulations and has been an important element in determining their physical properties. On the other hand, the relationship between several complex relaxations and spatial heterogeneity, which is essential for the practical use of metallic glasses, has not yet been clarified. In this study, IXS measurements were performed on metallic glass samples before and after structural relaxation, and the effect of structural relaxation on spatial inhomogeneity was investigated by comparing the sound velocity reflecting the nanoscopic structure with that reflecting the macroscopic structure obtained by using the electromagnetic acoustic resonance method (EMAR). Here the effect of structural relaxation on spatial inhomogeneity was investigated by using a PdNiCuP metallic glass.

Pd<sub>42.5</sub>Ni<sub>7.5</sub>Cu<sub>30</sub>P<sub>20</sub> (PNCP), a typical fragile metallic glass, was prepared by the arc melting method. The sample thickness was adjusted to an appropriate thickness for the X-ray scattering measurement by machining and polishing. IXS was measured using the beamline BL35XU at SPring-8, and the results were analyzed to derive the sound velocity reflecting the nanoscopic structure of the sample. The sound velocity reflecting the macroscopic structure of the sample was determined by using the laboratory's EMAR system for the bulk sample before and after aging.

Figure 1 (left) shows the results of EMAR measurements on PNCPs aged for different times, which show a decrease in internal friction and an increase in resonance frequency of the same vibration mode depending on the aging time. Analysis of the results shows that after aging, the elastic modulus of the sample

increases by 2~3% and, therefore, the sound velocity of the macroscopic system increases. On the other hand, Figure 1 (right) shows that no significant differences were observed in the sound velocities determined by IXS measurements before and after aging, which indicates that the elasticity of strongly-bonded regions (SBRs) remains unchanged before and after structural relaxation. The results of both measurements indicate that the macroscopic elastic modulus increases with structural relaxation because the weakly-bonded regions (WBR) elasticity is enlarged, although the SBR elastic modulus is not substantially changed. This may be due to the elimination of structural inhomogeneity in the glass structure by the progress of structural relaxation. This suggests that the structural relaxation in the glass structure is spatially inhomogeneous, and supports that the static spatial inhomogeneity is intrinsically present in the glass structure. In our talk, we will present the results of both measurements in more detail and discuss the effect of heat treatment on spatial inhomogeneity within metallic glass structures.

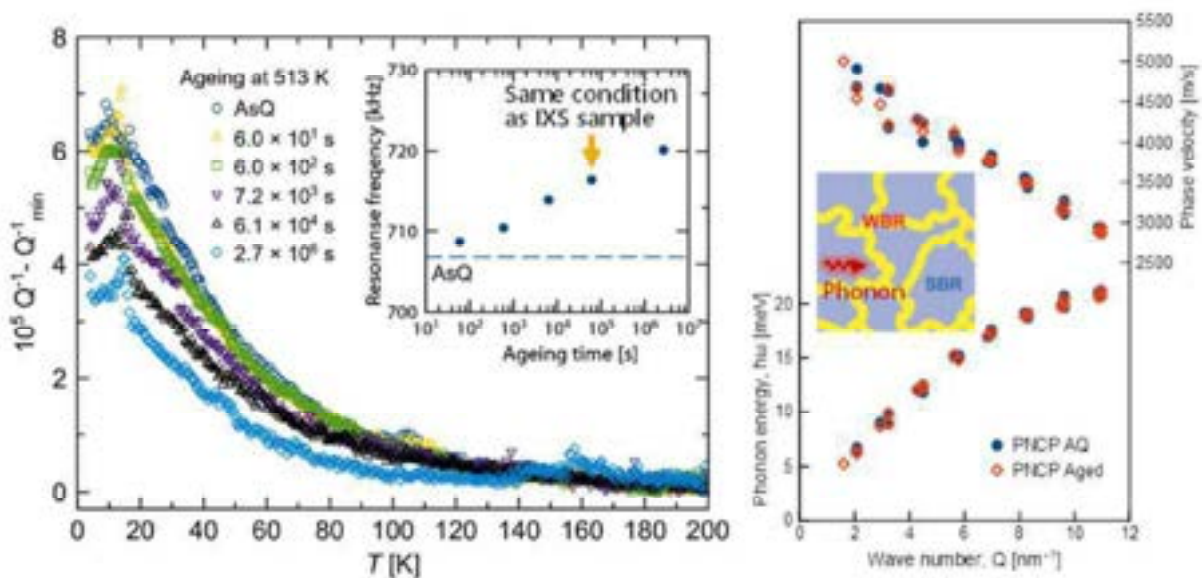


Fig. 1. (left) Internal friction measured by EMAR. The results are shown together with the change in resonance frequency with aging time. A following structural relaxation treatment, sub-T<sub>g</sub> annealing for 17h at 513 K (30 K lower than T<sub>g</sub>), was done for a PNCP glass material. (right) Phonon dispersion relations of as-quenched (AQ) sample and sub-T<sub>g</sub>-annealed (Aged) sample obtained by the IXS measurements.

[1] M. Chen, NPG Asia Mater., 3, 82 (2011).

[2] T. Ichitsubo, et al. Phys. Rev. B. 76 140201 (R) (2007)

## **Magnetomechanical effects in ferromagnetic microwires of Co-rich compositions**

Larissa V. Panina<sup>1,2,3\*</sup>, Makhsudsho Nematov<sup>2</sup>, Junaid Alam<sup>1</sup>, Nikolay Yudanov<sup>1</sup>, Anatoliy Samohvalov<sup>1</sup>, Alexander Morchenko<sup>1</sup>

<sup>1</sup> *Institute of Novel Materials and Nanotechnology, National University of Science and Technology (MISiS), Moscow 119991, Russia;*

<sup>2</sup> *Institute of Physics, Mathematics & IT, Immanuel Kant Baltic Federal University, Kaliningrad 236041, Russia*

<sup>3</sup> *Institute for Design Problems in Microelectronics RAS, Moscow 124681, Russia;*  
*\*drlpanina@gmail.com*

Ferromagnetic microwires are very attractive for wide range of applications exploiting their anisotropic magnetic properties and miniature dimensions [1]. In particular, Co-rich microwires produced by rapid quenching techniques may have a well-defined circular anisotropy and extremely high permeability, which is promising for the development of high-sensitivity sensors of low magnetic field, stress/strain and temperature. In the absence of a crystalline structure the magnetic anisotropy has a dominant contribution coming from the magnetoelastic interactions which explains stress-sensitive magnetic responses for both low and high frequency excitations. The magnetomechanical properties can be tuned by various annealing treatments affecting the saturation magnetostriction, internal stress distribution and induced anisotropy [2-4]. In this work we discuss the conditions how to realize thermally stable and stress-sensitive magnetic hysteresis and magnetoimpedance (MI) in microwires of a number of compositions based on CoFeSiB amorphous alloy.

Varying the Fe-content within few atomic percents, the saturation magnetostriction in these alloys can be made almost zero and extremely soft magnetic properties realized at this condition ensure huge sensitivities of the magnetically related effects. However, the amorphous state is thermally unstable: heating by moderate temperatures in the industrial range of below 80 C produces internal stress relaxation causing enormous changes in the magnetoelastic anisotropy. Such behavior hinders all the technical applications. To avoid uncontrolled structural relaxation various annealing treatments are employed. Annealing originates the changes in chemical and topological short-range orders which can be used to optimize the induced anisotropy and magnetostriction. This makes it possible to realize a unique combination of the easy anisotropy axis and the magnitude and sign of the saturation magnetostriction. For example, current annealing of amorphous wires with moderate current intensities induces a circumferential easy anisotropy and positive magnetostriction. The application of tensile stress along the wire contributes to long-range axial anisotropy and strongly affects the re-magnetization process and magnetoimpedance as shown in Fig. 1 [4]. Therefore, this magnetic configuration is desirable for stress/strain sensing with the use of microwires and is in the focus of this work.

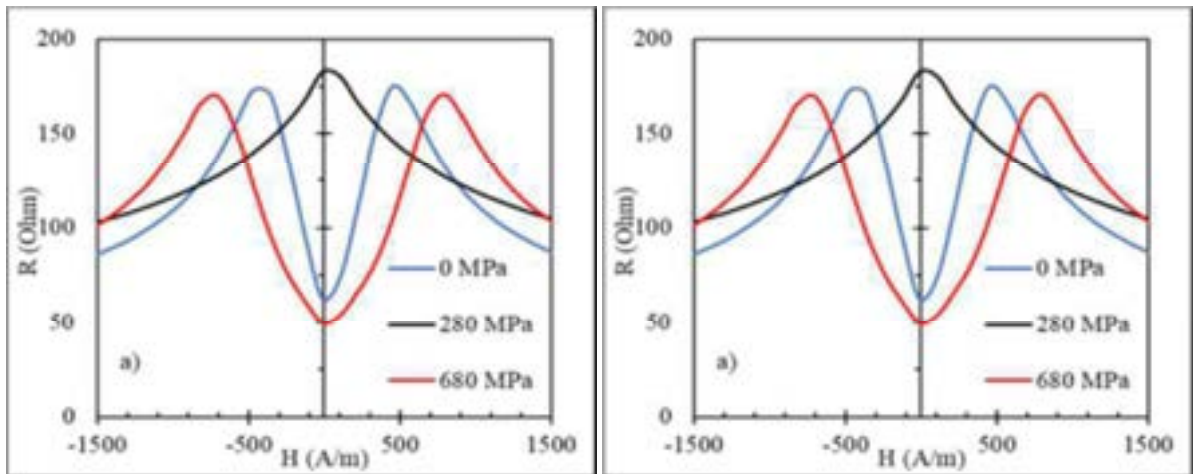


**Figure 1.** Effect of tensile stress on magnetoimpedance of glass-coated amorphous  $\text{Co}_{71}\text{Fe}_5\text{B}_{11}\text{Si}_{10}\text{Cr}_3$  microwires after current annealing (a) at 50 mA for 60 min, (b) at 60 mA for 60 min. Frequency is 50 MHz.

### References:

- K.Mohri, T. Uchiyama, L.Panina, M. Yamamoto, K. Bushida, Recent Advances of Amorphous Wire CMOS IC Magneto-Impedance Sensors: Innovative High-Performance Micromagnetic Sensor Chip. *J. Sensors* **2015** (2015), 1–8.
- A. Zhukov, M. Ipatov, M. Churyukanova, M. Talaat, A. Blanco, V. Zhukova, Trends in optimization of giant magnetoimpedance effect in amorphous and nanocrystalline materials. *J. Alloys Compd.* **727** (2017) 887–901.
- C.Gomez-Polo, M. Vázquez, Structural relaxation and magnetic properties of Co-rich amorphous wire. *J. Magn. Magn. Mater.* **118** (1993) 86–92.
- M.G.Nematov, A.M.Adam, L. V. Panina, N.A.Yudanov, A.Dzhumazoda, A.T.Morchenko, D.P.Makhnovskiy, F.X. Qin, Magnetic anisotropy and stress-magnetoimpedance (S-MI) in current-annealed Co-rich glass-coated microwires with positive magnetostriction. *J. Magn. Magn. Mater.* **474** (2019) 296–300.

## Relaxation behavior of an Al-Y-Ni-Co metallic glass in as-prepared and cold-rolled state

<sup>1</sup>\*Berezner A.D., <sup>1</sup>Fedorov V.A., <sup>2</sup>Zadorozhnyy M.Yu.,  
<sup>3,4</sup>Louzguine-Luzgin D.V.

<sup>1</sup>*Derzhavin Tambov State University, Tambov, Russia*

<sup>2</sup>*The National University of Science and Technology MISiS, Moscow, Russia*

<sup>3</sup>*Advanced Institute for Materials Research (WPI-AIMR), Sendai, Japan*

<sup>4</sup>*MathAM-OIL, National Institute of Advanced Industrial Science and Technology (AIST), Sendai, Japan*

\*a.berezner1009@gmail.com

Al-based metallic glasses (MGs) are of great interest for the various technological applications because of their superior mechanical strength and low density. Deformation-induced structure changes and crystallization of the Al<sub>85</sub>Y<sub>8</sub>Ni<sub>5</sub>Co<sub>2</sub> rolled at room and elevated temperature were studied recently [1,2]. It gives to us an opportunity for the further investigation in this field.

The ingot of the Al<sub>85</sub>Y<sub>8</sub>Ni<sub>5</sub>Co<sub>2</sub> alloy was prepared by arc-melting the mixtures of Al 99.99 mass% purity, Y 99.9 mass% purity, Ni 99.9 mass% purity and Co 99.9 mass% purity in an argon atmosphere purified with a Ti getter. Ribbon samples of about 40 μm thickness and about 4.5 mm width were prepared by rapid solidification of the melt on a single copper wheel at the wheel tangential velocity of 42 m/s. The samples with a working length of 18.5 mm were studied by using a dynamic mechanical analyzer (DMA), Q800 TA Instruments. They were studied on heating up to 673 K at the heating rate of 5 K/min. A sinusoidal-type elastic tensile deformation (±0.4N – variable loading force) was applied at the oscillation frequency of 3 Hz in order to measure the storage modulus ( $E'$ ), loss modulus ( $E''$ ) and the internal friction ( $Q^{-1}$ ) of materials.

Al<sub>85</sub>Y<sub>8</sub>Ni<sub>5</sub>Co<sub>2</sub> metallic glassy ribbon samples subjected to cold rolling showed a stronger  $\beta$ -relaxation peak and faster deformation on heating compared to those studied in the as-prepared state. Application of dynamic loading leads to mechanical deformation starting at a lower temperature compared to static load. The resonance processes are found to be possible due to simultaneous superposition of the thermal and mechanical vibration components. Such an effect can lead to increased fluidity and premature failure of the sample at certain frequencies. The model for estimation of deformation rate, reaction force, the main values of DMA, thermal capacity, sound speed etc. is proposed here. By the model equations, deformation of as-cast and rolled Al<sub>85</sub>Y<sub>8</sub>Ni<sub>5</sub>Co<sub>2</sub> MG is related to thermal (DSC) maximum as a function of loading frequency and heating rate. The main relationship of this alternatively can be given graphically (in Fig.1).

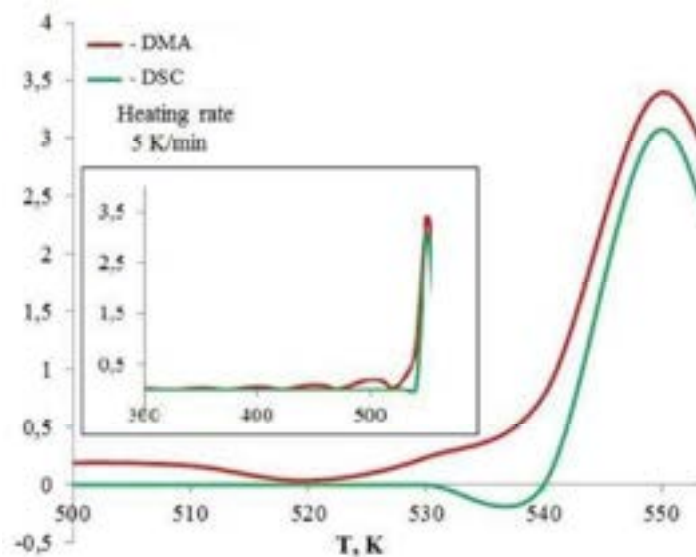


Fig.1 The calculated curve of the normalized heat capacity of the studied metallic glass. The entire view of the plots in the interval from 300 to 553 K is shown in the inset.

Simulation of DMA experiment permits estimation of the sound speed in MG specimen, for example, that simplifies acoustic investigation of ribbon MGs and other materials at the same conditions. The analysis of Non-Newtonian types of flow is carried out at non-isothermal DMA. As a result, the rheological mechanisms of deformation are proposed for the as-cast and rolled alloys. The proposed model permits systematization of different aspects of structural relaxation by the consistent mathematical reasoning. This work can be interested from the fundamental and applied viewpoints in physics and engineering.

*This work was supported within the framework of the program of the Ministry of Science and Higher Education of the Russian Federation «Russian Academic Excellence Project», and also by the Russian Science Foundation (grant No. 22-22-00226). The authors sincerely thank A. Bazlov and A.G. Igrevsckaya for assistance in preparation and cold rolling of the Al samples.*

- [1] D.V. Louzguine-Luzgin and A. Inoue, *J. Non-Cryst. Solids*, 352, 390 (2006);  
 [2] V.S. Zolotarevsky, A.I. Bazlov, A.G. Igrevsckaya, A.S. Aronin, G.E. Abrosimova, D.V. Louzguine-Luzgin, *JOM*, 71, 11, 4079 (2019);

# DYNAMIC MECHANICAL ANALYSIS OF $Zr_{65}Cu_{17.5}Ni_{10}Al_{7.5}$ METALLIC GLASS

R.A. Sergiienko<sup>1\*</sup>, O.A. Shcheretskyi<sup>1</sup>, V.Yu. Zadorozhnyy<sup>2</sup>, O.M. Myslyvchenko<sup>3</sup>, A.M. Verkhovliuk<sup>1</sup>

<sup>1</sup> *Physico-Technological Institute of Metals and Alloys, National Academy of Sciences of Ukraine, 34/1, Vernadsky Ave., Kyiv-142, 03680, Ukraine*

<sup>2</sup> *National University of Science and Technology «MISIS», Leninsky Prosp., 4, 119049, Moscow, Russia*

<sup>3</sup> *Frantsevich Institute for Problems of Materials Sciences of the NAS of Ukraine, 3 Krzhyzhanovsky Str., Kyiv, 03142, Ukraine*

\*e-mail: [rsruslan17@gmail.com](mailto:rsruslan17@gmail.com)

To understand the nature of the phenomena that occur during the heating of amorphous alloys, studies of the transition of zirconium-based alloys from an amorphous to a crystalline state using dynamic mechanical analysis (DMA) are promising and important [1, 2]. The DMA method was used to study the features of structure formation in the as-cast bulk (20×2×1 mm) and the as-spun ribbon (18×1.5×0.030 mm) samples during their heat treatment and under controlled dynamic and static loads. DMA studies were carried out by the three-point bending method for the bulk sample and under tensile load for ribbon sample using DMA 242C instrument of the German firm NETZSCH under the following conditions: dynamic stress of 4 H, static stress of 6 H, at a constant frequency of 1 Hz and different heating rates of 5 °C/min, 10 °C/min. When the bulk metallic glass sample of the  $Zr_{65}Cu_{17.5}Ni_{10}Al_{7.5}$  alloy was heated up to 325°C, the storage modulus,  $E^I$ , remains almost constant and in the amorphous state. With further heating, the elastic modulus decreases and at 420 °C takes a minimum value. Loss factor,  $\tan \delta$ , begins to grow up markedly from a temperature of 372 °C and reaches its maximum at 407 °C. At a temperature of minimum on the curve of  $E^I$  and maximum on the curve of  $\tan \delta$ , the alloy has maximum plastic properties; it is higher than the glass transition temperature ( $T_g = 368$  °C), which is confirmed by differential scanning calorimetry (DSC). During crystallization of the  $Zr_{65}Cu_{17.5}Ni_{10}Al_{7.5}$  alloy, the elastic modulus,  $E^I$ , increases, the loss factor,  $\tan \delta$ , also increases above 455 °C. Irreversible changes are induced by heating above the crystallization temperature, since the sample becomes crystalline. A similar change in the elastic modulus and loss factor on heating was found for the alloys of the Zr-Cu-Ni-Al system in other works [1-3].

When heating a ribbon sample under tensile load, a behavior of the elastic modulus,  $E^I$ , and loss factor,  $\tan \delta$ , is similar to that for the bulk sample. In contrast to the bulk sample, a change in the length of the ribbon sample during heating occurs abnormally (Fig. 1). At the beginning a decrease in sample length,  $dL$ , is observed and appears minimum at 239 °C, then the sample length gradually increases, and dramatic  $dL$  growth occurs above 300 °C (Fig.1).

Figure 2 shows the temperature dependence of the elastic modulus,  $E^I$ , (Fig. 2a) and loss factor,  $\tan \delta$ , (Fig. 2b) of the  $Zr_{65}Cu_{17.5}Ni_{10}Al_{7.5}$  alloy. There are totally seven heating processes until finally heating to 430 °C, each heating was

performed after the cooling to room temperature. Six times the sample was heated up to 250°C and 300°C at a rate of 10°C/min, and the seventh time the heating rate was 5°C/min. At each heating, the values of  $E^I$  and  $\tan \delta$  increase and significantly differ from each other, which can be explained by gradual relaxation processes occurring in the sample.

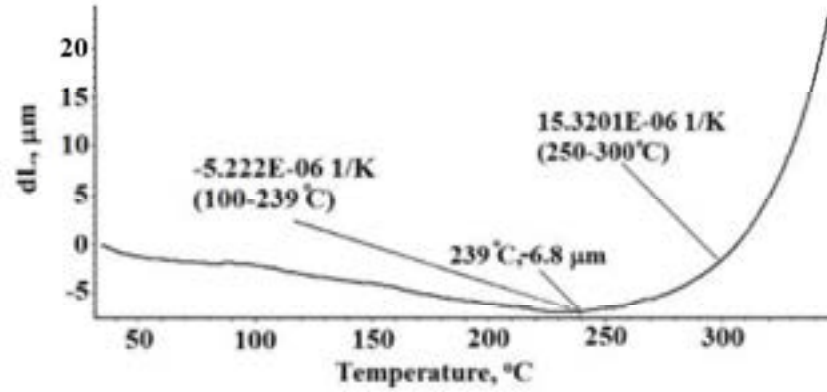


**Fig. 1.** DMA curve of sample length (dL) versus temperature of amorphous alloy  $Zr_{65}Cu_{17.5}Ni_{10}Al_{7.5}$

The room temperature storage modulus and loss factor of the 7<sup>th</sup> heating increase by about 15% and by a factor of three, respectively in comparison with the initial state for the first heating (Figs.2 a, b).

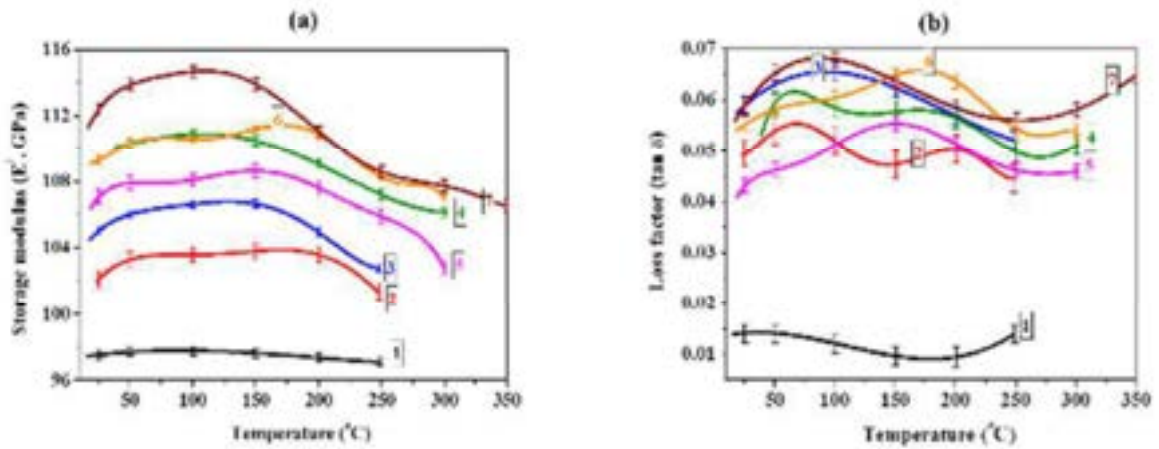


**Fig. 2.** Temperature dependence of storage modulus ( $E^I$ ) (a) and loss factor ( $\tan \delta$ ) (b) in  $Zr_{65}Cu_{17.5}Ni_{10}Al_{7.5}$  bulk metallic glass sample during successive heating to different temperatures measured at heating rates of 10 °C/min (for the 1st, 2nd, 3rd, 4th, 5th, 6th runs), 5 °C/min (for the 7th run) and constant driving frequency of 1 Hz. Error bars limits the scatter of experimental points relative to the fitting curves for 95% confidence probability interval.

[1] O. A. Shcheretsky, V. L. Lakhnenko, V. S. Shumikhin, A. A. Bepalyy, and A. V. Soloviova, *Metallofiz. Noveishie Tekhnol.*, **33** (2011) 1323-1332.

[2] R.A. Sergiienko, O.A. Shcheretskyi, V.Yu. Zadorozhnyy, *J. Alloys Compd.*, **791** (2019) 477-482.

[3] J.C. Qiao, R. Casalini, J.M. Pelletier, *J. Non-Cryst. Solids*, **407** (2015) 106-109.

# Fe-based alloys

# Internal friction phenomena in a wide temperature range up to 1073K in stable Fe-(0–30 at.%) Ga Alloys

Meng Sun, Lan Li, Weibin Jiang, Yunxia Gao, Xianping Wang, Qianfeng Fang\*

Key Laboratory of Materials Physics, Institute of Solid State Physics, HFIPS, Chinese Academy of Sciences, Hefei 230031, PR China

\*qffang@issp.ac.cn

**Keyword:** Fe-Ga alloys; Internal friction; Zener relaxation; Phase transition;

## Abstract:

The high damping capacity and high magnetization of Fe-Ga alloys are closely related to the phase structure and atomic relaxation behavior. Therefore, both scientifically and technically, an in-depth study of the relaxation and phase transition behaviors in Fe-Ga alloys is needed to understand the mechanism of the extraordinary functional properties and promote the application of Fe-Ga alloys. Although substantial progress has been made in the study of the IF behavior of Fe-Ga alloys, there are still some open questions. For example, the IF investigation of Fe-Ga alloy with Ga content greater than 28at% has rarely been reported and only a small part of studies on the IF behavior of Fe-Ga alloys involves the temperature domain above 600°C, where several phase transitions would occur based on the equilibrium phase diagram of Fe-Ga alloys.

The internal friction (IF) phenomena were systematically studied in a temperature range from room temperature to 1073K for Fe-(0–30 at.%)Ga alloys annealed at 480°C for 14 days, which include the magnetic-related high damping plateau (HDP) and the point of ferro-paramagnetic transition ( $T_c$ ), grain boundary relaxations, Zener relaxations, and the IF peaks associated with phase transitions. It was found that the Curie point  $T_c$ , as well as the rapid decay temperature of the HDP, decreases with the increasing Ga content, and the HDP disappears when the Ga content is greater than 18at.%. In the stable Fe-30at.%Ga alloy a frequency-independent phase transition IF peak was observed and its mechanism was suggested as phase transition of  $L1_2 \rightarrow A2/B2$ . The phase transitions in Fe-(0–30 at.%)Ga alloys evaluated by the IF technique are in good agreement with the equilibrium phase diagram. In addition, a new relaxation peak was observed before the displacive phase transitions of  $L1_2 \rightarrow D0_{19}$  and  $L1_2 \rightarrow A2/B2$ , and its mechanism could be related to Zener relaxation in FCC matrix.

## Mechanical spectroscopy of atomic ordering in Fe-(16–21)Ga-RE alloys

V.V. Palacheva<sup>a\*</sup>, A.K. Mohamed<sup>a</sup>, J. Cifre<sup>b</sup>, L.Yu. Dubov<sup>c</sup>, N.Yu. Samoylova<sup>d</sup>,  
A.M. Balagurov<sup>a,d,e</sup>, I.S. Golovin<sup>a</sup>

<sup>a</sup> National University of Science and Technology “MISIS”, Leninsky ave. 4/1, Moscow 119049, Russia

<sup>b</sup> Universitat de les Illes Balears, Ctra. De Valldemossa, km.7.5, Palma de Mallorca E-07122, Spain

<sup>c</sup> National Research Center Kurchatov Institute - ITEP, Moscow 117218, Russia

<sup>d</sup> Frank Laboratory of Neutron Physics, Joint Institute for Nuclear Research, Dubna 141980, Russia

<sup>e</sup> Lomonosov Moscow State University, Moscow, Russia

\*palacheva@misis.ru

Anelasticity of Fe-(16-21)at.%Ga-RE (rare earth RE = La, Tb elements) alloys at room and elevated temperatures is studied in a sub-resonance mechanical spectroscopy. Two thermally-activated and two transient effects are recorded in most of the studied alloys. To explain these phenomena, structure and phase transitions in several binary and ternary Fe-Ga alloys are investigated. The D0<sub>3</sub> ordering of rapidly cooled alloys with the A2 structure at heating at around 300 °C and the disordering at heating and the D0<sub>3</sub> ordering at cooling around 500 °C for annealed samples are proved using three in situ techniques: neutron diffraction, vibrating sample magnetometry, and internal friction and supported by positron annihilation experiments. Thermally activated transitory effects are tentatively explained by stress-induced reorientation of Ga-Ga and carbon atoms jumps.

Figure 1a shows the TDIF curves for the as-quenched Fe-19.5Ga binary alloy measured at heating using six different frequencies of forced bending vibrations in a single cantilever mode. Two thermally activated effects (P1 and P2), whose temperature position depends on measuring frequency, and two transient effects (P<sub>Tr1</sub> and P<sub>Tr2</sub>), whose temperature position is practically independent on measuring frequency, are marked in the figure. These four effects can be observed at heating on the TDIF curves for all the studied alloys, but their intensity depends on the alloy's composition and heat treatment.

At cooling (see Fig. 1b), the P1 and P<sub>Tr1</sub> disappear, whereas the P2 and P<sub>Tr2</sub> effects are recorded in this alloy as well as in most of other studied compositions. The second, third, and fourth ‘heating and cooling’ runs of the same sample are rather similar to those measured at cooling (Fig. 1c). To make the P<sub>Tr2</sub> effect distinguishably better, it is underlined by yellow colour. As shown in Fig. 1c,d the P2 peak at heating for low frequencies is influenced by the transitory effect (P<sub>Tr1</sub>).

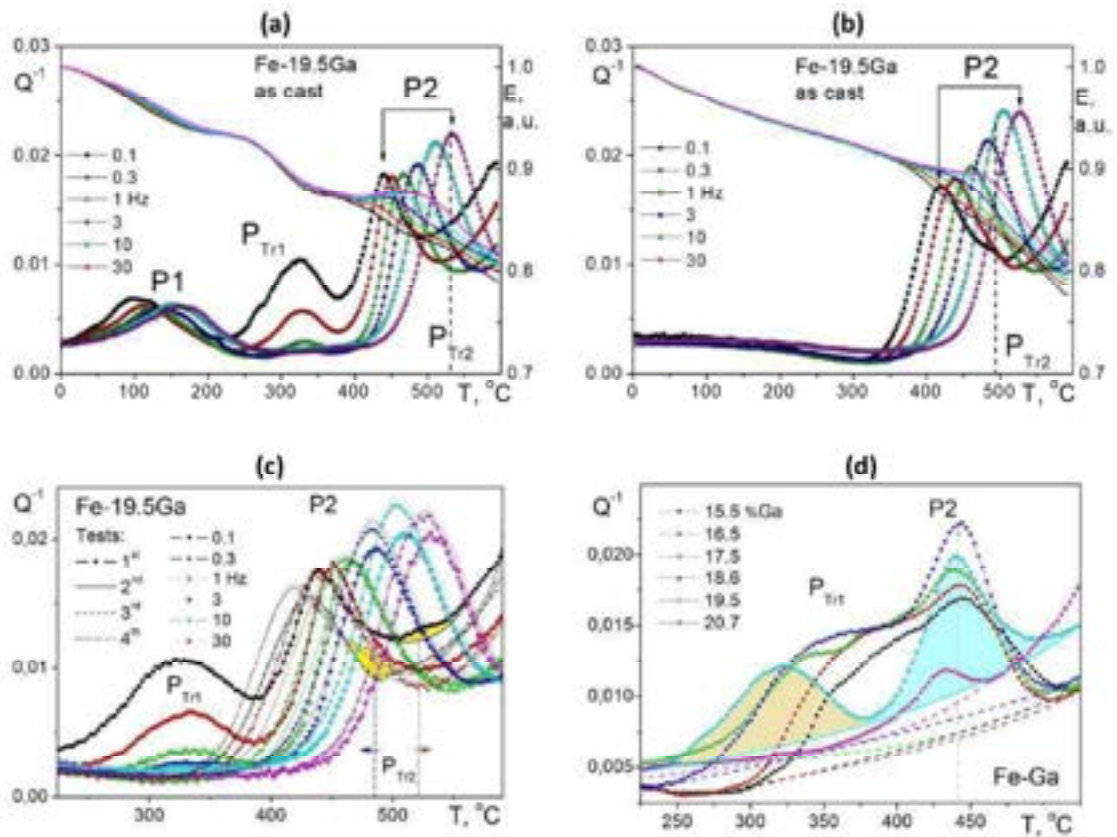


Fig. 1. TDIF curves at six different frequencies for the Fe-19.5Ga binary alloy as measured at heating (a), cooling (b), and three subsequent heating and cooling runs (c); the TDIF curves at heating for several binary Fe-Ga alloys in the range of the  $P_{Tri1}$  and P2 peaks as measured at 0.1 Hz (d).

We can conclude that mechanical spectroscopy is a very sensitive method that gives a response to even slight changes of the structure, including atomic jumps and weak ordering effects. The temperature-dependent internal friction spectra of Fe-Ga and Fe-Ga-RE (with 16-19at. %Ga, RE = La, Tb) alloys are rather complicated and dependent on samples pre-history. After summarizing and analyzing about thirty TDIF spectra (each measured from 0° to 600 °C at forced vibrations using six frequencies from 0.1 to 30 Hz) of as-cast, as quenched and annealed samples, we reliably distinguished two thermally activated and two transient effects in most samples.

This study was supported by Russian Science Foundation project 19-72-20080.

#### References:

- [1] I.S. Golovin, Anelasticity of Fe-Ga based alloys, Mater. Des. 88 (2015) 577-587. doi:10.1016/j.matdes.2015.08.160
- [2] I.S. Golovin, V.V. Palacheva, J. Cifre, C. Jiang, Internal friction in Fe-Ga alloys at elevated temperatures, J. Alloys Compd. 785 (2019) 1257-1263. doi:10.1016/j.jallcom.2019.01.265

# Mechanical spectroscopy of phase transitions in Fe-(23-38)Ga-RE alloys

A.K. Mohamed<sup>1,2\*</sup>, V.V. Palacheva<sup>1</sup>, E.N. Zanaeva<sup>1</sup>, J. Cifre<sup>3</sup>,

E.B. Cherepetskaya<sup>1</sup> N.Yu. Samoylova<sup>1,4,5</sup>, A.M. Balagurov<sup>1,3,6</sup>, I.S. Golovin<sup>1</sup>

<sup>1</sup> National University of Science and Technology "MISIS", Leninsky ave. 4, 119049, Moscow, Russia

<sup>2</sup> Shoubra Faculty of Engineering, Benha University, Cairo, 11629, Egypt

<sup>3</sup> Universitat de les Illes Balears, Ctra. De Valldemossa, km.7.5, E-07122, Palma de Mallorca, Spain

<sup>4</sup> Frank Laboratory of Neutron Physics, Joint Institute for Nuclear Research, 141980, Dubna, Russia

<sup>5</sup> Skobeltsyn Institute of Nuclear Physics, Lomonosov Moscow State University, Moscow, Russia

<sup>6</sup> Lomonosov Moscow State University, Moscow, Russia

\*Speaker' e-mail: abdelkarim.abdelkarim@feng.bu.edu.eg

As cast Fe-Ga alloys with metastable A2 structure with D0<sub>3</sub> and B2 clusters [1] are subjected to several phase transitions at heating from B.C.C.-derived phases (A2, D0<sub>3</sub>, B2) → F.C.C.(L1<sub>2</sub>) → H.C.P.(D0<sub>19</sub>) → B.C.C. (equilibrium) phases [2]. These structures are shown in Fig. 1 for alloys with about 27%Ga. At cooling from 600°C the equilibrium L1<sub>2</sub> phase remains unchanged until room temperature. For alloys with Ga > 30%, additional phases: β-Fe<sub>6</sub>Ga<sub>5</sub> in as cast state and α-Fe<sub>6</sub>Ga<sub>5</sub> after annealing.

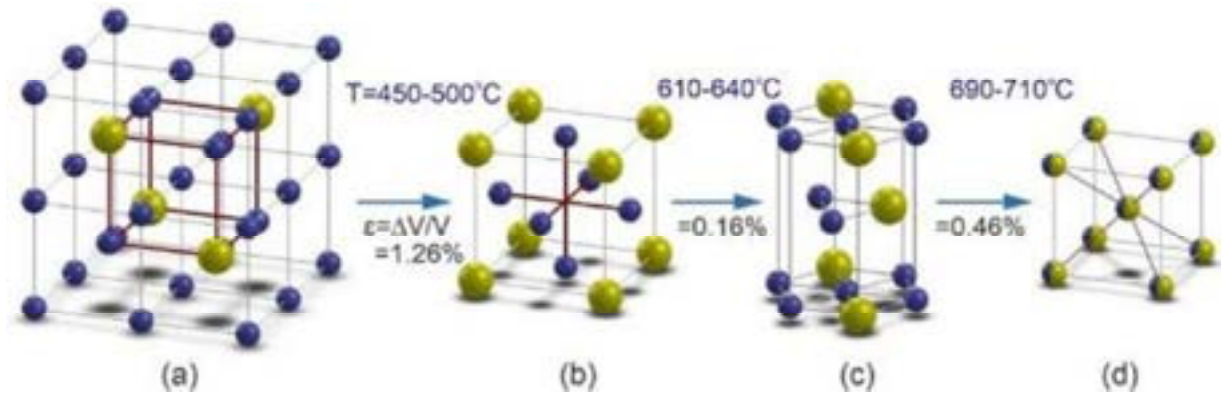


Fig. 1. Sequence of phase transitions from D0<sub>3</sub> (a) to L1<sub>2</sub> (b) to D0<sub>19</sub> (c) and to A2 (d) structures. Transition temperatures and deformation strain accompanied these transitions are given near arrows.

For Fe-Ga alloys with Ga content from 25 to 33 at.% the metastable phases (B.C.C. derived phases are indicated as D0<sub>3</sub> structure in diffraction patterns) transform to equilibrium L1<sub>2</sub> phase at T > 450°C if heating rate is 2 K/min. These phases play a key role in the formation of functional properties of Fe-Ga alloys: the A2 and D0<sub>3</sub> phases have positive- and the L1<sub>2</sub> has negative magnetostriction [3].

In this work we used temperature dependent internal friction (TDIF) tests to record first order phase transition between B.C.C. derived and F.C.C. phases. VSM, dilatometry, DSC were used to support this study and to interpret the TDIF results. The results of *in situ* neutron diffraction tests carried out earlier on the same samples [4] were also used to interpret the results.

Anelastic effects in Fe-(23-38)Ga binary and ternary alloys doped with rare earth (RE) elements, RE = Pr, Sm, Tb, Er, and Yb are studied in a sub-resonance frequency through heating and cooling in the range from 0 to 600 °C. In situ neutron diffraction, vibrating sample magnetometry (VSM), and differential scanning calorimetry (DSC) are used to trace the phase transition during heating and cooling, and to interpret anelastic effects due to phase transitions. Besides the thermally activated effects, two transient effects due to the first order transitions  $D0_3 \rightarrow L1_2$  and  $B2/D0_3 \rightarrow Fe_{13}Ga_9$  (later in alloys with Ga content > 29 at.%) are carefully studied. In most cases the RE elements decrease the rate of phase transitions. The obtained results demonstrate excellent correlation between temperature dependent internal friction, in situ neutron diffraction and vibrating sample magnetometry tests.

Temperature dependent internal friction and modulus of elasticity (Fig. 2a,c) and VSM and dilatometry (first derivative) curves (Fig. 2b,d) help to assign several anelastic effects to different structures or to phase transitions. Values of temperature dependent modulus are given in arbitrary units due to insufficient stiffness of DMA apparatus. Absolute values were determined in as cast state and after 90% transition to  $L1_2$  phase and given in Fig. 2a.

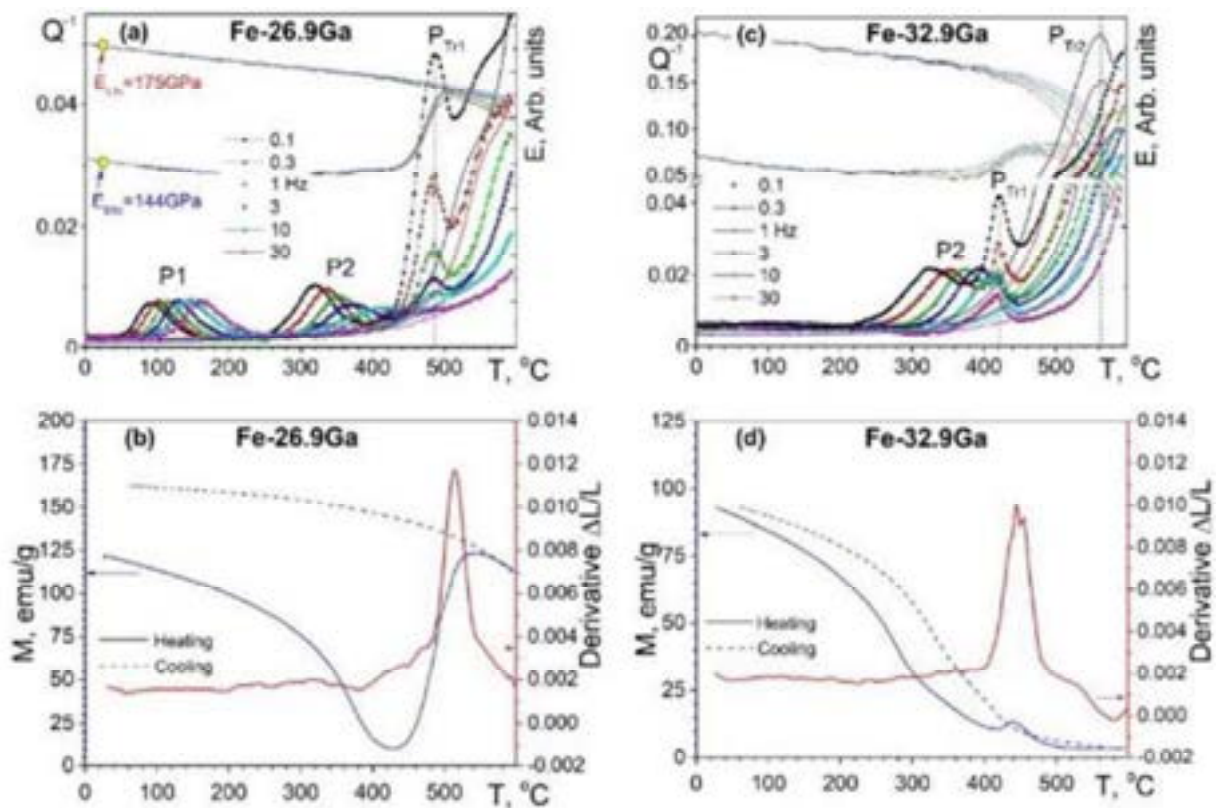


Fig. 2. Temperature dependent internal friction and modulus of elasticity (a, c) and VSM and dilatometry (first derivative) curves (b, d) for Fe-26.9 and 32.9Ga, respectively.

Heating rate 2K/min (DMA), 5K/min (dilatometry) and 6K/min (VSM).

Parameters of two thermally activated (P1 and P2) and two transient ( $P_{Tr1}$ ,

$P_{Tr2}$ ) effects, and the nature of these effects will be discussed in the presentation.

The work is supported by RFBR project № 18-58-52007 and by Russian Science Foundation project 19-72-20080.

References:

- [1] I.S. Golovin, A.M. Balagurov, I.A. Bobrikov et al. *Intermetallics*. 114 (2019) 106610. doi:10.1016/j.intermet.2019.106610.
- [2] I.S. Golovin, A.M. Balagurov, A. Emdadi et al. *Intermetallics*. 100 (2018) 20–26. doi:10.1016/j.intermet.2018.05.016.
- [3] V. V. Palacheva, A. Emdadi, F. Emeis et al. *Acta Mater.* 130 (2017) 229–239. doi:10.1016/j.actamat.2017.03.049.
- [4] I.S. Golovin, A.K. Mohamed, V.V. Palacheva et al. *J. Alloys Compd.* 811 (2019) 152030. doi:10.1016/j.jallcom.2019.152030.

**References:**

- [1] N. Srisukhumbowornchai, S. Guruswamy, Large magnetostriction in directionally solidified FeGa and FeGaAl alloys, *J. Appl. Phys.*, 90 (11) (2001), 5680-5688.
- [2] O. Ikeda, R. Kainuma, I. Ohnuma, K. Fukamichi, K. Ishida, Phase equilibria and stability of ordered bcc phases in the Fe-rich portion of the Fe-Ga system, *J. Alloys Compd.*, 347 (1) (2002), 198-205.
- [3] A.E. Clark, M. Wun-Fogle, J.B. Restorff, K.W. Dennis, T.A. Lograsso, R.W. McCallum, Temperature dependence of the magnetic anisotropy and magnetostriction of  $Fe_{100-x}Ga_x$  ( $x= 8.6, 16.6, 28.5$ ), *J. Appl. Phys.*, 97 (10) (2005)10M316.
- [4] I.S. Golovin, V.V Palacheva, A.K. Mohamed, A.M. Balagurov, Structure and Properties of Fe–Ga Alloys as Promising Materials for Electronics, *Physics of Metals and Metallography*, 2020, Vol. 121, No. 9, pp. 851–893.

# Effect of phase composition on the internal friction and magnetostriction in the L<sub>12</sub>/D<sub>03</sub> biphase Fe-27Ga alloys

L. Li<sup>1,2</sup>, Y.X. Gao<sup>\*1</sup>, M. Sun<sup>1</sup>, K. Jing<sup>1,2</sup>, Z. Zhuang<sup>\*1</sup>, X.P. Wang<sup>1</sup>, W.B. Jiang<sup>1</sup>, Q.F. Fang<sup>1</sup>

<sup>1</sup> Key Laboratory of Materials Physics, Institute of Solid State Physics,  
Chinese Academy of Sciences, Hefei 230031, China

<sup>2</sup> University of Science and Technology of China, Hefei 230026, China

\*E-mail address: [yxgao@issp.ac.cn](mailto:yxgao@issp.ac.cn)

Fe-Ga alloys exhibit unique functional properties such as magnetostriction and high damping that can be adjusted by the phase transitions (D<sub>03</sub> to L<sub>12</sub>) through a proper compositions and heat treatments. In our work, the effect of phase composition on the internal friction (IF) and magnetostriction in Fe-27Ga alloys were systematically investigated. It was found that proportion of L<sub>12</sub> phase in the biphase (L<sub>12</sub>/D<sub>03</sub>) Fe-27Ga alloys can be controlled by adjusting the annealing temperature and holding time. Two temperature-dependent IF peaks, i.e., a Snoek-type relaxation peak ( $P_1$ ) associated with the stress-induced jump of interstitial C atoms in the BCC-structured D<sub>03</sub> phase and a Zener-type relaxation peak ( $P_2$ ) associated with stress-induced jump of Ga-pairs in the D<sub>03</sub> phase were observed. The height of both peaks decreases gradually with the increasing content of L<sub>12</sub> phase. The absolute value of magnetostriction at an applied magnetic field higher than 2000 Oe and the amplitude-dependent IF at a strain amplitude up to 10<sup>-3</sup> decreases at first and then increases with the increasing content of L<sub>12</sub> phase. With the increasing strain amplitude, magneto-mechanical damping of D<sub>03</sub> phase increases at first and then decreases, while that of the L<sub>12</sub> phase increases monotonously. This indicates that the magnetic domain walls of D<sub>03</sub> phase can move easily under a low stress, while those of L<sub>12</sub> phase can be driven only when the stress is high enough. Such researches could provide a design concept for high damping Fe-Ga alloys to meet the requirements in different application fields such as micro-vibration field, strong vibration field, magnetic or non-magnetic field.

# **Metallic alloys**

## Mechanical spectroscopy of Al-based alloys with L<sub>12</sub> precipitates

A.V. Mikhaylovskaya\*, A.V. Pozdniakov,  
A.G. Mochugovskiy, R.Yu. Barkov, I.S. Golovin

NUST "MISiS", 119049 Russian Federation, Moscow, Leninskiy ave. 4,  
e-mail: mihaylovskaya@misis.ru

Small additions of transition/rare-earth metals (TM/REM) increase strength properties of Al-based alloys due to precipitation hardening and recrystallization resistance. TM/REMs form the supersaturated Al-based solid solution during solidification and L<sub>12</sub>-type nanoprecipitates after subsequent heat treatment. Chemical composition of the alloys and heat treatment influence significantly on the precipitation mechanism and the dispersoids parameters. A high number density of nanoscale precipitates is required to provide a strong Zener pinning force and a high recrystallization resistance. Present study is focused on the L<sub>12</sub>-phase precipitation and recrystallization kinetics analysis using mechanical spectroscopy.

The temperature dependent and amplitude dependence internal friction (TDIF and ADIF) were studied by means a DMA Q800 TA Instruments. Optical, scanning, transmission electron microscopy techniques and X-ray diffractometry were performed to analyse the microstructure of the alloys studied.

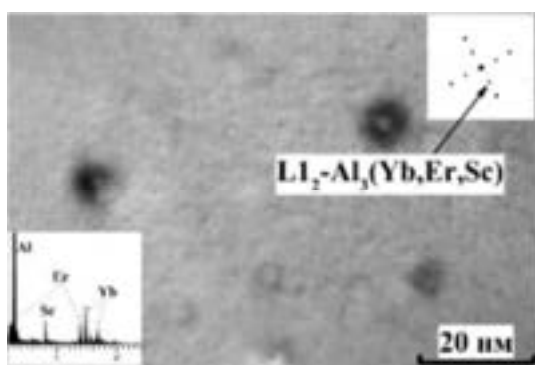


Fig. 1. TEM images of the AlErYbSc alloy after annealing at 300 °C for 3 h (SAED pattern in [011] zone axis and EDS spectra from nanoscale precipitate)

The aluminum-based solid solution (in short, (Al)) and Al<sub>3</sub>(Er, Yb) eutectic particles with size of 50-200 nm are detected in as-cast structure of the alloys. Sc and Zr are completely dissolved in (Al). The hardening is observed during annealing at 300-420 °C due to the precipitation of the coherent L<sub>12</sub> nanoprecipitates with a size range of 4-8 nm (Fig. 1). The one-step annealing of as-cast alloy provides discontinuous and continuous precipitation of the L<sub>12</sub>-phase. The two-steps annealing lead to the formation of a high density of continuously formed precipitates.

The HV(T<sub>ann</sub>) curves for cold-rolled samples demonstrate the hardening effect in the range of 100-350 °C and softening at higher annealing temperatures. The softening is the result of recrystallization and related phenomena. The recrystallized grain structure and IF “pseudo” peak (P<sub>R</sub>) were recorded at about 370°C at TDIF curves for the alloys with low fraction of L<sub>12</sub> phase (Fig. 2a,b). The P<sub>R</sub> peaks temperature coincides with an intense hardness decrease. If the grain structure is non-recrystallized, the P<sub>R</sub> peak was not recorded for the samples (Fig. 2c,d). The samples with a high density of precipitates have structure with a high fraction of low-angle grain boundaries up to temperature of 450-500°C.

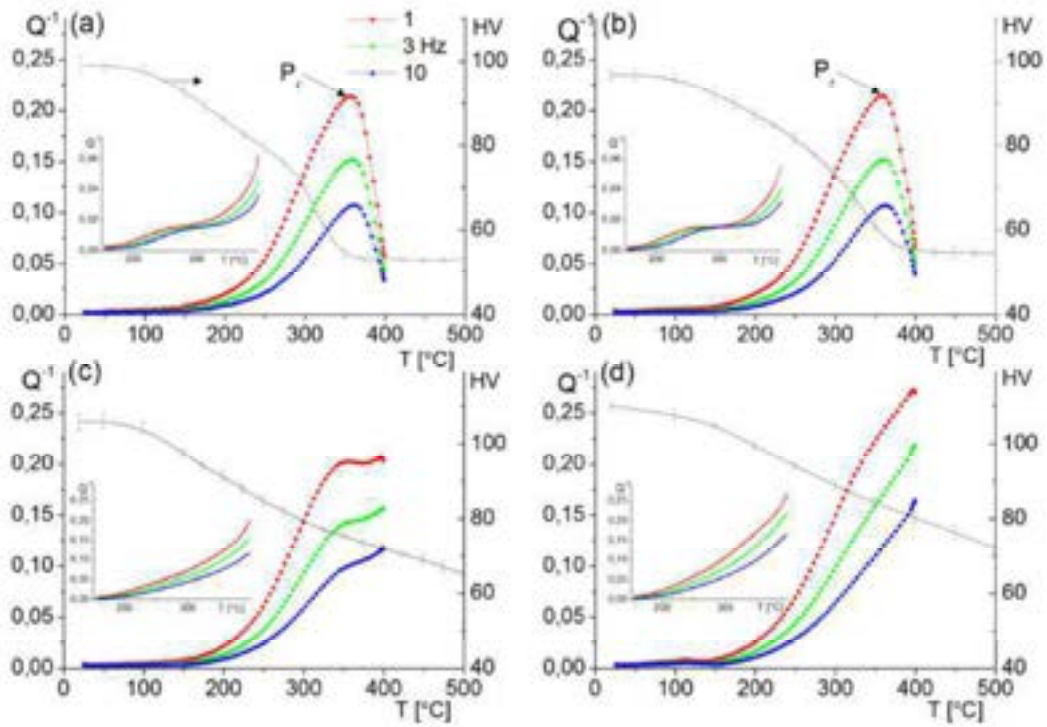


Fig. 2. TDIF curves at heating and cooling (inserts) and hardness curves as a function of temperature of 30 min annealing for cold rolled samples of Al-Mg-Zr alloy pre-annealed at 360 °C (a), 420 °C (b), and in two steps at 360 °C +420 °C (c,d)

The values of IF background activation energy  $H=0.74\text{--}0.80$  eV and characteristic relaxation time  $\tau_0=1.9\times 10^{-10}\text{--}3.1\times 10^{-11}$  s are typical for dislocation relaxation in the deformed and recovered states. In the recrystallized state, IF background is mainly controlled by the vacancies.

The ADIF curves for as rolled, 1h annealed at 300 °C (peak of HV) and 1h annealed at 550 °C (recrystallized state) samples are different. In the alloy with a small fraction of precipitates, IF background significantly decreased after annealing, while, in the alloy with a high number density of precipitates the IF decreased insignificantly. The increase in the hardness, observed at annealing of as-rolled sample as well as a weak IF background decrease, is accompanied with additional precipitation of the  $L1_2$ -dispersoids. Their formation is stimulated by a high concentration of the lattice defects accumulated during rolling. The two-step homogenization and low temperature thermomechanical treatment provide a high density of the  $L1_2$  precipitates and increase the recrystallization resistance. As a result, the strength properties are significantly increased.

This study demonstrates that the mechanical spectroscopy is an effective tool to investigate and characterize recrystallization kinetics and to identify the optimal regimes to achieve required microstructure and advanced properties.

*The study of Al-Er-Yb-Sc alloys was supported by Russian Foundation for Basic Research Grant # 20-33-70170, and Al-Mg-Zr alloy by Russian Science Foundation Grant # 17-79-20426.*

## Mechanical spectroscopy study of as-cast and additive manufactured AlSi10Mg

M. Cabibbo<sup>1</sup>, R. Montanari<sup>2,\*</sup>, A.Pola<sup>3</sup>, M.Tocci<sup>3</sup>, A.Varone<sup>2</sup>

<sup>1</sup>*Dipartimento di Ingegneria Industriale e Scienze Matematiche (DIISM), Università Politecnica delle Marche, Via Brecce Bianche 12, 60131 - Ancona, Italy*

<sup>2</sup>*Dipartimento di Ingegneria Industriale, Università di Roma "Tor Vergata", Via del Politecnico 1, 00133- Roma, Italy*

<sup>3</sup>*Dipartimento di Ingegneria Industriale, Università di Roma "Tor Vergata", Via del Politecnico 1, 00133- Roma, Italy*

\*roberto.montanari@uniroma2.it

The AlSi10Mg alloy produced by casting (AC) and additive manufacturing (AM) technology of laser powder bed fusion (L-PBF) has been investigated through mechanical spectroscopy. In addition to the grain boundary peak  $P_{GB}$  the  $Q^{-1}$  curves of both materials exhibit two other relaxation peaks,  $P1$  ( $H = 0.8 \pm 0.05$  eV;  $\tau_0 = 10^{-11 \pm 1}$  s) and  $P2$  ( $H = 1.0 \pm 0.05$  eV;  $\tau_0 = 10^{-13 \pm 1}$  s), depending on the interaction of dislocations with solute elements (Si and Mg). Relaxation strengths of  $P1$ ,  $P2$  and  $P_{GB}$  of AM alloy are greater than those of the AC one owing to the finer structure of Al cells and the higher amount of Si and Mg in supersaturated solid solution induced by the rapid solidification typical of the L-PBF process. After successive MS test runs relaxation strengths of  $P1$  and  $P2$  peaks in both the examined materials decrease due to the precipitation of Si atoms and dislocation density recovery. Such decrease is more pronounced in AM alloy where change of cell shape and increase of cell size is observed. Dynamic modulus of AM alloy exhibits an anomalous trend in the first test run that is no more present in successive runs. The irreversible process giving rise to such anomalous behavior is the closure of pores of nanometric size.

# Kinetics of diffusionless isothermal and athermal omega transformations in Ti alloys

M. Tane<sup>1\*</sup>, N.L. Okamoto<sup>2</sup>, K. Inoue<sup>2</sup>, M. Luckabauer<sup>2</sup>, Y. Nagai<sup>2</sup>  
T. Sekino<sup>1</sup>, T. Nakano<sup>3</sup>, T. Ichitsubo<sup>2</sup>

<sup>1</sup> Graduate School of Engineering, Osaka Metropolitan University, Osaka, Japan

<sup>2</sup> Institute for Materials Research, Tohoku University, Sendai, Japan

<sup>3</sup> Division of Materials and Manufacturing Science, Graduate School of Engineering, Osaka University, Suita, Japan

\*mtane@omu.ac.jp

In titanium alloys that are indispensable for structural and biomedical materials, the control of  $\omega$ (hexagonal)-phase transformation from body-centered cubic  $\beta$  phase has attracted much attention, because it can be utilized for the formation of various unique nanostructures. Conventionally, the  $\omega$ -phase transformation has been categorized either as a diffusion-mediated isothermal transformation or an athermal transformation that occurs spontaneously via a diffusionless mechanism. However, we recently found a new type of diffusionless  $\omega$  transformation that isothermally occurs during aging near room temperature [1]. Notably, the diffusionless isothermal  $\omega$  transformation occurs in locally unstable  $\beta$  regions having fewer  $\beta$ -stabilizing elements, formed by quenched-in compositional fluctuations.

To clarify the difference in kinetics between the diffusionless isothermal and athermal  $\omega$  transformations, we measured the change in internal friction during room-temperature aging and the temperature dependence of internal friction at low temperature in Ti-V alloys. The internal-friction measurements revealed that the  $\{111\}_\beta$  plane pairs dynamically collapse in locally unstable  $\beta$  regions formed by the quenched-in compositional fluctuations, as shown in Fig. 1. The analysis using the Debye relaxation model revealed that the activation energy of the dynamic  $\{111\}_\beta$  collapse is  $\sim 0.05$ - $0.30$  eV, and this activation process

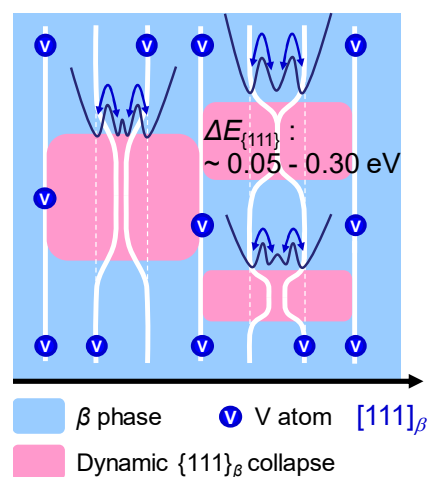


Fig. 1. Schematic illustration showing dynamic  $\{111\}_\beta$  collapse, which is an elementary process of diffusionless isothermal and athermal  $\omega$  transformations in a Ti-V alloy [1].

dominates the transformation rates of both the diffusionless isothermal and athermal  $\omega$  transformations, in addition to the nucleation process of  $\omega$  phase. In the diffusionless isothermal transformation, the  $\omega$ -phase nucleation requires relatively high activation energy owing to the coherent  $\beta/\omega$  interface, because it occurs locally unstable  $\beta$  regions, surrounded by stable  $\beta$  regions. Thus, the transformation occurs at slower rates than the athermal transformation, which occurs in widely-

spread unstable  $\beta$  regions.

[1] M. Tane, H. Nishiyama, A. Umeda, N.L. Okamoto, K. Inoue, M. Luckabauer, Y. Nagai, T. Sekino, T. Nakano, T. Ichitsubo, *Phys. Rev. Materials*, **3** (2019) 043604.

# INFLUENCE OF Nb ON THE Ti DIFFUSION IN $\gamma$ -TiAl INTERMETALLICS STUDIED BY MECHANICAL SPECTROSCOPY

M.L. Nó<sup>1\*</sup>, J. Ibáñez<sup>2</sup>, M. Oehring<sup>3</sup>, J. M. San Juan<sup>2</sup>

<sup>1</sup> *Dpt. of Applied Physics II, Faculty of Science and Technology, University of the Basque Country, UPV/EHU, Apdo. 644, 48080-Bilbao, Spain.*

<sup>2</sup> *Dpt. Physics of Condensed Matter, Faculty of Science and Technology, University of the Basque Country, UPV/EHU, Apdo. 644, 48080-Bilbao, Spain.*

<sup>3</sup> *Helmholtz-Zentrum Geesthacht, Institute of Materials Research, Max-Planck-Str. 1, 21502 Geesthacht, Germany.*

\*e-mail maria.no@ehu.es

In the last decades there has been a growing interest in developing new intermetallic families, which would be able to improve the specific performances provided by superalloys at high temperature, and the  $\gamma$ -TiAl alloys were developed to fulfill the required performances. In particular, the creep resistance should be improved and consequently the study of the diffusion mechanisms and the associated relaxation processes becomes very useful to get a deep understanding of the physics involved during creep. Mechanical spectroscopy was used to study these diffusion mechanisms and previous works on several  $\gamma$ -TiAl alloys showed a relaxation peak P( $\alpha_2$ ) associated to the diffusion of Ti in the  $\alpha_2$  phase [1,2], as well as an internal friction background at high temperature, which is associated to the creep behavior [3]. Thus, in order to optimize the mechanical behavior at high temperature, the diffusion processes of the different atomic species and its mutual interaction, must be understood. In particular, we focused our attention on Nb, which is a common alloying element in many  $\gamma$ -TiAl alloys. Then, the aim of the present work is to do a quantitative analysis of the influence of Nb, on the diffusion of Ti in the  $\alpha_2$  phase.

Three different  $\gamma$ -TiAl alloys with a variable amount of Nb, between 5 and 9 at.%, were studied by mechanical spectroscopy up to 1300 K and at different frequencies between 2 Hz and  $10^{-3}$  Hz. The internal friction spectra were measured in a low frequency mechanical spectrometer [4] under high vacuum,  $2 \cdot 10^{-5}$  mbar, to avoid oxidation. In the frame of the present research work, previous data from the literature of internal friction on  $\gamma$ -TiAl samples, with 4 at.% Nb [1] and without Nb [2], were also considered. In all cases, the concentration of Nb in the  $\alpha_2$  phase was precisely measured in a Field-Emission-Gun (FEG) Scanning Electron Microscope equipped with microanalysis, or in a Transmission Electron Microscope FEI-TITAN Cube 300 kV equipped with the four detectors X-ray microanalysis system.

The series of spectra measured in the  $\gamma$ -TiAl alloy with 5 at.% of Nb is shown, as an example, in Figure 1. To precisely measure the activation energy of the peak  $P(\alpha_2)$ , appearing in all the different alloys, the high temperature background (HTB) was subtracted following the method previously described [2], in order to isolate the relaxation peak, and then the activation parameters were determined by conventional methods. This procedure was performed for all measured samples.

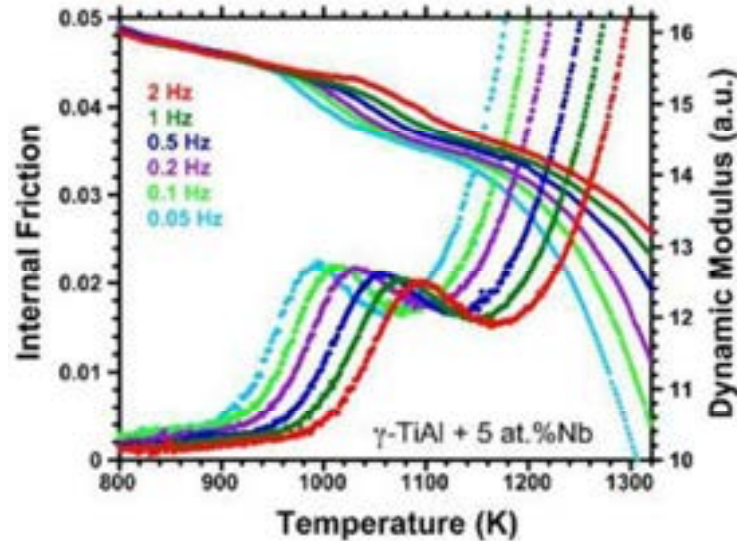


Fig. 1. Internal friction spectra measured on a sample of  $\gamma$ -TiAl with 5 at.% of Nb, where the relaxation peak  $P(\alpha_2)$ , together with its associated modulus variation and the HTB, are shown.

The obtained results show clearly that there is an increase of the activation energy of the peak  $P(\alpha_2)$  when the Nb concentration increases. An atomic model for the  $P(\alpha_2)$  relaxation associated to the diffusion of Ti in presence of Nb, is proposed and discussed at the light of the experimental results. It can be concluded that Nb increases the activation energy for diffusion of Ti and this influence was quantified in the present work.

- [1] J. San Juan, P. Simas, T. Schmoelzer, H. Clemens, S. Mayer, M.L. Nó, *Acta Materialia* **65** (2014) 338-350.
- [2] M. Castillo-Rodriguez, M.L. Nó, J.A. Jimenez, O. Ruano, J. San Juan, *Acta Materialia* **103** (2016) 46-56.
- [3] T. Klein, L. Usategui, B. Rashkova, M.L. Nó, J. San Juan, H. Clemens, S. Mayer, *Acta Materialia* **128** (2017) 440-450.
- [4] P. Simas, J. San Juan, R. Schaller, M.L. Nó, *Key Engineering Materials* **423** (2010) 89-95.

# EFFECT OF ANNEALING ON LOW-TEMPERATURE ACOUSTIC PROPERTIES OF NANOCOMPOSITES Cu-Fe OBTAINED BY BATCH HYDROEXTRUSION TECHNIQUES

P.P. Pal-Val<sup>1\*</sup>, L.N. Pal-Val<sup>1</sup>, V.Yu. Dmitrenko<sup>2</sup>, A.N. Pilipenko<sup>2</sup>, A.P. Rybalko<sup>3</sup>

<sup>1</sup> *B.Verkin Institute for Low-Temperature Physics & Engineering,  
National Academy of Sciences of Ukraine, Kharkov, Ukraine*

<sup>2</sup> *A.Galkin Donetsk Institute for Physics & Engineering,  
National Academy of Sciences of Ukraine, Kiev, Ukraine*

<sup>3</sup> *S. Kuznets Kharkov National University of Economics, Kharkov, Ukraine*

[\\*pppalval@gmail.com](mailto:pppalval@gmail.com)

Copper-based composites are widely used in power engineering, transport, microelectronics, etc. The Cu-Fe composites have high thermal and electrical conductivity, high mechanical properties, wear and corrosion resistance as well as a low cost of iron when compared with other reinforcing materials. In this work, we have studied the low-temperature acoustic properties of Cu-Fe fibrous nanocomposites with a different number of Fe fibers. The samples were fabricated by the batch hydroextrusion method.

The structure of the samples was studied by X-ray diffraction analysis and optical metallography. X-ray diffraction analysis showed that Cu-Fe composites are the two-phase systems with a component ratio close to the calculated ones. The sizes of the coherent scattering regions (CSRs) monotonically decreased down to ~20 nm with decreasing fiber diameters which indicated the formation of the nanocrystalline structures in the samples investigated.

Acoustic measurements were carried out in the temperature range  $2\text{ K} < T < 310\text{ K}$  using the two-component composite vibrator technique [1]. Longitudinal standing waves were excited in samples at oscillation frequencies  $f \sim 50 - 350\text{ kHz}$ . The measurements were made in the amplitude-independent region at the constant strain amplitude  $\varepsilon_0 \approx 10^{-7}$ . Along

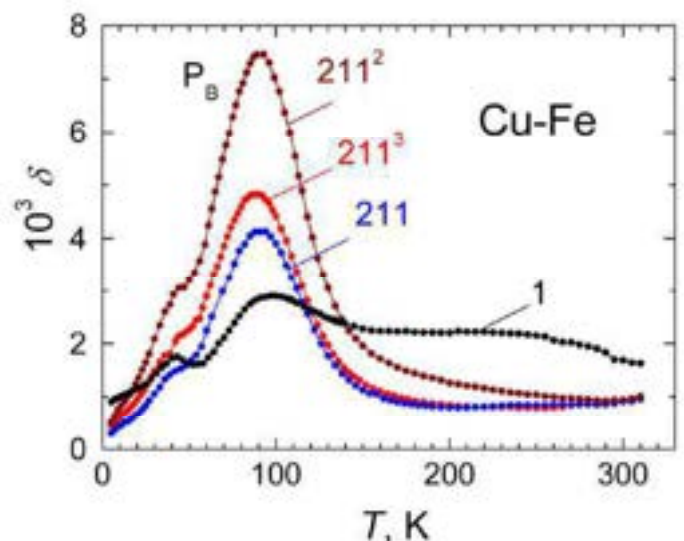


Fig. 1. Peak Bordoni in temperature dependences of the decrement  $\delta(T)$  in Cu-Fe nanocomposites

with the logarithmic decrement, the (figures show the number of Fe fibers). measurements of the dynamic Young's modulus  $E$  were carried out. Fig. 1 shows the temperature dependences of the logarithmic decrement  $\delta$  in the as-prepared samples. The pronounced relaxation peak Bordoni  $P_B$  was revealed near  $T \approx 90$  K at frequencies of  $f \sim 73$  kHz. Activation parameters of the peak are close to those obtained earlier in pure copper subjected to ECAP procedure [2], ultrafine-grained FRTP copper [3,4] and in Cu-Nb nanocomposites [5] both subjected to hydroextrusion and drawing. It was shown that the dynamic relaxation process observed is caused by the thermoactivated motion of dislocations in the first order Peierls' relief of copper.

When annealing the samples at elevated temperature  $T_{ann}$ , the height of the Bordoni peak is reduced starting from  $T_{ann} \sim 200$  °C (Fig. 2a). That is due to a decrease in the dislocation density in the Cu matrix of nanocomposites. Unlike pure Cu samples, this process proceeds most intensively at annealing temperatures of 200–320°C, i.e. at significantly higher temperatures than it was found in unreinforced copper (135°C) [2,4]. Thus, the dislocation structure of a Cu-based nanocomposite is more stable than that of pure ultrafine-grained Cu.

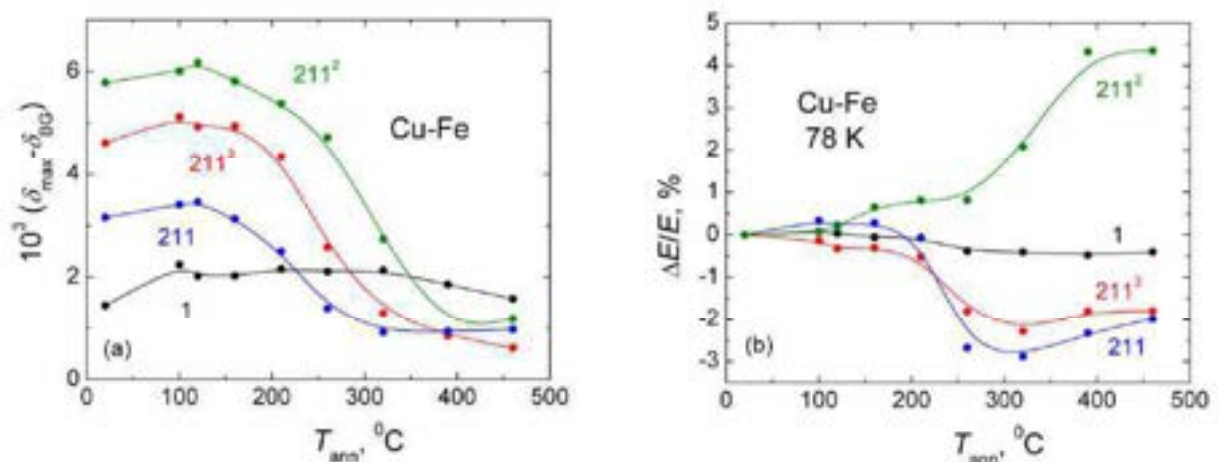


Fig. 2. The effect of annealing on (a) the height of the Bordoni peak and (b) the relative changes of the dynamic Young's modulus at 78 K in composites with different contents of Fe fibers.

In the same interval 200 – 320°C, the noticeable changes in the dynamic Young's modulus were occurred (Fig. 2 b). These changes are apparently caused by transition from the deformation to the annealing textures in the samples [3].

- [1] V.D. Natsik, P.P. Pal-Val, S.N. Smirnov, *Acoust. Phys.*, **44** (1998) 553-560.
- [2] I.S. Golovin, P.P. Pal-Val, L.N. Pal-Val, E.N. Vatazhuk, Y. Estrin. *Solid State Phenom.*, **184** (2012) 289-294.
- [3] P.P. Pal-Val, Yu.N. Loginov, S.L. Demakov, A.G. Illarionov, V.D. Natsik, L.N. Pal-Val, A.A. Davydenko, A.P. Rybalko. *Mater. Sci. & Eng. A* **618** (2014) 9-15.

- [4] P.P. Pal-Val, I.S. Braude, L.N. Pal-Val, V.G. Geidarov. *Visnyk V. Karazin KhNU, Ser. Fizyka*, № 30 (2019) 17-23.
- [5] E.N. Vatazhuk, P.P. Pal-Val, L.N. Pal-Val, V.D. Natsik, M.A. Tikhonovsky, A.A. Kupriyanov. *Low Temp. Phys.* **35** (2009) 417-423.

# Low damping materials

## Comparing amorphous silicon prepared by *e*-beam evaporation and sputtering toward eliminating atomic tunneling states

X. Liu<sup>1\*</sup>, M. R. Abernathy<sup>1</sup>, T. H. Metcalf<sup>1</sup>, B. Jugdersuren<sup>2</sup>, J. C. Culbertson<sup>1</sup>, M. Molina-Ruiz<sup>3</sup>, F. Hellman<sup>3</sup>

<sup>1</sup>*Naval Research Laboratory, Washington, D.C. 20375, USA*

<sup>2</sup>*Jacobs Engineering Group, Hanover, MD 21076, USA*

<sup>3</sup>*Department of Physics, University of California Berkeley, Berkeley, CA 94720, USA*

\*xiao.liu@nrl.navy.mil

Amorphous thin films devoid of atomic tunneling two-level systems (TLS) would untangle a plethora of current challenges in technological areas, such as superconducting quantum bits [1] and the next generation gravitational-wave detectors [2]. It has previously been shown that amorphous silicon (*a*-Si) thin films can be produced free of TLS by *e*-beam evaporation onto substrates at elevated temperatures, and there appears to be a strong correlation between the atomic density of these films and the number density of TLS [3, 4]. We have prepared higher-density films using magnetron sputtering at substrate temperatures from room temperature to elevated temperatures comparable to those used in the *e*-beam studies. We compare the atomic densities measured using Rutherford backscattering, and the shear moduli, the speeds of sound and the densities of TLS calculated using internal friction measurements at cryogenic temperatures of sputtered *a*-Si films to those of the *e*-beam films. Our results show that despite higher atomic densities, sputtered *a*-Si films have lower speeds of sound and higher densities of TLS at elevated substrate temperatures, which we attribute to the different film growth mechanism from that of *e*-beam evaporation. We conclude that a collaborative improvement of both local structural order and network structural connectivity, determined by atomic density and speed of sound, respectively, to approach their crystalline values is required to eliminate atomic tunneling states.

[1] C. Müller, J.H. Cole, J. Lisenfeld, *Rep. Prog. Phys.* **82**, (2019) 124501.

[2] R. Birney, J. Steinlechner, Z. Tornasi, S. MacFoy, D. Vine, A. S. Bell, D. Gibson, J. Hough, S. Rowan, P. Sortais, S. Sproules, S. Tait, I. W. Martin, S. Reid, *Phys. Rev. Lett.*, **121** (2018) 191101.

[3] D.R. Queen, X. Liu, J. Karel, T.H. Metcalf, and F. Hellman, *Phys. Rev. Lett.*, **110** (2013) 135901.

[4] X. Liu, D.R. Queen, T.H. Metcalf, J.E. Karel, F. Hellman, *Phys. Rev. Lett.*, **113** (2014) 025503.

## Internal friction measurements of low energy excitations in amorphous germanium thin films

T. H. Metcalf<sup>1\*</sup>, X. Liu<sup>1</sup>, G. Jernigan<sup>1</sup>, J. C. Culbertson<sup>1</sup>, M. R. Abernathy<sup>2,1,2</sup>,  
M. Molina-Ruiz<sup>3</sup>, F. Hellman<sup>3</sup>,

<sup>1</sup>*US Naval Research Laboratory, Washington DC, USA*

<sup>2</sup>*Present address: Johns Hopkins University Applied Physics Laboratory, Laurel MD, USA*

<sup>3</sup>*Department of Physics, University of California-Berkeley, Berkeley CA, USA*

[\\*tom.metcalf@nrl.navy.mil](mailto:tom.metcalf@nrl.navy.mil) (use [thmetcalf@mac.com](mailto:thmetcalf@mac.com) for .ru domains)

Motivated to create a germanium analog to nearly two-level-tunneling-system (TLS)-free amorphous silicon [1], six germanium films, all about 350nm thick, were deposited by molecular beam epitaxy onto substrates held at temperatures between room temperature and 280°C. The internal friction and speed of sound of the films was measured between 375 mK and 300K. Although the intent was to study amorphous thin films, those grown at 200°C and higher were shown to be at least partially crystalline. The tunneling strength  $C$ , a measure of the interaction between phonons and two-level tunneling systems, decreased monotonically with increasing substrate growth temperature, and for films grown on substrates at temperatures above room temperature,  $C$  was below the glassy range. The lowest value for an amorphous film, for the 160°C -grown film, was  $C=1.9\times 10^{-5}$ . which is one order of magnitude higher than the lowest accomplished in e-beam a-Si. We conclude that the lower crystallization temperature inhibits taking full advantage of an elevated substrate temperature for increased surface mobility in a-Ge to reduce TLS.

[1] X. Liu, D. R. Queen, T. H. Metcalf, J. E. Karel, F. Hellman, Phys. Rev. Lett. **113**, 025503 (2014)

## Stability of samples in coating research: from edge effect to ageing.

Lumaca D.<sup>1,2\*</sup>, Amato A.<sup>3</sup>, Bischi M.<sup>4</sup>, Cagnoli G.<sup>5</sup>, Cesarini E.<sup>2</sup>, Fafone V.<sup>1,2</sup>, Granata M.<sup>6</sup>, Guidi M. G.<sup>4</sup>, Lorenzini M.<sup>1,2</sup>, Martelli F.<sup>4</sup>, Mereni L.<sup>6</sup>, Minenkov Y.<sup>2</sup>, Montani M.<sup>4</sup>, Nardecchia I.<sup>2</sup>, Piergiovanni F.<sup>4</sup>, Placidi E.<sup>7</sup>, Rocchi A.<sup>2</sup>

<sup>1</sup>*Università degli Studi di Roma Tor Vergata, Roma, Italy*

<sup>2</sup>*INFN, Sezione Roma Tor Vergata, Roma, Italy*

<sup>3</sup>*GWFP, Faculty of Science and Engineering - Maastricht University, Maastricht, Netherlands*

<sup>4</sup>*Università degli Studi di Urbino "Carlo Bo", Urbino (PU), Italy*

<sup>5</sup>*Université de Lyon, Université Claude Bernard Lyon 1, CNRS, Institut Lumière Matière, Villeurbanne, France*

<sup>6</sup>*Laboratoire des Matériaux Avancés, IP2I, CNRS, Université de Lyon, Université Claude Bernard Lyon 1, Villeurbanne, France*

<sup>7</sup>*Università di Roma "La Sapienza", Roma, Italy*

\*[diana.lumaca@roma2.infn.it](mailto:diana.lumaca@roma2.infn.it)

Mechanical and optical thermal noises play an important role in many precise opto-mechanical experiments, in which positions of test bodies are monitored by laser beams. Much of the experimental and theoretical research in this area was driven by the physics of gravitational wave interferometers, where thermal fluctuations induced within the mirror's multi-layered dielectric coating are expected to be the dominant source of noise in the frequency band between about 10 and 300 Hz [1].

Coating thermal noise is directly related to structural dissipation inside the material through the loss angle [2]. In view of future upgrades of gravitational wave detectors, increasing the mechanical performances of reflective coatings, by lowering the loss angle ( $\varphi$ ) and retaining their outstanding optical and morphological properties, is fundamental.

The mechanical characterization of substrates and coatings can be performed measuring  $\varphi$  in small disk-shaped samples, on which different coatings materials can be deposited. The  $\varphi$  measurements can be performed through the ring-down method, exciting the resonant mode of the sample and measuring the exponential decrease in the free oscillation amplitude. The sample has to be held by some kind of suspension or clamping, making the coupling between the two negligible: in the Gentle Nodal Suspension (GeNS) system the sample is placed in equilibrium from its centre on top of a sphere, providing a mechanically stable support without affecting the measurements [3].

Coating loss angle can be derived by a differential measurement of the

sample before and after the coating deposition. To perform a precise coating mechanical characterization, the substrate on which it is deposited must be pre-characterized and must be stable with respect to its dissipative behaviour. Many different materials are used as substrate for coating deposition and studies. Among amorphous materials, fused silica ( $\text{SiO}_2$ ) is widely used in coating thermal noise research. Mechanical losses of commercial  $\text{SiO}_2$  substrates even if very low at room temperature, show a frequency dependent behaviour and are subjected to ageing. Despite the annealing treatments reduce the losses, the level of stability obtained over time is not sufficient. These effects compromise the accuracy or even the detectability of the coating loss angle. The source of this deterioration can be related to the ground, unpolished lateral surface according to the edge effect model [4]. The effect of spurious losses can be quantified from the loss angle separation of different classes of mode shapes, since different resonant modes store different amount of elastic energy at the edge. In this work we show that the polishing of the samples edge reduces the amount of spurious losses and ageing effects coming from the absorption of impurities through the edge itself.

A new procedure through  $\text{CO}_2$  laser polishing of the edge surface is proposed, explained and put in place. The results of these procedures, in terms of roughness and losses behaviour will be shown (see Fig. 1). The loss angle measurements are compared with edge losses model and other existing models.

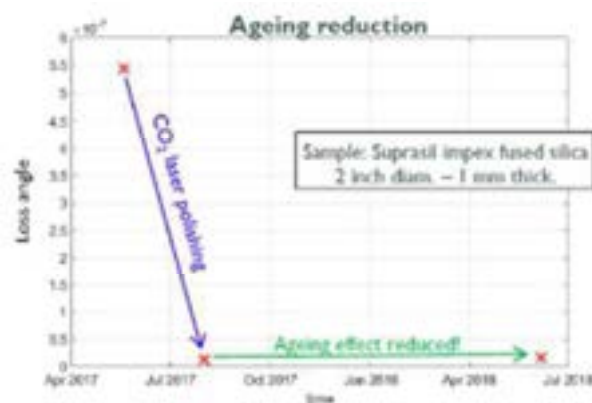


Fig. 1. Reduction of ageing effect of the mechanical loss angle after  $\text{CO}_2$  polishing procedure.

[1] Gregory M Harry *et al* 2002 Thermal noise in interferometric gravitational wave detectors due to dielectric optical coatings *Class. Quantum Grav.* 19 897

[2] Harry G. M., Bodiya T. P. and De Salvo R. 2012 Optical Coatings and Thermal Noise in Precision Measurement Cambridge University Press New York

- [3] Cesarini E., Lorenzini M. et al. 2009 A "gentle" nodal suspension for measurements of the acoustic attenuation in materials *Rev. Sci. Instrum.* 80
- [4] Cagnoli G. et al. 2017 Mode-dependent mechanical losses in disc resonators *Phys. Lett. A* 382

# Domain Walls

## Local properties of domain walls

W. Schranz<sup>1\*</sup>, A. Tröster<sup>1</sup>, I. Rychetsky<sup>2</sup>

<sup>1</sup>University of Vienna, Faculty of Physics, Boltzmannngasse 5, 1090 Wien, Austria

<sup>2</sup>Institute of Physics, Academy of Sciences of the Czech Republic, Na Slovance 2, 18221 Prague 8  
Czech Republic

\*wilfried.schranz@univie.ac.at

The discovery of novel domain wall (DW) properties has stirred up much attention for their potential use in nanoelectronics [1, 2]. In the present talk we discuss the local properties of domain walls of various materials using a recently developed method of combining layer group analysis [3] with order parameter symmetry and Landau-Ginzburg theory [4, 5] and compare the results with some experimentally determined properties of the corresponding materials [6,7] and with results from computer simulations [8].

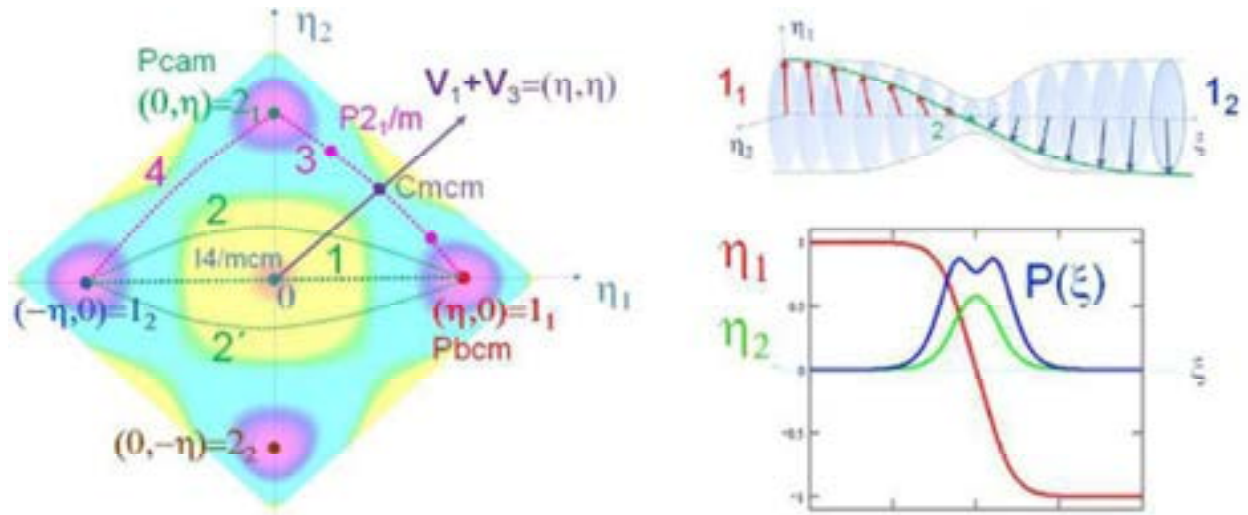


**Fig. 1.** Left: Free energy landscape of a system with a two component order parameter  $(\eta_1, \eta_2)$ . The lines indicate different pathways in OP space, which obey different local symmetries. Right: Spatial variations of the OP components  $\eta_1(\xi)$  and  $\eta_2(\xi)$  and in-plane polarization  $P(\xi)$  for a rotational antiphase boundary  $1_1 \rightarrow 1_2$  (path 2 in the free energy landscape; from [4]).

- [1] G. Nataf, M. Guennou, J. Gregg, D. Meier, J. Hlinka, E. Salje, and J. Kreisel, *Nature Reviews Physics* **2**, 634 (2020).
- [2] P. Sharma, Q. Zhang, D. Sando, C. H. Lei, Y. Liu, J. Li, V. Nagarajan, and J. Seidel, *Science advances* **3**, e1700512 (2017).
- [3] V. Janovec, *Ferroelectrics* **12**, 43 (1976).
- [4] W. Schranz, I. Rychetsky and J. Hlinka, *Phys. Rev. B* **100**, 184105/1-14 (2019).
- [5] W. Schranz, C. Schuster, A. Tröster and I. Rychetsky, *Phys. Rev. B* **102**, 184101/1-12 (2020).
- [6] W. Schranz, A. Tröster and I. Rychetsky, *Journal of Alloys and Compounds* **890**, 161775 (2022).
- [7] I. Rychetsky, W. Schranz and A. Tröster, *Phys. Rev. B* **104**, 224107 (2021).

[8] A. Tröster, C. Verdi, C. Dellago, I. Rychetsky, G. Kresse and W. Schranz, Hard Antiphase Domain Boundaries in Strontium Titanate unravelled using Machine-Learned Force Fields, *submitted to Phys. Rev. Lett.*

## Attenuation of low-frequency sound in the $\text{Na}_{0.875}\text{Li}_{0.125}\text{NbO}_3$ solid solution

S.A. Gridnev<sup>1</sup>, M.A. Belousov<sup>1</sup>, L.A. Reznichenko<sup>2</sup>, L.N. Korotkov\*<sup>1</sup>

<sup>1</sup> *Voronezh State Technical University, 394026, Voronezh, Russia.*

<sup>2</sup> *Southern Federal University, Research Institute of Physics, Rostov-on-Don, Russia  
e-mail: l\_korotkov@mail.ru*

Lead-free piezoelectric materials, due to their environmental friendliness, are currently attracting close attention as an alternative to widely used today the “toxic”  $\text{Pb}(\text{Zr},\text{Ti})\text{O}_3$  type ferroelectric ceramics. Solid solutions based on  $\text{NaNbO}_3$  occupy a leading place among such materials. They are characterized by a large number of structural phase transitions and have a unique combination of physical characteristics, which make these materials interesting for practical use.

The crystal structure and electro-physical properties of  $(\text{Na}_{1-x}\text{Li}_x)\text{NbO}_3$  system are well studied at present in contrast to the elastic and inelastic properties. Therefore, this work was devoted to studying the low frequency sound attenuation in  $\text{Na}_{0.875}\text{Li}_{0.125}\text{NbO}_3$  solid solution.

The results of the studies have shown that solid  $\text{Na}_{0.875}\text{Li}_{0.125}\text{NbO}_3$  solution undergo two structural phase transitions within the temperature range of 300 - 700 K. Along with the ferroelectric phase transition near the temperature  $T_1 \approx 620$  K, another structural phase transition was found near the temperature  $T_2 \approx 559$  K.

The  $Q^{-1}$  maxima observed near of both phase transitions are mainly due to the motion of the interphase boundaries and can be satisfactory described in the framework of the low-frequency fluctuation mechanism of internal friction.

The analysis of obtained data revealed that both low-temperature phases are ferroelectric one, whereas the phase that occurs above the temperature  $T_1$  is paraelectric ones. Both phase transitions at  $T_1$  and  $T_2$  are first-order transitions. The volumes of the critical nucleus at both phase transitions estimated as  $V_0 \approx 10^{-23} \text{ m}^3$ . We revealed that the main contribution to mechanical losses in the ferroelectric region, excluding the temperature regions near structural phase transitions is associated with the domain walls kinetics.

Besides, a noticeable increase in the value of internal friction with the deformation amplitude of the sample was found. The amplitude dependences of  $Q^{-1}(x_m)$  can be satisfactory described within the framework of Friedel dislocation model. The study showed that the parameter  $s$ , which characterizes the dependence of internal friction on the deformation amplitude, depends on temperature in the same way as the shear modulus  $G$ . The abrupt increase in the parameter  $s$  during the transition to the paraelectric phase is presumably associated with a significant increase in the modulus  $G$  above  $T_1$  and redistribution of elastic stresses in the sample because of the disappearance of the domain structure.

# **Ceramics and ferroelectrics**

# Lattice dynamics in niobium doped $\text{PbZrO}_3$ single crystals

D. Kajewski

*Country Institute of Physics, University of Silesia in Katowice,  
75 Pułku Piechoty 1, 41-500 Chorzów, Poland*

\*dariusz.kajewski@us.edu.pl

Lead zirconate  $\text{PbZrO}_3$  has been of interest for dozens of years since its discovery [1]. Antiferroelectric character of the phase below  $T_C$  was not questioned and a relatively small number of papers reported on the properties of this phase. Even mechanism of transition to antiferroelectric order was not so frequently discussed as so called intermediate phase appearing directly below transition at  $T_C$  [2-7]. It was because of role of defects which could not be omitted while seeking an origin of the intermediate phase existence.

Moreover introduction of heterovalent dopant could cause creation or compensation of defects leading to the changes in stability of the crystal lattice. Recently we have proved that small concentration of niobium dopant leads to the existence of new, never observed before, intermediate phase [8] of the unknown crystal structure and properties dependent on the dopant concentration.

Therefore this work will present the acoustic anomalies and precursor dynamics of high-quality niobium doped lead zirconate single crystals investigated by Brillouin light scattering in comparison with Raman light scattering and the birefringence measurements in the wide temperature range above and below Curie Temperature ( $T_C$ ). The acoustic anomalies were correlated with the anomalous birefringence, piezoelectric effect, and the deviation of the Curie-Weiss law.

- [1] G. Shirane, E. Sawaguchi, A. Takeda, *Phys. Rev.*, **80**, (1950) 485.
- [2] V. J. Tennery, *J. Electrochem. Soc.*, **112** (1965) 1117.
- [3] L. Goulpeau, *Sov. Phys. Solid State*, **8** (1967) 1970
- [4] L. Benguigui, *J. Solid State Chem.*, **3** (1971) 381.
- [5] B. A. Scott and G. Burns, *J. Am. Ceram. Soc.*, **55** (1972) 331.
- [6] Z. Ujma and J. Hańderek, *Phys. Stat. Solidi (a)*, **28** (1975) 489.
- [7] J.-H. Ko, M. Górny, A. Majchrowski, K. Roleder, A. Busmann-Holder, *Phys. Rev. B*, **87** (2013) 184110.
- [8] D. Kajewski, Z. Ujma, P. Zajdel, K. Roleder, *Phys. Rev. B*, **93** (2016) 054104.

# Depolarization of ferroelectrics measured by their piezoelectric and elastic response

O. Aktas,<sup>1,\*</sup> Z. W. He,<sup>1</sup> G. Linyu,<sup>1</sup> L.-N. Liu,<sup>2</sup> X.-M. Chen,<sup>2</sup> P. S. da Siva Jr.,<sup>3</sup> L.H. Li,<sup>4</sup> F. Yang,<sup>5</sup> F. Cordero,<sup>6</sup> X. Ding,<sup>1,\*</sup> and E. K.H. Salje<sup>7</sup>

<sup>1</sup>State Key Laboratory for Mechanical Behavior of Materials, Xi'an Jiaotong University, Xi'an 710049, China

<sup>2</sup>School of Physics and information Technology, Shaanxi Normal University, Xi'an 710119, China

<sup>3</sup>Department of Physics, Federal University of São Carlos, 13565-905 São Carlos, São Paulo, Brazil

<sup>4</sup>Sir Robert Hadfield Building, Department of Materials Science & Engineering, Mappin Street, University of Sheffield, Sheffield, S1 3JD, UK

<sup>5</sup>Institute of Fuel Cells, School of Mechanical Engineering, Shanghai Jiao Tong University, Shanghai, 200240, China.

<sup>6</sup>Istituto di Struttura della Materia-CNR (ISM-CNR), Area della Ricerca di Roma-Tor Vergata, Via del Fosso del Cavaliere 100, I-00133 Roma, Italy

<sup>7</sup> Department of Earth Sciences, University of Cambridge, Cambridge CB2 3EQ, UK

\*oktayaktas@xjtu.edu.cn (O. Aktas)

Along with current efforts to replace toxic lead-based materials, the increasing demand for piezo-devices has led to intensive research to find new materials that are environmentally friendly and suitable for future applications [1, 2]. These applications require knowledge about the thermal evolution of the piezoelectric coefficient (usually  $d_{33}$ ) as well as the depolarization temperature ( $T_d$ ), which often determines the upper temperature limit for their operation [1, 2]. However,  $T_d$  of ferroelectrics is often determined by dielectric constant measurements, which provide no information on the thermal evolution of the piezoelectric coefficient. In this talk, Resonant Piezoelectric Spectroscopy (RPS) [3, 4] is demonstrated to be a convenient and complementary method to measure the temperature dependence of the piezoelectric coefficient  $d_{33}$  with reasonable accuracy and determine  $T_d$  through piezoelectric and elastic anomalies with examples on  $\text{BaTiO}_3$  and  $\text{PbSc}_{0.5}\text{Ta}_{0.5}\text{TaO}_3$ . Then, it is applied to lead-free piezoelectric  $\text{Na}_{0.5}\text{Bi}_{0.5+x}\text{TiO}_{3+0.15x}$  ( $x = -0.02, -0.01, 0, 0.01, 0.015$ ) to investigate the role of Bi-nonstoichiometry on the depolarization temperature in  $\text{Na}_{0.5}\text{Bi}_{0.5}\text{TiO}_3$ . The sample with minimal concentration of defects ( $x = 0.01$ ) had a  $T_d$  depressed by  $40^\circ\text{C}$  with respect to other samples. This indicates the role of defects in domain wall pinning in increased  $T_d$ . Results are particularly important for applications of NBT-based materials, which require tuning of  $T_d$  depending on whether probed applications are based on piezoelectricity (below  $T_d$ ) or large strains needed in actuators (above  $T_d$ ).

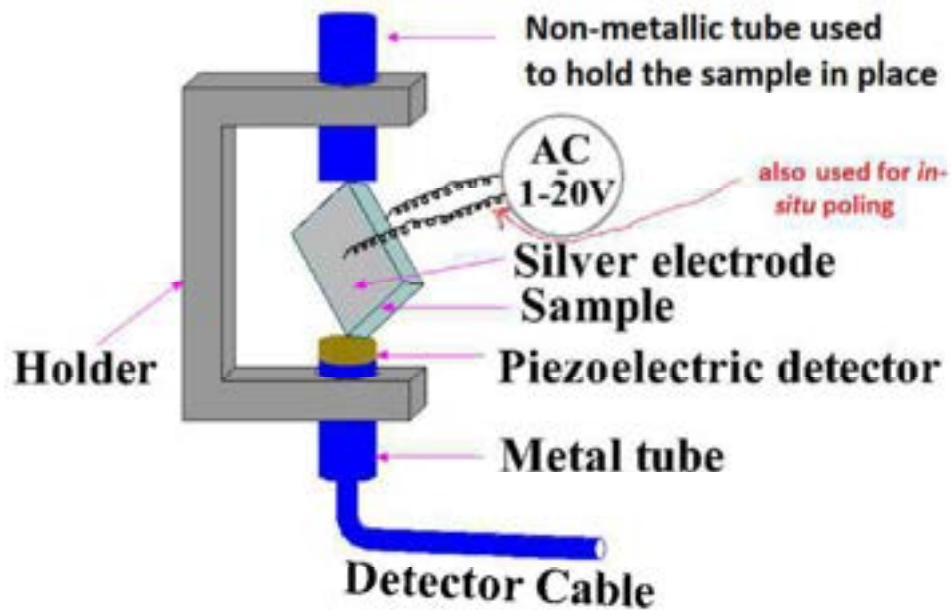


Fig. 1. Schematic of RPS used for investigation of direct and converse piezoelectric effects. An AC voltage applied across the sample through the wires attached to the electrodes on parallel faces of the sample generates mechanical resonances of the sample, which is picked up by the piezoelectric transducer, which acts as the detector. The same wires can be used for in-situ electrical poling of the sample. Alternatively, the AC voltage can be applied across the piezoelectric transducer to generate mechanical resonances. The voltage develops across the sample due to the direct piezoelectric effect of the sample and is collected via the wires attached to the electrodes on opposite faces of the sample. The same arrangement can be used for RUS measurements if a second transducer is attached to the upper tube in contact with the transducer so that elastic resonances can be excited mechanically.

- [1] A. J. Bell, T. P. Comyn, T. J. Stevenson, Expanding the application space for piezoelectric materials, *APL Mater.* 9 (2021) 010901.
- [2] T. Zheng, J. G. Wu, D. Q. Xiao, J. G. Zhu, Recent development in lead-free perovskite piezoelectric bulk materials, *Prog. Mater. Sci.* 98 (2018) 552-624.
- [3] O. Aktas , M. Kangama, G. Linyu, G. Catalan , X. Ding, A. Zunger, E. K. H. Salje, Piezoelectricity in nominally centrosymmetric phases, *Phys. Rev. Res.* 3 (2021) 043221.
- [4] O. Aktas, M. Kangama, G. Linyu, X. Ding, M. A. Carpenter, E. K. H. Salje, Probing the dynamic response of ferroelectric and ferroelastic materials by simultaneous detection of elastic and piezoelectric properties, *J. Alloys and Compounds* 903 (2022) 163857.

## Low-frequency internal friction in ferroelectric $\text{Ba}_{0.8}\text{Sr}_{0.2}\text{TiO}_3$ and $\text{Ba}_{0.8}\text{Sr}_{0.2}\text{TiO}_3 + 0.2$ mass. % La ceramics

S.A. Gridnev, I.I. Popov\*, M.A. Kashirin, A.I. Bocharov  
Voronezh State Technical University, Voronezh, Russia  
\*popovich\_vano@mail.ru

Barium-strontium titanate ceramics is widely studied for many years, with the main attention of researchers directed to the investigation of dielectric properties. However, there are not many works devoted to the investigation of elastic and anelastic properties [1], particularly internal friction, especially at low frequencies [2]. A great advantage of the low-frequency internal friction method is its high sensitivity to structural defects, impurity atoms, and motion of domain walls [3]. Therefore, the aim of this work was to study the phase transformation kinetics, as well as to investigate the effect of an external dc electric field and electronic subsystem on low-frequency internal friction in ferroelectric  $\text{Ba}_{0.8}\text{Sr}_{0.2}\text{TiO}_3$  ceramics.

The effect of the heating rate and the frequency of oscillations on the internal friction peak height near the Curie temperature were studied in ferroelectric  $\text{Ba}_{0.8}\text{Sr}_{0.2}\text{TiO}_3$ . The fluctuation model of low-frequency internal friction [4] is used to explain the obtained dependences and to estimate the nuclei volume of a new phase arising at a phase transition. The estimated value of the nuclei volume  $V \approx 1.77 \cdot 10^{-24} \text{ m}^3$  coincides in order of magnitude with the Känzig region sizes [5]. The applied dc electric field increases the internal friction both in the ferroelectric phase and in the region of the phase transition. It indicates a domains contribution to internal friction. After a dc electric field switched on in the ferroelectric phase, the time decrease of internal friction was observed, which had an exponential form. The addition of 0.2 mass. % La in  $\text{Ba}_{0.8}\text{Sr}_{0.2}\text{TiO}_3$  led both to an increase in the internal friction level in the ferroelectric phase and to a decrease in the internal friction maximum near the Curie temperature. In the first case, this was explained by a decrease in the interaction energy of charged point defects with ferroelectric domain walls [6], and in the second case, by the pinning of domain walls by lanthanum ions.

- [1] F. Cordero, *Ceramics*, **1** (2018) 211-228.
- [2] H. Frayssignes, B.L. Cheng, G. Fantozzi, T.W. Button, *J. Eur. Ceram. Soc.*, **25** (2005) 3203-3206.
- [3] L.B. Magalas, *Mater. Sci. Eng. A*, **521–522** (2009) 405-415.
- [4] S.A. Gridnev, *Ferroelectrics*, **112** (1990) 107-127.
- [5] W. Känzig, *Helv. Phys. Acta.*, **24** (1951) 175-216.
- [6] S.A. Gridnev, B.M. Darinskii, V.N. Netchaev, *Ferroelectrics*, **46** (1983) 5-11.

## Ferroic glass behavior in (Bi,Na)TiO<sub>3</sub> – based lead-free electroceramics

Julio Cesar Camilo Alborno Diaz<sup>1,2</sup>, Michel Venet<sup>1</sup>, Ariano De Giovanni Rodrigues<sup>1</sup>, David Antonio Barbosa Quiroga<sup>1</sup>, Francesco Cordero<sup>3</sup> and Paulo Sergio da Silva Jr<sup>1\*</sup>

<sup>1</sup> *Department of Physics, Federal University of São Carlos, Brazil*

<sup>2</sup> *Center of Science and Technology of Materials, Energy and Nuclear Research Institute, São Paulo, SP, Brazil.*

<sup>3</sup> *CNR-ISM, Istituto di Struttura della Materia, Area della Ricerca di Roma-Tor Vergata, Roma, Italy.*

\*psergio@ufscar.br

Ferroic glass materials, that is, relaxors, spin glasses, and strain glasses attract special attention because of their intriguing physical properties and potential for novel technological applications. The ferroic glass state emerges from a gradual freezing process of the disordered ferroic state, resulting in the so-called ferroic glass transition, which has unique features absent in a typical ferroic transition [1]. For instance, the strain glass behavior of materials can be identified by a peculiar thermal and frequency evolution of the mechanical response around the phase-transition region, measured from their anelastic properties. This mechanical phenomenon has been reported mainly for metallic systems [2,3], and recently, also in a few ceramics systems [4,5].

In the last two decades, Bi<sub>0.5</sub>Na<sub>0.5</sub>TiO<sub>3</sub>-based (BNT) lead-free electroceramics have received considerable attention, particularly the binary xBi<sub>0.5</sub>Na<sub>0.5</sub>TiO<sub>3</sub>-yBaTiO<sub>3</sub> (BNT-BT) solid solutions because of their technological potential [6]. However, the ternary xBi<sub>0.5</sub>Na<sub>0.5</sub>TiO<sub>3</sub>-yBi<sub>0.5</sub>K<sub>0.5</sub>TiO<sub>3</sub>-zBaTiO<sub>3</sub> (BNT-BKT-BT or BNBK) system has been less studied despite its possible technological applications and the interesting phenomenology behind a more complex system. Relaxor characteristics have been also reported for several (Bi,Na)TiO<sub>3</sub>- based ferroelectric compositions [7], however, despite ferroic glass states manifest mainly in disordered systems, the possible presence of these states (relaxor and/or strain glass) in ternary BNBK compositions has not been still investigated.

In this work, several characterization techniques are used to demonstrate the occurrence of simultaneous relaxor and strain glass states in the ternary lead-free BNBK system. Hysteresis and current density loops measurements at different temperatures for a BNBK ceramic showed typical characteristics observed in BNT-based ceramics containing the tetragonal P4bm phase. Above 400 K, slim loops like those of ferroelectric relaxors are observed. For temperatures between 400 and 450 K, a phase transition with simultaneous relaxor and strain glass character is revealed by the dielectric and anelastic characterizations (Fig. 1). The minimum of elastic modulus shifts to higher temperatures as the frequency increases, obeying the Vogel-Fulcher relation, which clearly shows the occurrence of a strain glass state in this material. Similar characteristics are observed in the imaginary part of the dielectric permittivity, which demonstrates the relaxor character of this phase transition.

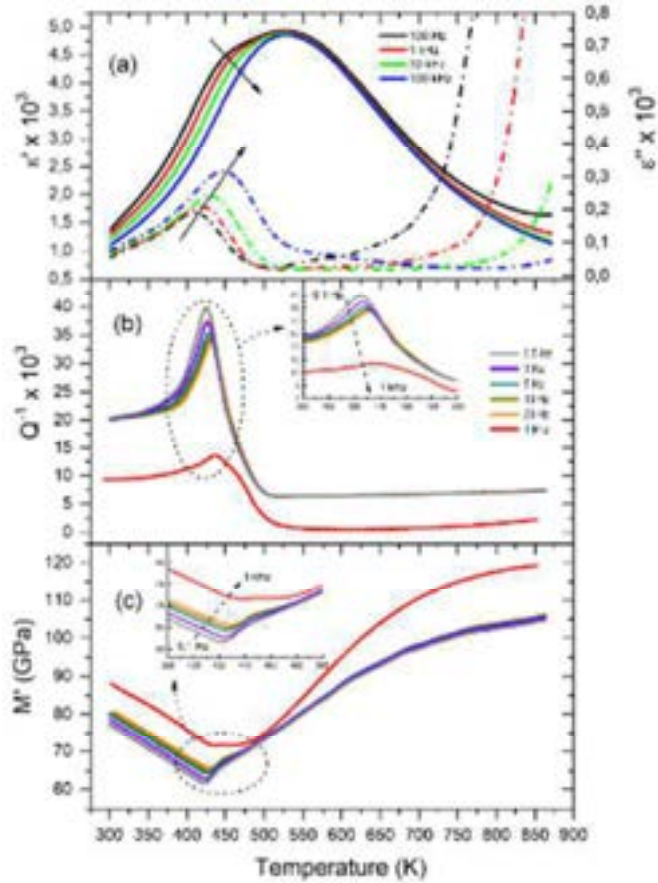


Fig. 1. Temperature dependence of the dielectric and mechanical responses, at different frequencies, for a BNBK82 ceramic. (a) Real  $\epsilon'$  and imaginary  $\epsilon''$  parts of dielectric permittivity, (b) Internal friction  $Q^{-1}$  and (c) Young's modulus  $M'$ .

The origin of this phenomenon was elucidated with the help of structural characterizations, such as Raman spectroscopy and high-resolution synchrotron X-ray diffraction, at different temperatures. Coexistence of the tetragonal  $P4mm$  and  $P4bm$  phases occurs at room temperature with approximate phase fractions of 75 and 25%. As the temperature increases, the  $P4mm$  tetragonal phase begins to transform into cubic  $Pm-3m$  near 330 K until about 450K, where it disappears. From this temperature, the material is composed of  $P4bm$  PNRs embedded in a non-polar cubic matrix, which is the origin of the observed relaxor state. The typical octahedra tilts of the  $P4bm$  PNRs result in spontaneous strain and hence, a tilt strain glass state also arises. Knowing the origin of the phenomenon observed in this BNT-based ternary system, new lead-free ferroic glass materials with improved properties can be designed.

- [1] X. Ren, *Phys. Status Solidi B* **251**, 1982 (2014).
- [2] D. Wang, et al. *Acta Mater.* **58**, 6206 (2010).
- [3] Y. Wang, et al., *Sci. Rep.* **4**, 3995 (2014).
- [4] Y. Ni, et al., *J. Alloys Compd.* **577**, S468 (2013).
- [5] Y. Ji, et al., *Acta Mater.* **168**, 250 (2019).
- [6] J. Rödel, et al., *J. Am. Ceram. Soc.* **92**, 1153 (2009).
- [7] J. Glaum, et al., *Phys. Rev. Mater.* **3**, 54406 (2019).

## Cation reorientation and octahedral tilting in the metal-organic perovskites MAPI and FAPI

F. Cordero<sup>1\*</sup>, F. Trequatrini<sup>2+</sup>, F. Craciun,<sup>1</sup> A.M. Paoletti<sup>3</sup> and G. Zanotti<sup>3</sup>  
<sup>1</sup>*Istituto di Struttura della Materia-CNR (ISM-CNR), Area della Ricerca di Roma - Tor Vergata, Via del Fosso del Cavaliere 100, I-00133 Roma, Italy*  
<sup>2</sup>*Dip. di Fisica, Università di Roma “La Sapienza”, p.le A. Moro 2, I-00185 Roma, Italy*  
<sup>3</sup>*Istituto di Struttura della Materia-CNR (ISM-CNR), Area della Ricerca di Roma 1, Via Salaria, I-00015 Monterotondo Scalo, Roma, Italy*

\*francesco.cordero@ism.cnr.it [+francesco.trequatrini@roma1.infn.it](mailto:francesco.trequatrini@roma1.infn.it)

The metal-organic halide perovskites are the object of great interest since it has been recently found that they have excellent photovoltaic properties, and can therefore be used to create cheap and efficient solar cells, photodetectors and LEDs with a wide range of colors. Much of the research is focused on two issues: the scarce stability of the materials and the mechanisms that allow the photocarriers to have so long lifetimes. These phenomena are closely connected to the structural transformations and to the dynamics of the reorienting organic cations, both of which can be studied by anelastic measurements [1,2].

The anelastic spectra of MAPbI<sub>3</sub> (MAPI, MA = methylammonium = CH<sub>3</sub>NH<sub>3</sub>) and FAPbI<sub>3</sub> (FAPI, FA = formamidinium = CH(NH<sub>2</sub>)<sub>2</sub>) have been measured on samples obtained by pressing the powders and electrostatically excited on their free flexural modes at kHz frequencies. Both perovskites are cubic at and above room temperature ( $\alpha$  phase), with freely rotating FA and MA cations and undergo two tilt transitions of the PbI<sub>6</sub> octahedra into a tetragonal ( $\beta$ ) phase and orthorhombic ( $\gamma$ ) phase, accompanied by losses of the orientational degrees of freedom of the MA and FA. All these phenomena are clearly visible in the anelastic spectra (Fig. 1), together with an additional phase transition (I) in FAPI at low temperature. According to the Landau theory of phase transitions with coupling between the rotation angle of the octahedra  $\phi$  and the ensuing strain  $\varepsilon$  of the form  $\varepsilon\phi^2$ , at a tilt transition with order parameter  $\phi$  the elastic constant associated with  $\varepsilon$  undergoes a steplike softening, as observed at the  $\alpha \rightarrow \beta$  transitions in Fig. 1. The stiffening at the  $\beta \rightarrow \gamma$  transitions is unexpected, but actually observed in few oxide perovskites when entering the *Pnma* phase with  $a^-b^+a^-$  tilts (the rotations of the octahedra about the cubic axes are alternately  $\pm\phi$  along *a* and *c* and in-phase along *b*). It has been suggested that this behaviour is due to a sort of blocking of the tilt degrees of freedom due to the concomitant in-phase and out-of-phase tilts, but this explanation can reasonably account, at most, for a complete loss of the softening associated with

the tilted  $\beta$  phase (up to the horizontal dashed lines in Fig. 1). Instead, FAPI and MAPI restiffen well above the value in the untilted  $\alpha$  phase. At least this excess restiffening, if not

more, has to be attributed to the freezing of the residual rotational degrees of freedom of the FA and MA molecules.

In MAPI the stiffening below  $T_{\beta\gamma}$  is partly due to the modulus defect of an intense thermally activated relaxation, identified with the residual reorientation of the MA major axis with strong antiferroelectric correlations, since their electric dipoles do not cause a concomitant dielectric relaxation [1]. In FAPI, instead, the freezing of the reorientation of the FA major axes must progress together with the order parameter of the transition, since the stiffening, though rather structured, does not show a dependence on frequency of the relaxation type and is accompanied by a drop of  $Q^{-1}$  rather than a peak. This fact points to a coupling between FA orientation and tilt of the surrounding octahedra larger than in MAPI, in agreement with the larger size of FA. As a consequence, the  $\beta/\gamma$  transition in FAPI is not a traditional displacive transition as octahedral tilting normally is, but has a dominant kinetic component due to the FA reorientation. This is evident also from the fact that its temperature and the shape of the elastic anomaly depend on sample and thermal history and may even show an inverted thermal hysteresis.

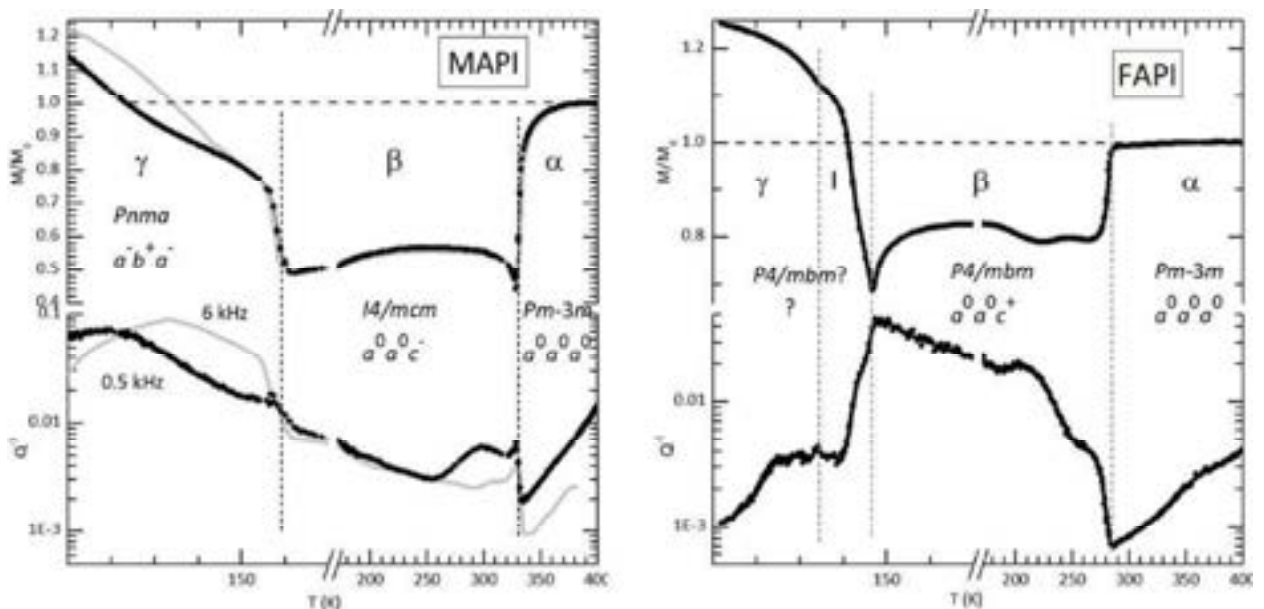


Fig. 1. Anelastic spectra of MAPI and FAPI. The various structural phases are indicated with their conventional names, symmetry groups and octahedral tilt patterns in Glazer's notation.

[1] F. Cordero, F. Craciun, F. Trequattrini, P. Imperatori, A. M.

Paoletti, and G.Pennesi, *J. Phys. Chem. Lett.*, **9** (2018) 4401–4406.  
[2] F. Cordero, F. Craciun, F. Trequattrini, A. Generosi, B. Paci,  
A. M. Paoletti, and G. Pennesi, *J. Phys. Chem. Lett.*, **10** (2019) 2463–2469.

# Point defects

## Interaction between interstitial-substitutional solute atoms and formation of their clusters in bcc iron

NUMAKURA Hiroshi

*Osaka Metropolitan University (formerly Osaka Prefecture University), Sakai, Japan*  
numakura@omu.ac.jp

Influences of substitutional solute atoms on the Snoek relaxation of C and N can be understood as arising from local interaction between the two solute species, i.e., trapping of the mobile interstitial solute atom by the substitutional solute atom [1,2]. Since this interaction is an important factor in the microstructure and properties of steels, it could be useful if one can obtain quantitative information on the atomic interaction from how the relaxation spectrum is affected. This is the aim of our foregoing work on the dilute Fe-Cr-N and Fe-V-N alloys [3,4].

In the first part of this talk we present systematic analyses of the Snoek relaxation of N in the two systems mentioned above. The anisotropy of relaxation has been studied using single crystal specimens of Fe-Cr-N alloys. The results indicate that the favourable configuration is the first neighbour N-Cr pair, which agrees well with our ab initio calculations. With such piece of information the interaction energy evaluated from the effects of the substitutional solute on the Snoek relaxation and the solubility [4] can be consistently understood.

In the second part we discuss formation of interstitial-substitutional solute atoms clusters. When dilute Fe-M-C/N alloys are solution-treated and then subjected to ageing, clusters of the two species of atoms develop in the bcc matrix, as first discovered in surface nitriding of Fe-Ti/V/Cr alloys [5]. They are few-layers-thick precursors of alloy carbides (MC) or nitrides (MN), and are effective in increasing strength, probably without much deteriorating ductility, like the case of G-P zones in age-hardening aluminium alloys. We show latest results on Fe-Cr-N, Fe-Ti-N and Fe-Ti-C alloys studied by measurements of electrical resistivity, microhardness, and the Snoek relaxation.

- [1] H. Numakura, M. Koiwa, M<sup>3</sup>D: Mechanics and Mechanisms of Material Damping, ASTM STP 1304, 1997, pp 383-393.
- [2] M. Koiwa, Philos. Mag. 24 (1971), 107-122.
- [3] X.-S. Guan, Y. Nishizawa, K. Okamura, H. Numakura, M. Koiwa, Mater. Sci. Eng. A 370 (2004), 73-77.
- [4] H. Numakura, Arch. Metall. Mater. 60 (2015), 2061-2068.
- [5] G. Miyamoto, T. Tomio, H. Aota, K. Oh-ishi, K. Hono, T. Furuhashi, Mater. Sci. Tech. 27 (2011), 742-746.

## Stress-induced ordering due to oxygen present in Ti-15Mo alloy

J.R.S. Martins Jr<sup>1</sup>, R.A. Nogueira<sup>2</sup>, R.O. Araújo<sup>3</sup>, C.R. Grandini<sup>2\*</sup>

<sup>1</sup>*IFSP – Câmpus Caraguatatuba, 11.665-071, Caraguatatuba, SP, Brazil*

<sup>2</sup>*UNESP, Laboratório de Anelasticidade e Biomateriais, 17.033-360, Bauru, SP, Brazil*

<sup>2</sup>*IFSP – Câmpus Barretos, 14.781-502, Barretos, SP, Brazil*

\*carlos.r.grandini@unesp.br

Ti and its alloys have a very interesting set of properties such as low density, excellent corrosion resistance, high mechanical strength, and biocompatibility, making it a special material for various chemical, aerospace, sports, and biomedical applications industries [1]. Among Ti alloys, Ti-15Mo (wt%) is very promising for use as a biomaterial because they have excellent corrosion resistance and good mechanical properties such as fatigue, hardness, and wear resistance. These alloys have a predominant body-centered cubic (bcc) crystalline structure and have their mechanical properties strongly changed with the addition of interstitial elements atoms such as oxygen and nitrogen [2]. This study's objective was to analyze the effect of oxygen on the anelastic properties of Ti-15Mo alloy using mechanical spectroscopy measurements.

The used samples are Ti containing 15 wt% of Mo. The sample was produced by arc melting in an argon atmosphere, using Ti (purity of 99.7%) and Mo (purity of 99.5%), both supplied by Aldrich Inc. After melting, the samples were characterized by x-ray diffraction, optical and scanning electron microscopy measurements [3]. The internal friction spectra as a function of temperature were obtained using dynamical mechanical analysis (DMA) measurements, in the temperature range of 300–720 K, with a heating rate of 1.0 K/min and a frequency range of 1–40 Hz. All samples were measured in the tension mode [4].

The internal friction and frequency spectra as a function of temperature for Ti-15Mo alloy, measured with oscillation of 35 Hz in the temperature range of 100 to 700 K, are shown in Fig. 1. It is possible clearly to observe a relaxation structure at 400 K. To analyze the characteristics of this relaxation structure. The samples were measured with another two frequencies, where it was observed that the relaxation structure moves to regions of higher temperature as the oscillation frequency increases, showing the thermally activated characteristic of the relaxation process.

The anelastic spectroscopy measurements showed complex structures, identifying relaxation processes due to stress-induced ordering of oxygen and nitrogen atoms around the elements that compose the alloy. They were associated with the interstitial diffusion of oxygen atoms in a solid solution in the alloy [5]. It was observed relaxation processes due to stress-induced ordering of single oxygen atoms around single molybdenum solute atoms (Mo-O process); stress-induced ordering of single oxygen atoms around single titanium atoms of the metallic matrix (Ti-O process); stress-induced ordering of single nitrogen atoms around single molybdenum solute atoms (Mo-N process) and stress-induced ordering of single nitrogen atoms around single titanium atoms of the metallic

matrix (Ti-N process) [6].

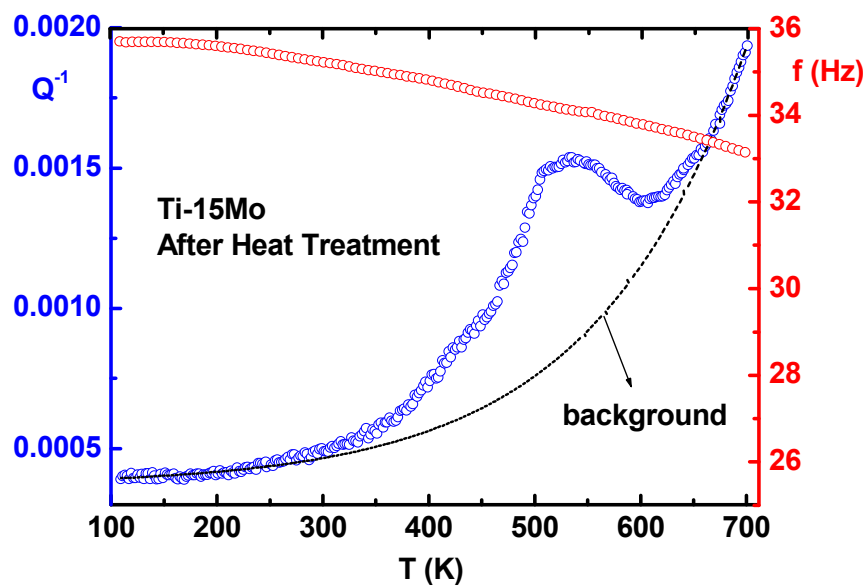


Fig. 1. Internal friction as a function of temperature for Ti-15Mo alloy measured around 35 Hz.

The authors would like to thank Brazilian Agencies Capes, CNPq, and FAPESP for their financial support.

- [1] S.S. Sidhu, H. Singh, M.A.-H. Gepreel, *Mat. Sci. Eng. C* **121** (2021) 111661.
- [2] X. Min, P. Bai, S. Emura, X. Ji, C. Cheng, B. Jiang, K. Tsuchiya, *Mat. Sci. Eng A* **684** (2017) 534.
- [3] J.R.S. Martins Jr., R.O. Araújo, T.A.G. Donato, V. Arana-Chavez, M.A.R. Buzalaf, C.R. Grandini, *Materials* **7** (2014) 232.
- [4] ASTM E1876–01, ASTM International, Philadelphia (USA), 2002.
- [5] M.R. Silva, R.O. Araújo, G.P.S. Suarez, C.R. Grandini, *Oxidation of Metals* **97** (2022) 183.
- [6] J.R.S. Martins Jr, R.O. Araújo, R.A. Nogueira, C.R. Grandini, *Arch. Metall. Mat.* **61** (2016) 25.

# Hopping and clustering of oxygen vacancies in $\text{BaTiO}_{3-\delta}$ and the influence of the off-centred Ti atoms

F. Cordero,<sup>1\*</sup> F. Trequattrini,<sup>2+</sup> D. A. B. Quiroga,<sup>3</sup> and P. S. Silva, Jr.<sup>3</sup>

<sup>1</sup>*Istituto di Struttura della Materia-CNR (ISM-CNR), Area della Ricerca di Roma - Tor Vergata, Via del Fosso del Cavaliere 100, I-00133 Roma, Italy*

<sup>2</sup>*Dip. di Fisica, Sapienza Università di Roma, p.le A. Moro 2, I-00185 Roma, Italy*

<sup>3</sup>*Department of Physics, Federal University of São Carlos, 13565-905 São Carlos (SP), Brazil*

\*francesco.cordero@ism.cnr.it +francesco.trequattrini@roma1.infn.it

The diffusion and aggregation of oxygen vacancies ( $V_O$ ) in perovskites are still poorly understood, even though they are involved in a wide range of applications and phenomena, from solid state electrolytes for fuel cells to ferroelectric fatigue. The only case where a satisfactory picture has been obtained is cubic  $\text{SrTiO}_{3-\delta}$ , through fitting of the anelastic spectra at several O deficiencies [1]. In this manner it has been shown that the activation energy of 1 eV, commonly identified with the barrier for  $V_O$  diffusion, is actually associated with pairs and larger complexes of  $V_O$ , which are stable also for  $\delta < 0.01$  and above 600 K, while the barrier for the hopping of isolated  $V_O$  is only 0.6 eV. Similar clean results cannot be obtained in highly doped perovskites, as ionic conductors are, or in the presence of structural phase transitions, including the ferroelectric (FE) ones, because the anelastic spectra become very complicated and/or dominated by domain wall relaxations.

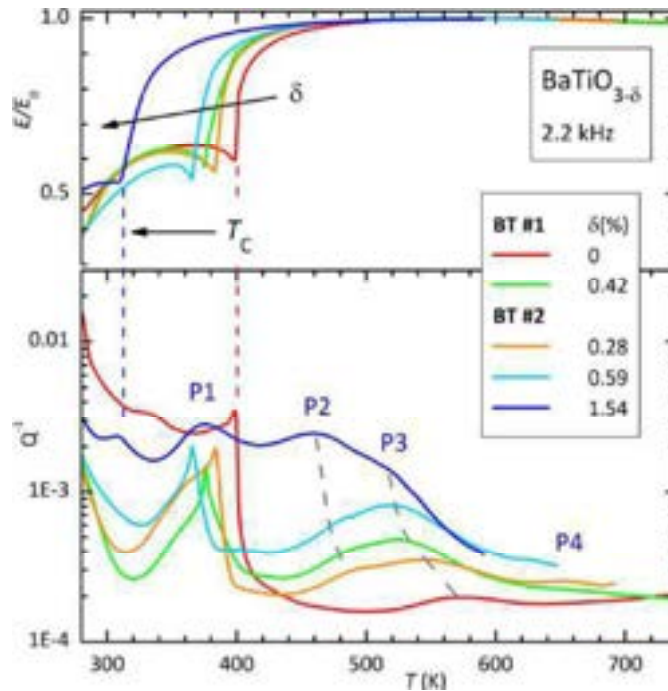


Fig. 1. Anelastic spectra of two samples of  $\text{BaTiO}_{3-\delta}$  with  $0 \leq \delta \leq 0.016$ .

We present similar experiments in barium titanate [2], where the

ferroelectric transition at  $T_C = 400$  K partially hides the anelastic relaxation processes due to  $V_O$ . The introduction of  $V_O$ , however, depresses  $T_C$ , and it has been possible to lower it enough to reveal all the relaxation processes due to free and clustered  $V_O$ . The resulting anelastic spectra are similar to those of  $\text{SrTiO}_{3-\delta}$  but there are also important differences. In  $\text{BaTiO}_{3-\delta}$  the anisotropy of the elastic dipole of the isolated  $V_O$  is about three times larger, the anelastic relaxation peaks markedly shift to lower temperature with doping, the activation energy for the diffusion of the isolated  $V_O$  is 0.72 eV, larger than 0.60 eV in  $\text{SrTiO}_3$ , while that for the pair reorientation is smaller, 0.86 eV compared to 0.97 eV. All these observations are explained by taking into account that, unlike in  $\text{SrTiO}_3$ , Ti is dynamically disordered over eight off-centre positions. A strong indication in this sense comes from the temperature dependence of Young's modulus, with anharmonic stiffening perfectly linear in temperature down to 200 K in  $\text{SrTiO}_3$ , but with anomalous softening already below 750 K in  $\text{BaTiO}_3$ .

[1] F. Cordero, *Phys. Rev. B*, **76** (2007) 172106.

[2] F. Cordero, F. Trequattrini, D. A. B. Quiroga and P. S. Silva Jr., *J. Alloys and Compounds* **874** (2022) 159753.

## The role of Ag on the stress-induced ordering of oxygen in the Ti-15Zr-15Mo alloy

J. E. Torrento<sup>1</sup>, D. R. N. Correa<sup>2,\*</sup>, M. R. da Silva<sup>3</sup>, C. R. Grandini<sup>1,4</sup>

<sup>1</sup>UNESP – Univ Estadual Paulista, Laboratório de Anelasticidade e Biomateriais, 17.033-360, Bauru (SP), Brazil

<sup>2</sup>IFSP – Federal Institute of Education, Science and Technology of São Paulo, 18095-410, Sorocaba (SP), Brazil

<sup>3</sup>IFSP – Federal Institute of Education, Science and Technology of São Paulo, 14804-296, Araraquara (SP), Brazil

<sup>4</sup>IBTN/BR – Institute of Biomaterials, Tribocorrosion and Nanomedicine, Brazilian Branch, 17.033-360, Bauru (SP), Brazil

\*diego.correa@ifsp.edu.br

In this study, the effect of substitutional Ag on the stress-induced ordering of oxygen in the Ti-15Zr-15Mo (wt%) alloy was investigated by dynamic mechanical analysis. The Ti-15Zr-15Mo-xAg (x = 0, 1, and 3) samples were produced by argon arc melting, submitted to a posterior homogenization heat treatment, hot rolling, and solution heat treatment. The dynamic mechanical analysis was performed in the tensile mode, at a maximum strain amplitude of 0.02%, between 425 and 725 K, at 1 K/min, and frequencies from 10 up to 30 Hz. The results showed a broadened and asymmetric anelastic relaxation peak around 450 and 725 K in all samples, with step decay in Young's modulus typical of stress-induced ordering phenomena. The peaks shifted towards high temperature with the increase of the frequency, indicating a thermally activated process. The peak fitting stated the presence of oxygen-type processes, produced by the interaction of matrix (Ti-O) and substitutional (Zr-O) elements, and one clustering (Ti-O-O). The amount of Ag exhibited a significant effect on the  $Q_p^{-1}$  and  $T_p$  relationship (Fig. 1) and in the diffusional parameters  $D_0$  and  $\tau_0$  of the metallic matrix, which could be related to the changes in the bcc crystalline structure's atomic bonding. Thus, the results show that the interaction of interstitial oxygen in the Ti-15Zr-15Mo alloy can be tunable by the addition of Ag, which could bring novel insights about industrial applications beyond the biomedical area [1].

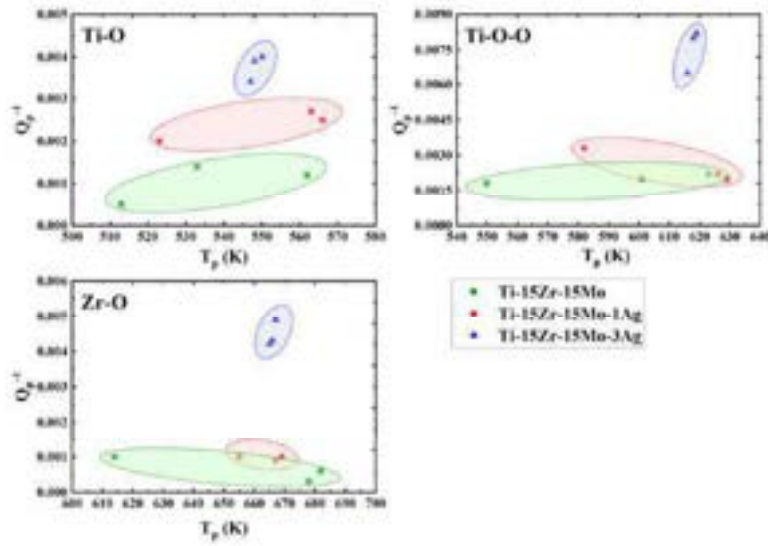


Fig. 1.  $Q_p^{-1}$  and  $T_p$  relationship of the peaks as a function of the Ag quantity.

[1] J.E. Torrento, D.R.N. Correa, M.R. da Silva, C.R. Grandini, *Journal of Alloys and Compounds*, (2021) 159641. (In Press).

# Thermo-kinetic modelling of the giant Snoek effect in carbon-supersaturated iron

P. Maugis<sup>1\*</sup>

<sup>1</sup>*Aix-Marseille University, CNRS, IM2NP, France*

\*philippe.maugis@im2np.fr

Snoek relaxation in interstitial bcc solid solutions is the origin of the Snoek peak in frequency-dependent and temperature-dependent internal friction measurements. The internal friction profiles of low-carbon steels show a linear dependence of the peak height with carbon content. However, recent Monte Carlo simulations of frequency-dependent internal friction exhibited a non-linear giant peak height at high carbon contents. To investigate this effect in temperature-dependent internal friction, we developed a thermo-kinetic mean-field theory of the Snoek relaxation phenomenon. By taking into account the collective behavior of the interstitial atoms, our theory predicts:

- 1) A non-linear dependence of the peak height with composition when approaching the order-disorder transition of the alloy;
- 2) A shift in the temperature of the peak;
- 3) A composition-dependent activation enthalpy of the relaxation time.

The theory is exemplified by the case of carbon-supersaturated iron.

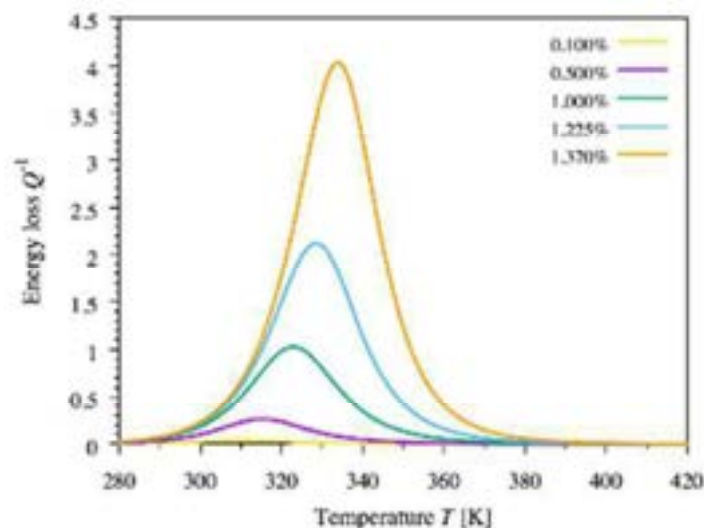


Fig. 1. Snoek relaxation profiles for various carbon contents computed with our linearized model. The oscillation frequency is  $f = 1$  Hz.

- [1] P. Maugis, Giant Snoek peak in ferrite due to carbon-carbon strain interactions, *Materialia* **12** (2020) 100805.
- [2] P. Maugis, Thermo-kinetic modelling of the giant Snoek effect in carbon-supersaturated iron, *J. Alloys Compd.* **877** (2021) 160236.

# Atomistic investigation on the impact of substitutional Al and Si atoms on the carbon kinetics in ferrite

Liangzhao Huang<sup>1\*</sup>, Paul Eyméoud<sup>2</sup>, Philippe Maugis<sup>1</sup>

<sup>1</sup>Aix Marseille Université, CNRS, IM2NP, Marseille, France

<sup>2</sup>Université de Toulon, Aix Marseille Université, CNRS, IM2NP, Toulon, France

\*e-mail address of corresponding author

The pairwise interactions of substitutional solute atom  $X = \text{Al}, \text{Si}$  with interstitial carbon at stable (octahedral) and saddle-point (tetrahedral) positions in body-centered-cubic iron are computed using first principles. These pairwise interactions are used in atomistic kinetic Monte Carlo approach to simulate carbon internal friction and tracer diffusion measurements in Fe-Si, Fe-Al, and Fe-Al-Si ferritic alloys without any adjusting parameters. The good agreement between the simulated and experimental Snoek relaxation profiles validates the pair interaction model for kinetic simulations (cf. Fig. 1). The predicted effect of Al on slowing down carbon diffusion is consistent with previous studies. We highlight a size effect on the Si-carbon interactions obtained from first principles. Using a carefully tested database, it is shown that the introduction of Si into ferrite only decreases the carbon diffusivity below a critical temperature.

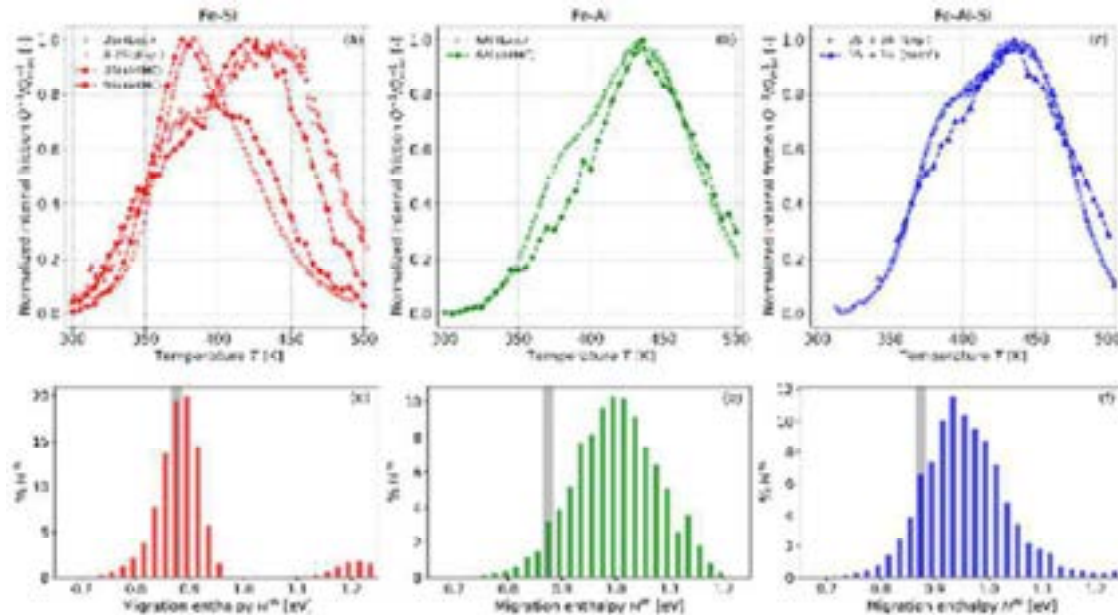


Fig. 1. (a)--(c): Experimental and simulated carbon Snoek relaxation profiles in bcc Fe-Si, Fe-Al and Fe-Al-Si alloys. The alloy compositions are expressed in at.%. The experimental profiles are reproduced from the results of Sinning et al. [1], in which all the samples were water-quenched from 1000K. The experimental excitation frequency of Fe-6.7Si system is 320–410Hz, and the one of Fe-6Al and Fe-3Al-3Si is about 600Hz. The excitation frequency of AKMC simulation is set to 400Hz for Fe-6Si, and 600Hz for Fe-6Al and Fe-3Al-3Si. (d)--(f): Distribution of carbon migration enthalpy  $H^m$  in Fe-6Si, Fe-6Al and Fe-3Al-3Si alloys measured

by AKMC simulation at 400K. The shaded area indicates the carbon migration enthalpy in substitutional solute-free bcc Fe.

[1] H. R. Sinning, I. S. Golovin, A. Strahl, O. A. Sokolova, T. Sazonova, Interactions between solute atoms in Fe-Si-Al-C alloys as studied by mechanical spectroscopy, *Mater. Sci. Eng. A* 521-522 (2009) 63–66. doi:10.1016/j.msea.2008.09.110.

# Theory

# MOBILITY OF DISLOCATIONS IN THE IRON-BASED C-, N-, H-SOLID SOLUTIONS MEASURED USING INTERNAL FRICTION: EFFECT OF ELECTRON STRUCTURE

V.G. Gavriljuk\*, V.N. Shyvaniuk, S.M. Teus  
G.V. Institute for Metal Physics, Kiev, Ukraine  
\*gavr@imp.kiev.ua

Snoek-Köster (S-K) relaxation and the amplitude-dependent internal friction (ADIF) in the interstitial iron-based solid solutions are studied in terms of mobility of dislocations. The effect of interstitial elements on the S-K relaxation amplitude, as well as on the internal friction background measured in the ADIF experiments, is analyzed as consequence of a change in the electron structure.

The electron structure of the  $\alpha$ - and  $\gamma$ -iron containing carbon or nitrogen and hydrogen has been *ab initio* calculated using the Wien2k program package based on the Kohn-Hohenberg-Sham density functional theory. It was obtained that carbon in the both iron phases decreases the density of electron states at the Fermi level, whereas nitrogen and hydrogen increase it [1-4].

Correspondingly, using the measurements of electron spin resonance in the  $\gamma$ -iron alloys, the concentration of free electrons is found to be decreased by carbon and increased due to nitrogen and hydrogen [5, 6]. On the account of a strong binding of these elements to dislocations, the concentration of free electrons is suggested to be locally changed in the vicinity of dislocations encased in the clouds of interstitial atoms. Consequently, a change in dislocation properties is expected, namely in the line tension which controls mobility of dislocations. Therefore, it should reveal itself in relaxation phenomena of which mechanism is related with dislocation vibrations.

Such a correlation was found for the S-K relaxation caused by carbon and nitrogen in the iron martensite [7], see Fig. 1. At equal contents of interstitials in the solid solution, the S-K relaxation amplitude is higher in case of nitrogen in comparison with carbon, which is consistent with the earlier obtained results in the pure iron [8]. In case of S-K relaxation caused by hydrogen in the  $\alpha$ -iron, the convincing data were obtained in [9], see Fig. 2.

Examples for the ADIF in austenitic steels are presented in Figures 3 and 4. The area swept by the vibrating dislocations significantly increases by nitrogen and hydrogen in comparison with carbon.

The both, S-K relaxation and ADIF, evidence a change of the dislocation line tension in its correlation with C-, N- and H-effect on the electron structure.

[1] S.M. Teus, V.N. Shyvanyuk, B.D. Shanina, V.G. Gavriljuk. *Phys. Stat. Sol. (a)* **204** (2007) 4249-4258.

[2] V.G. Gavriljuk, B.D. Shanina, V.N. Shyvanyuk, S.M. Teus. *J. Appl. Phys.* **108** (2010) 083723.

[3] V.G. Gavriljuk, B.D. Shanina, V.N. Shyvanyuk, S.M. Teus. *Corrosion Reviews* **31** (2013) 33-50.

- [4] S.M. Teus, V.G. Gavriljuk. *Mater Letts* **258** (2020) 126801
- [5] V.G. Gavriljuk, B.D. Shanina, N.P. Baran, V.M. Maximenko. *Phys. Rev. B* **48** (1993) 3224-3231.
- [6] B.D. Shanina, V.G. Gavriljuk, S.P. Kolesnik, V.N. Shyvanyuk. *J. Phys. D: Appl. Phys.* **32** (1999) 298-304.
- [7] V.G. Gavriljuk, V.N. Shyvanyuk, B.D. Shanina. *Acta Mater* **53** (2005) 5017-5024.
- [8] K. Kamber, D. Keefer, C Wert. *Acta Metall* **9** (1961) 403-414.
- [9] K. Takita , K. Sakamoto. *Scripta Metall* **10** (1976) 399-403.

# On Internal Friction due to Elastic Waves Radiation during Dislocation Bending Vibrations in the Peierls Relief

V.V. Dezhin

*Voronezh State Technical University, Voronezh, Russian Federation*

viktor.dezhin@mail.ru

In present work, consideration of small bending vibrations of an infinite dislocation in a nondissipative medium is continued. It was believed that braking of dislocation oscillations was caused only by radiation of elastic waves. Presence of the Peierls relief in real crystals is taken into account. Expression for inverse generalized susceptibility of dislocation is found, which differs from expression obtained in [1] by a constant  $\pi\sigma_P$ , where  $\sigma_P$  is the Peierls stress. Internal friction was calculated by the formula  $Q^{-1} = \frac{\Delta W \rho_d}{2\pi W_0}$ . Here  $\Delta W = \frac{2\pi}{\omega} W$  is radiated energy for oscillation period,  $\rho_d$  is dislocation density,  $W_0 = \frac{\sigma_0^2}{2\mu}$  is total vibration energy of unit volume,  $\omega$  is dislocation vibration frequency,  $\sigma_0$  is amplitude of alternating stress in the crystal,  $\mu$  is shear modulus. To find average energy emitted per unit time per unit length of dislocation, we use formula from [2]  $W = (\omega/2) \text{Im} \alpha(k_z, \omega) |\sigma b|^2$ , where  $\alpha(k_z, \omega)$  is generalized susceptibility of dislocation,  $k_z$  is wave vector component along dislocation line,  $\sigma$  is amplitude of variable external stress acting on the dislocation,  $b$  is the Burgers vector length. Presence of two different cases for elastic waves radiation  $|k_z| < \omega/c_l$  and  $\omega/c_l < |k_z| < \omega/c_t$  is established. Fig. 1-4 shows dependence of internal friction on frequency of dislocation bending vibrations for aluminum crystal. It can be seen that internal friction due to elastic waves radiation is very small compared to total dislocation internal friction [3]. Figures 1-4 show the resonant peaks of internal friction.

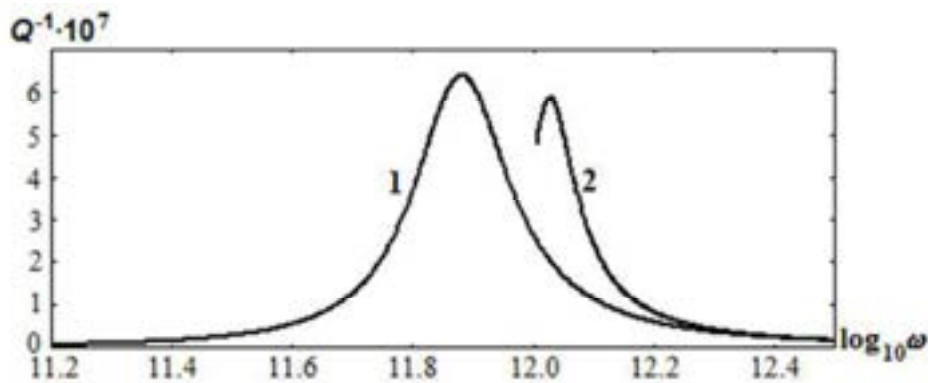


Fig. 1. Frequency dependence of internal friction at  $|k_z| < \omega/c_l$  of infinite screw dislocation bending vibrations; 1 –  $k_z = 10^3 \text{ m}^{-1}$ , 2 –  $k_z = 10^{8.2} \text{ m}^{-1}$

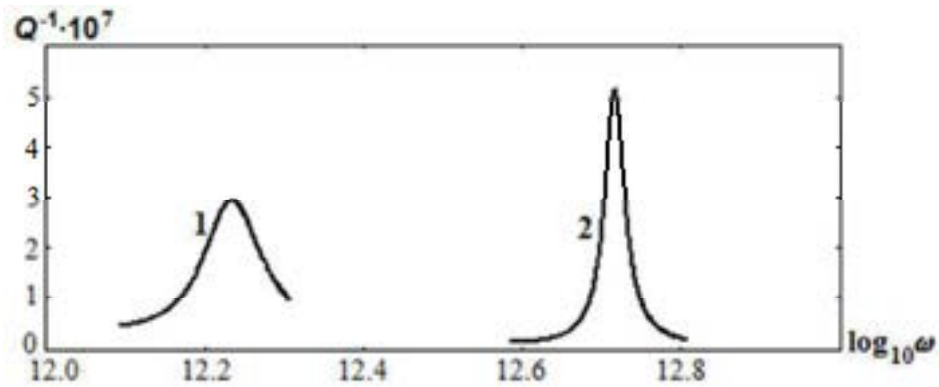


Fig. 2. Frequency dependence of internal friction at  $\omega/c_l < |k_z| < \omega/c_t$  of infinite screw dislocation bending vibrations; 1 –  $k_z = 10^{8.5} \text{ m}^{-1}$ , 2 –  $k_z = 10^9 \text{ m}^{-1}$

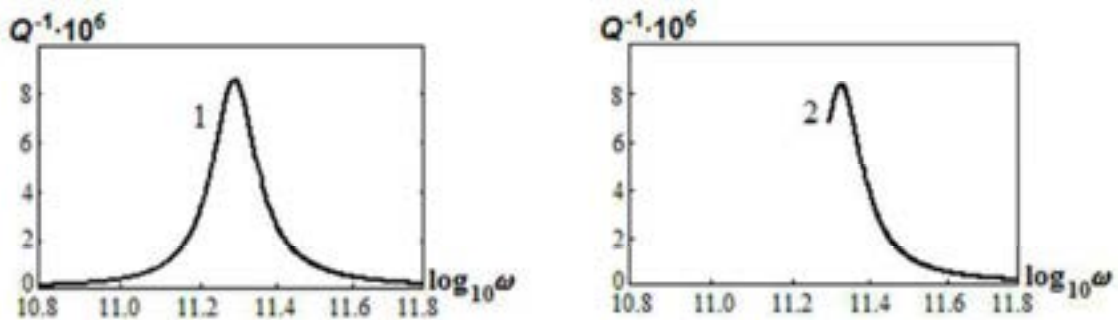


Fig. 3. Frequency dependence of internal friction at  $|k_z| < \omega/c_l$  of infinite edge dislocation bending vibrations; 1 –  $k_z = 10^3 \text{ m}^{-1}$ , 2 –  $k_z = 10^{7.5} \text{ m}^{-1}$ .

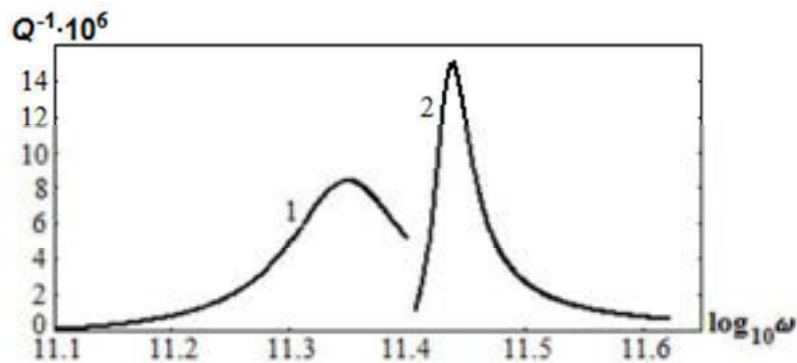


Fig. 4. Frequency dependence of internal friction at  $\omega/c_l < |k_z| < \omega/c_t$  of infinite edge dislocation bending vibrations; 1 –  $k_z = 10^{7.6} \text{ m}^{-1}$ , 2 –  $k_z = 10^{7.9} \text{ m}^{-1}$

- [1] I.L. Bataronov, V.V. Dezhin, A.M. Roshchupkin, *Bulletin of the Russian Academy of Sciences: Physics*, **57** (1993) 1947-1955.
- [2] L.D. Landau, E.M. Lifshitz, *Statistical Physics, Part 1 (Course of Theoretical Physics, Vol 5)*, (Butterworth-Heinemann, Oxford, 1980).
- [3] M.S. Blanter, I.S. Golovin, H. Neuhäuser, H.-R. Sinning, *Internal Friction in Metallic Materials* (Springer-Verlag, Berlin, 2007).

# ELECTRICAL, ELASTIC PROPERTIES AND DEFECT STRUCTURES IN ISOTACTIC POLYPROPYLENE DOPED WITH NANOGRAFITE AND GRAPHENE NANOPARTICLES

L.V. Elnikova<sup>1\*</sup>, A.T. Ponomarenko<sup>2</sup>, P.M. Nedorezova<sup>3</sup>, V.G. Shevchenko<sup>2</sup>,  
A.N. Ozerin<sup>2</sup>, O.M. Palaznik<sup>3</sup>, V.V. Skoi<sup>4,5</sup>, A.I. Kuklin<sup>4,5</sup>

<sup>1</sup>*NIC "Kurchatov Institute" - A.I. Alikhanov Institute for Theoretical and Experimental Physics, Moscow, Russian Federation*

<sup>2</sup>*N.S. Enikolopov Institute of synthetic and polymeric materials RAS, Moscow, Russian Federation*

<sup>3</sup>*N.N. Semenov Federal Research Center for Chemical Physics RAS, Moscow, Russian Federation*

<sup>4</sup>*Joint Institute for Nuclear Research, Dubna, Russian Federation*

<sup>5</sup>*Moscow Institute of Physics and Technology, Dolgoprudny, Russian Federation*

\*elnikova@itep.ru

Conducting polymers have wide technological applications in sensors, actuators, electric and optical devices, solar cells *etc.* To improve their operational performance, mechanical, thermal, electrical, optical properties, such polymers are doped with carbon allotrope nanofillers such as graphene and nanographite particles, fullerenes, single-wall and multi-wall carbon nanotubes and so on [1].

Our report is devoted to analysis and characterization of structure, elastic, electric properties and of novel polymer nanocomposites, isotactic polypropylene (iPP) with high crystallinity filled with flat thin layered nanographite and graphene nanoparticles at different concentrations and sizes.

Dynamic mechanical analysis (DMA) for the iPP-graphene systems [2] revealed variations of the storage ( $E'$ ) and loss ( $\text{tg}\delta$ ) moduli with increasing of contents of graphene nanoparticles and temperature. In the temperature range between glass transition and degradation temperature defines the choice of optimal nanofiller concentrations, when the Young modulus and tensile strength increase (by 50 and 25% respectively). Three relaxation processes ( $\alpha$ ,  $\beta$ ,  $\gamma$ ) at the  $E'$  and  $\text{tg}\delta$  curves are possible for such composites ( $\beta$  relaxation is associated with generalized motion in the amorphous regions during the glass transition,  $\gamma$  address to the mobility of crystallites).

Similar data on DMA and other structural methods [3] for different ordered carbon allotrope structures, including graphene nanoplates, in the syndiotactic PP matrix in the temperature range from -60 to 160°C shown temperature decreasing of  $E'$ , temperature and concentration dependent peaks of mechanical and dielectric losses, as well as for graphene nanifillers (by 2.6wt%) in the iPP matrix [4,5].

Small-angle neutron scattering (SANS) [6] allows us to confirm changes in measured mechanical properties by the fact that nanographite and graphene nanoparticles in the iPP matrix form new aggregates, which possess fractal dimensionality. Such intrinsic morphology of material is caused by deformation

of nanofillers, *i.e.* by structural defects in nanographite and graphene nanoparticles.

For explanation changes in the Young modulus, plastic, elastic, electric properties and other features of these composites, we apply theoretical modeling describing gauge defect structures [7,8] with the tight-binding Hamiltonian [8,9]. We involve the concept of Cosserat elasticity with the gauge orientation field [10] and study topological defects disclinations and dislocations, point defects and grain boundaries [7,11,12] in the nanographite and graphene nanoparticles affected morphology and mesomorphism of the iPP nanocomposites. In terms of Cosserat elasticity, we propose numerical modeling, which contributes to estimation and prediction of mechanical behavior of novel nanocomposites in the wide range of nanofiller concentrations and temperatures for required technical realizations.

- [1] L.-J. Dai, C.-L. Fu, Y.-L. Zhu, Z.-Y. Sun, *J. Chem. Phys.* **150**, (2019) 184903-1-184903-11.
- [2] M.A. Milani, D. González, R. Quijada, N.R.S. Basso, M.L. Cerrada, D.S. Azambuja, G.B. Gallan, *Composites Science and Technology*. **84** (2013) 1-7.
- [3] S.V. Polschikov, P.M. Nedorezova, O.M. Komkova, A.N. Klyamkina, A.N. Shchegolikhin, V.G. Krasheninnikov, A.M. Aladyshev, V.G. Shevchenko, V.E. Muradyan, *Nanotech. in Russia*, **9**(3-4)(2014) 175-183.
- [4] S.V. Polschikov, P.M. Nedorezova, A.N. Klyamkina, V.G. Krasheninnikov, A.M. Aladyshev, A.N. Shchegolikhin, V.G. Shevchenko, E.A. Sinevich, V.E. Muradyan, *Nanotech. in Russia*, **8**(1-2)(2013) 69-80.
- [5] S.V. Polschikov, P.M. Nedorezova, A.N. Klyamkina, A.A. Kovalchuk, A. M. Aladyshev, A. N. Shchegolikhin, V.G. Shevchenko, V.E. Muradyan, *J. Appl. Polym. Sci.*, (2012) 1-8. DOI: 10.1002/APP.37837.
- [6] L.V. Elnikova, A.N. Ozerin, V.G. Shevchenko, P.M. Nedorezova, A.T. Ponomarenko, V.V. Skoi, A.I. Kuklin, *Fullerenes, Nanotubes and Carbon Nanostructures*, **29**(10) (2021) 783-792.
- [7] E.A. Kochetov, V.A. Osipov, P. Pincak, *J. Phys.: Condens. Matt.*, **22** (2010) 395502-1-395502-11.
- [8] M.A.H. Vozmediano, M.I. Katsnelson, F. Guinea, *Phys. Rep.*, **496** (2010) 109-148.
- [9] I.V. Fal'kovsky, M.A. Zubkov, *Symmetry*, **12** (2020) 317-1-317-29.
- [10] J. Li, C.S. Ha, R.S. Lakes, *Phys. Status Solidi B*, (2019) 1900140-1-1900140-6.
- [11] O.V. Yazyev, S.G. Louie, *Phys. Rev.*, **B 81**(2010) 195420-1-195420-7.
- [12] L.A. Openov and A.I. Podlivaev, *JETP Lett.*, **90** (2009) 459-463.

# Magnetic materials

# Enhancement of the magneto-mechanical properties in directional solidified $\text{Fe}_{80}\text{Al}_{20}$ alloys by doping Tb

H.W. Chang<sup>1\*</sup>, S.U. Jen<sup>2</sup>, Y.H. Liao<sup>1</sup>, D.H. Tseng<sup>1</sup>, H.Y. Hsieh<sup>1</sup>,  
W.C. Chang<sup>1</sup>, C.H. Chiu<sup>3</sup>, J. Cifre<sup>4</sup>, D.G. Chubov<sup>5</sup>, I.S. Golovin<sup>5,6</sup>

<sup>1</sup> Department of Physics, National Chung Cheng University, Chia-Yi, 621 Taiwan

<sup>2</sup> Institute of Physics, Academia Sinica, Taipei, 115 Taiwan

<sup>3</sup> New Materials Research & Development Dept., China Steel Corp., Kaohsiung, Taiwan

<sup>4</sup> Universitat de les Illes Balears, Ctra. De Valldemossa, km.7.5, E-07122 Palma de Mallorca, Spain

<sup>5</sup> National University of Science and Technology "MISIS", Leninsky Ave. 4, 119049, Moscow, Russia

<sup>6</sup> Moscow Polytechnic University, B. Semenovskay 38, 107023, Moscow, Russia

\*Corresponding author: H.W. Chang, E-mail: [wei0208@gmail.com](mailto:wei0208@gmail.com)

## Abstract

Enhancement of the magneto-mechanical properties in directional solidified  $\text{Fe}_{80}\text{Al}_{20}$  alloys by doping Tb is demonstrated. The  $\Delta E$  effect of 9.1%, large magnetostriction of 144 ppm, magnetostriction sensitivity of 0.28 ppm/Oe,  $\Delta G$  effect of 5.4%, and magneto-mechanical coupling of 29.74% reached for  $\text{Fe}_{79.9}\text{Al}_{20}\text{Tb}_{0.1}$  alloy are beneficial for applications. The increased magnetostriction with increasing the Tb content  $x$  from 0 to 0.1 is related to the increased degree of (110) texture with Tb doping. Notably, the increased magnetostriction sensitivity, resulted from the increased magnetostriction with Tb-doping, leads to the enhancement of  $\Delta E$  and  $\Delta G$  effects. Nevertheless, the degraded (110) texture for higher Tb content ( $x = 0.15$ ) results in the reduction of magneto-mechanical properties. Summarized with the experimental measured and theoretically estimated results, the micro eddy-current mechanism mainly governs the change of damping capacity with  $H$  for frequency of vibrations  $\sim 2.0$  kHz resulting from the magnetic domain wall motion. Moreover, the amplitude and temperature dependences of internal friction and elastic modulus data, measured by DMA, including damping capacity and Young's modulus, at a frequency of 0.1-30 Hz could characterize hysteretic damping and anelastic effects at heating. The result of this study suggests a cost-effective and simple method to obtain  $\text{Fe}_{80}\text{Al}_{20}$  based alloy with excellent magneto-mechanical properties via proper Tb-doping.

## Acknowledgment

This research was financially supported by the Ministry of Science and Technology of Taiwan, under grant No. MOST-109-2112-M-194-006 and the Russian Science Foundation project No. 19-72-20080.

# Anelasticity Study of Antiferromagnetic FeMnMo Alloy

H. Tanimoto\*, K. Matsumoto, F. Higashi  
*University of Tsukuba, Tsukuba Ibaraki 305-8573, Japan*

\*tanimoto@ims.tsukuba.ac.jp

Ferromagnetic Invar and Elinvar alloys are widely used for the precision measuring instruments, however, the designed properties are spoiled by external magnetic fields. Recently, antiferromagnetic Invar and Elinvar alloys attract interests because of the robustness against the external magnetic field. FeMn-based alloys are candidate for the antiferromagnetic Invar and Elinvar alloys [1] and an improvement of the properties was reported by addition of small amount of transition metals like Mo and Nb [2]. Since the magnetic moments in FeMn-based alloys are ordered antiparallely along the  $\langle 111 \rangle$  direction, the control of texture is also important for the desired Invar or Elinvar properties. We focus the columnar texture in the ingot prepared by arc-melting and the effect of the texture on the Elinvar property of FeMn-based alloy is investigated. Thin reeds with three different textures were prepared by changing the cutting direction from the ingot: A; the reed direction parallel to the columnar grains, B; the reed surface normally across the columnar grains, and C; the columnar grains along the reed width direction. Figure 1 shows the temperature change in the resonant frequency measured by using the flexural reed vibration technique. The temperature change in the frequency is very small for the three specimens at 200 to 300 K, especially specimen B. The further development of the preferred texture is expected after cold-rolling and the followed annealing and the results will be discussed as well as the effect on the anelasticity.

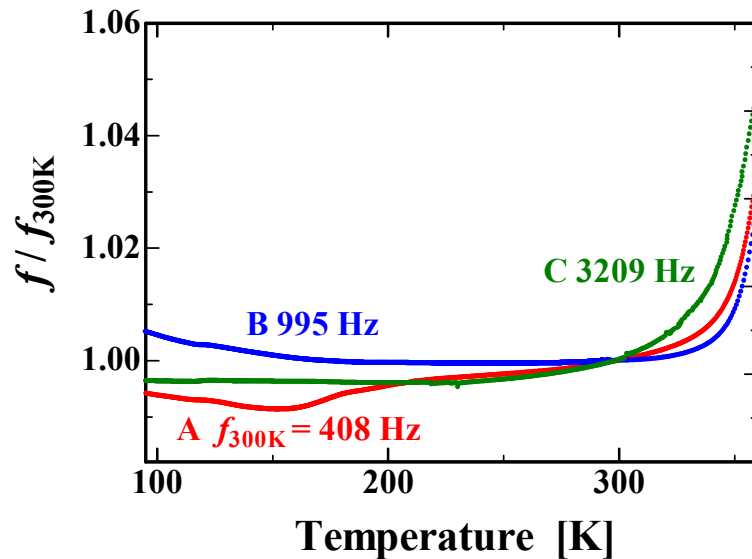


Fig. 1. Temperature change in the resonant frequency ( $f$ ) of Fe-25wt.%Mn-5wt.%Mo alloy, where the changes normalized by the value at 300 K is shown.

[1] Y. Zhang, X. Tian, Z. Qin, H. Jiang, *J. Mag. Mag. Mater.*, **324** (2012) 853-856.

[2] T. Masumoto, S. Ohnuma, K. Sugawara, H. Kimura, *Mater. Trans.* **55** (2017) 701-704

# Magneto-mechanical damping and phase transformations in iron-based alloys

D. Mari<sup>1\*</sup>, I. Tkalcec<sup>1</sup>, M. Kabchou<sup>2</sup>, I.S. Golovin<sup>3</sup>

<sup>1</sup>EPFL, Institute of Physics, CH-1015 Lausanne, Switzerland

<sup>2</sup>Polytech Clermont-Ferrand, 63178 Aubière, France

<sup>3</sup>National University of Science and Technology "MISIS", 119049 Moscow, Russia

\*daniele.mari@epfl.ch

Mechanical spectroscopy is a well-known technique that allows the measurement of the mobility of crystal defects. The defect movement produces damping i.e. energy dissipation during a periodic excitation cycle. Magnetic effects, in particular in ferromagnetic materials, cause damping as well. This damping is amplitude dependent in ferromagnetic alloys.

In this study, Amplitude Dependent Internal Friction (ADIF) measurements are made in a free pendulum capable to produce high strain amplitude oscillations up to  $2 \times 10^{-2}$ . Temperature scans are realized in a forced pendulum at a strain amplitude of  $1 \times 10^{-5}$  and at 1 Hz.

In fig. 1, the spectra measured in pure iron as a function of temperature are shown. Fig. 1a shows a Temperature Dependent Internal Friction (TDIF) spectrum up to 1250 K in two following cycles. The first cycle just stopped after the Curie temperature (expected at 1040 K) and the second one was carried out above the bcc-fcc transformation expected at 1180 K. Fig. 1b shows the modulus (in arbitrary units since measured in forced pendulum) as a function of temperature. Upon heating, one can observe a relaxation peak at around 780 K, which might be attributed to a grain boundary sliding effect. From Fig. 1a, it can be inferred that the onset of the ferromagnetic transition can be detected by mechanical spectroscopy via a sudden increase of damping. However, the transition is well visible only upon cooling (paramagnetic  $\rightarrow$  ferromagnetic transition). A slope change, corresponding to the Curie temperature, is also detected in the modulus. Notice that on first heating (the sample had been quenched from 1173 K) and a dip is observed in the modulus at around 1020-1040 K.

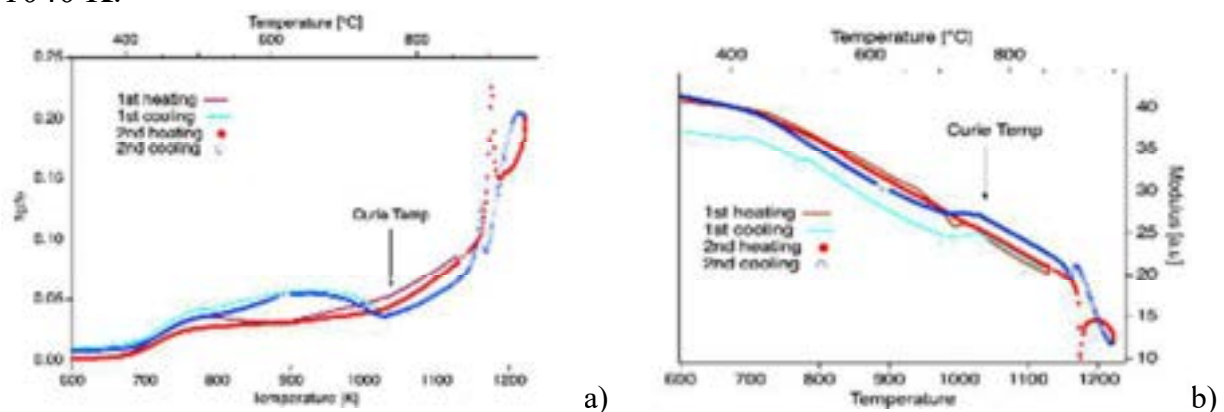


Fig. 1. TDIF measured in two successive cycles in pure iron: first heating-cooling cycle up to 1100 K and second heating-cooling cycle up to 1250 K. a) Measure of the mechanical loss.

b) Measurement of the relative shear modulus.

The bcc-fcc transition is marked by a sharp peak both on heating (1176 K) and on cooling (1163 K). The transformation of 1<sup>st</sup> order is hysteretic. The modulus shows a sharp dip in correspondence with the internal friction peak.

ADIF experiments were realized on the same sample. A magnetic field of 0.056 T was applied axially around the sample. As presented in fig. 2, a strong ADIF effect is observed without magnetic field with a maximum at a strain of  $5 \times 10^{-4}$ . The effect disappears completely when a magnetic field is applied.

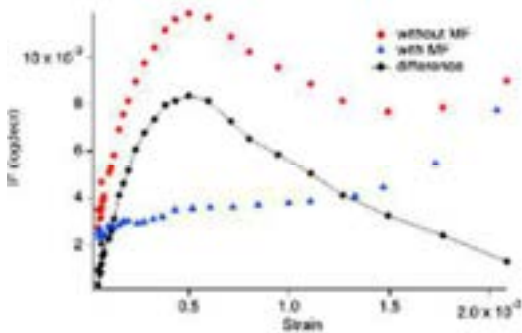


Fig. 2. ADIF measured in pure iron.

The features obtained in ferromagnetic alloys constitute a guideline to determine the characteristics of damping in magnetic transitions. In this paper, we also analyze the internal friction in a carbon steel martensite Fe-1.23wt%C,0.64wt%Cr. This material has been treated in order to make (Fe,Cr)<sub>3</sub>C spheroidal precipitates that are insoluble and that account for 12vol%. As confirmed in [1], the actual composition of the iron matrix is just below the eutectic and a certain amount of ferrite remains above the eutectic temperature. It is found that the Curie temperature of ferrite produces a strong drop of the internal friction (Fig. 3a) and a modulus increase (Fig. 3b). The ferrite to austenite transition produces some complex effects according to the solid solution state of carbon. When the alloy is kept above the eutectic point (heating cycle n+1 in fig. 3) a simple hysteretic behavior is observed.

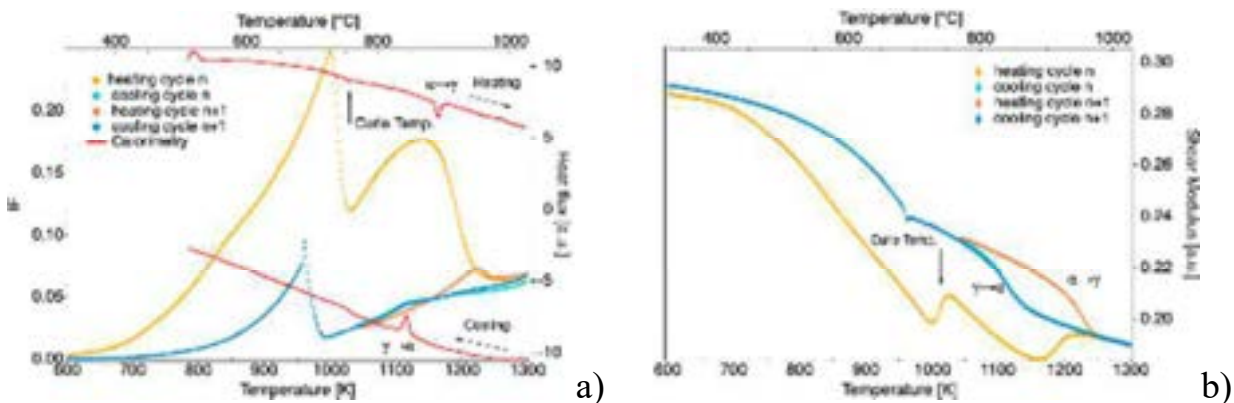


Fig. 3. TDIF measured in a 1.2wt%C steel a) Internal friction measured in two successive cycles. In the second the sample is not cooled below the Curie temperature. b) Shear modulus corresponding to measurements in a).

- [1] I. Tkalcec, D. Mari, W. Benoit, Correlation between internal friction background and the concentration of carbon in solid solution in a martensitic steel, *Mater. Sci. Eng. A.* 442 (2006) 471–475. <https://doi.org/10.1016/j.msea.2006.03.115>.

# Remanent magnetization of antiferromagnetic Dy through domain wall freezing: an acoustic study

M. Comas<sup>1\*</sup>, D. Salazar<sup>2</sup>, A. Paulsen<sup>3</sup>, J. Frenzel<sup>3</sup>, M. Corró<sup>1</sup>, S. Kustov<sup>1</sup>

<sup>1</sup>*Universitat de les Illes Balears, Palma de Mallorca, Spain*

<sup>2</sup>*BCMaterials, Leioa, Spain*

<sup>3</sup>*Ruhr-Universität Bochum, Bochum, Germany*

\*marticomas00@gmail.com

We report elastic, anelastic and magnetoelastic properties of single crystalline Dy in the para- and antiferromagnetic phases between 200 and 100 K at an ultrasonic frequency ca. 90 kHz using piezoelectric composite oscillator technique. Our attention is focussed on the puzzling conflict between essentially linear field dependence of the reversible inverse magnetostriction, RIM, (reflecting the canonical parabolic field dependence of the magnetostriction) and absence of scaling of continuous temperature spectra of RIM registered under different polarizing field. We show that the scaling does not exist if the sample is field-cooled across the Néel temperature  $T_N \approx 178$  K and is recovered if the field is applied below ca. 160 K. It is remarkable that the RIM-polarizing field hysteresis exists over a narrow temperature range above Néel temperature and its shape is typical for ferromagnetic structures. We argue that the loss of scaling in field-cooled samples originates from the remnant magnetization of the antiferromagnetic structure related with the magnetic moments of domain walls parallel to the c-axis. This magnetization can be induced only over the narrow temperature range of critical fluctuations down to 160 K. Between the Néel temperature and 160 K RIM versus polarized field dependences show hysteresis attributable to the domain walls. Below this temperature domain walls are “frozen”: (i) remnant magnetization is inhibited; (ii) RIM-polarizing field hysteresis vanishes and (iii) scaling of RIM temperature spectra is recovered. We argue that ferromagnetic-like type of the RIM-field hysteresis above  $T_N$  is due to the nuclei of the spiral antiferromagnetic structure which carry magnetic moments. Our conclusions confirm the results of the X-ray photon correlation spectroscopy on domain wall freezing in antiferromagnetic Dy.

# MAGNETIC BEHAVIOR IN COMMERCIAL IRON-SILICON ALLOYS CONTROLLED BY THE DISLOCATION DYNAMICS AT TEMPERATURES BELOW 420 K

O.A. Lambri<sup>1</sup>, B. Weidenfeller<sup>2</sup>, J.I. Pérez-Landazábal<sup>3</sup>, G.J. Cuello<sup>4</sup>, F.G. Bonifacich<sup>1</sup>, L. Weidenfeller<sup>5\*</sup>, V. Recarte<sup>3</sup>, G.I. Zelada<sup>1</sup>, W. Riehemann<sup>6</sup>

<sup>1</sup>*CONICET-UNR - Laboratorio de Materiales, Escuela de Ingeniería Eléctrica, Centro de Tecnología e Investigación Eléctrica, Facultad de Ciencias Exactas, Ingeniería y Agrimensura, Avda. Pellegrini 250, 2000 Rosario, Argentina*

<sup>2</sup>*Department of Materials Science – Institute of Electrochemistry Clausthal University of Technology, D-38678, Clausthal-Zellerfeld, Germany*

<sup>3</sup>*Departamento de Ciencias, Institute for Advanced Materials (INAMAT), Universidad Pública de Navarra, Campus de Arrosadía, 31006 Pamplona, Spain*

<sup>4</sup>*Institute Laue-Langevin, 71 Av. des Martyrs, B.P. 156, 38042 Grenoble Cedex 9, France*

<sup>5</sup>*Department of Mechanical Engineering, Ilmenau University of Technology, Max-Planck-Ring 12, 98693 Ilmenau, Germany*

<sup>6</sup>*Institute of Materials Science and Engineering, Clausthal University of Technology, D-38678 Clausthal-Zellerfeld, Germany (passed away)*

\*laura.weidenfeller@googlemail.com

Since the development of the grain oriented silicon steel (GOSS), several thermomechanical treatments and new production methods have been developed for improving the magnetic quality of iron silicon alloys [1-3]. The high silicon iron alloys, with silicon content around 6 – 6.5 wt.% exhibit high magnetization, low coercive force and a good degree of brittleness for technological applications[3]. Often the thermal treatments for iron silicon steels for electrical applications involve the annealing at elevated temperatures for controlling the second recrystallization, texture or the appearance of ordered phases. Indeed, the improvement of the magnetic quality requires a better understanding of the structure-properties relationship in soft magnetic materials.

In the present work, commercial samples of composition Fe-6 wt.% Si and Fe-3.1 wt.% Si (grain oriented, GOSS), have been studied. The microstructure from the samples was determined by means of neutron thermodiffraction (NTD) studies. NTD measurements were performed at the D20 installation in the Institute Laue-Langevin (ILL), from room temperature (RT) up to 1073 K with a neutron wavelength of 1.3Å. In addition, neutron diffraction (ND) studies were also carried out at RT under a magnetic field up to 6T. The magnetic properties have been determined by a computer-controlled A.C. digital hysteresis recorder, at 20 Hz, “in situ” as a function of temperature from RT up to 405K with a heating rate of around 1 K min<sup>-1</sup>. The dislocation dynamics, involving also the interaction with the domain walls, was studied through mechanical spectroscopy (MS) studies. MS measurements [4,5] (damping, Q<sup>-1</sup>, and natural frequency, f; f<sup>2</sup> being proportional to the elastic shear modulus) were performed in an inverted torsion pendulum, as a function of temperature, frequency and strain. MS studies were performed also as a function of temperature under the application of a direct magnetic field, HDC, of 30 kA m<sup>-1</sup>.

We are reporting an improvement in the magnetic quality of iron silicon alloys due to an enhancement in the mobility of the domains walls controlled by the increase in the dislocations mobility. In addition, the improvement was found in quenched samples and also in samples which were previously thermally treated to achieve the highest magnetic quality.

It will be demonstrated that the improvement in the coercive force  $H_c$ , up to around 370 K, shown in Figure 1, is controlled by an increase in the mobility of the domain walls due to the increase in the dislocation's mobility enhanced by the movement of vacancies. In addition, the subsequent increase in  $H_c$  is promoted by different kinds of interactions processes among domain walls, dislocations and point defects, which decrease the domain walls mobility. The dislocation dynamics as a function of temperature controlled by the degree of order, interactions with vacancy complexes and point defects are discussed both for ordered and disordered alloys.

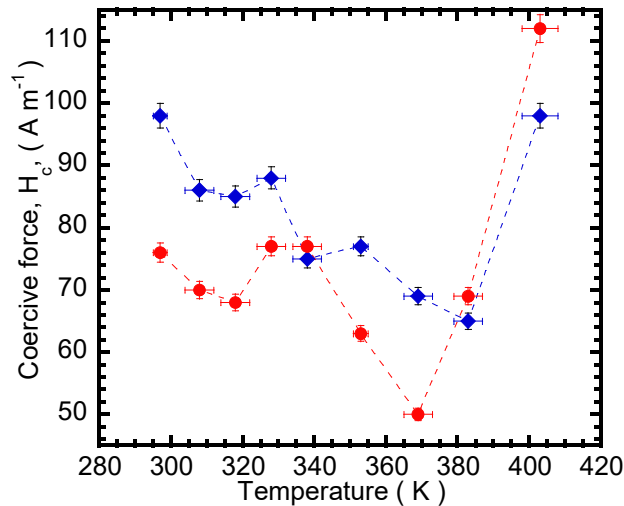


Fig.1. Coercive force,  $H_c$ , measured “in situ” as a function of temperature. Circles: Fe-6wt.%Si, annealed at 1273 K during 1 hour under a vacuum of  $10^{-5}$  Pa followed by quenching in water at RT. Fe-3.1 wt.% Si, annealed at 1073 K during 1 hour under a vacuum of  $10^{-5}$  Pa followed by slow cooling in the furnace (usual for the heat treatment of electrical grade GOSS [1]). Lines are a guide for the eyes.

- [1] R. M. Bozorth, Ferromagnetism, MacMillan, London, UK 1951.
- [2] M. Matsuo, Trans. Iron Steel Inst. Japan 1989, 29, 809.
- [3] K. M. Gupta, N. Gupta, in Advanced Materials Series (Ed: A. Tiwari), John Wiley & Sons, New Jersey, USA 2015.
- [4] R. Schaller, G. Fantozzi, G. Gremaud (Eds.), Mechanical Spectroscopy, Trans Tech, Switzerland, 2001.
- [5] M.S. Blanter, I.S. Golovin, H. Neuhäuser, H.-R. Sinning, Internal Friction in Metallic Materials. A Handbook, Springer, Berlin, 2007.

## Villari points in single crystalline Dy as an example of “horizontal hysteresis” in ferroic materials

M.L. Corró<sup>1\*</sup>, M. Comas<sup>1</sup>, A. Paulsen<sup>2</sup>, J. Frenzel<sup>2</sup>, D. Salazar<sup>3</sup>, S. Kustov<sup>1</sup>

<sup>1</sup>*Universitat de les Illes Balears, Cra Valldemossa km 7.5, Palma 07122, Spain*

<sup>2</sup>*Ruhr-Universität Bochum, Universitätsstr. 150, D-44801 Bochum, Germany*

<sup>3</sup>*BCMaterials, UPV/EHU Science Park, Barrio Sarriena s/n, 48940 Leioa, Spain*

\*miquel.corro@uib.cat

Internal friction, Young’s modulus and reversible inverse magnetostriction (Villari effect) of  $[11\bar{2}0]$  oriented Dy single crystals were studied either as a function of temperature under different applied magnetic fields or as a function of field at constant temperatures above and below the temperature of antiferromagnetic (AFM) ordering. Two Villari points, wherein the magnetoelastic coupling vanishes, were found at and slightly below the Néel temperature,  $T_N$ . The first one was, essentially independent on the applied field, was related to the para-antiferromagnetic transition and coincided with the  $T_N$ . The second one was observed a few degrees below the  $T_N$  and was displaced by polarising field. The peculiar behaviour of the magnetoelastic coupling and the existence of two Villari points in single crystalline Dy is explained by a combination of lattice magnetostriction and contribution of AFM domain walls. We compare magnetoelastic hysteresis around Villari points in AFM ordered Dy with the so-called “horizontal hysteresis” in some ferroelectrics close to the Curie temperature, which is also ascribed to a superposition of different polarization mechanisms. We conclude that the observation and the origin of “horizontal hysteresis” is generic in ferroic materials.

# Grain boundaries

# RELAXATION TIME SHIFT OF COBALT RELATED INTERNAL FRICTION PEAK IN WC-CO CEMENTED CARBIDE

L. Degeneve<sup>1\*</sup>, S. Adjam<sup>1</sup>, D. Mari<sup>1</sup>,

<sup>1</sup> *Ecole Polytechnique Fédérale de Lausanne (EPFL), SB IPHYS LQM,  
Station 3, 1015 Lausanne, Switzerland*

\* [lucas.degeneve@epfl.ch](mailto:lucas.degeneve@epfl.ch)

Cemented carbides are excellent hard materials used for nearly a century for cutting tools and wear resistant parts applications. This study presents investigations made on WC-Co cemented carbides using mechanical spectroscopy. This technique allows studying microplastic deformations in pure or composite crystalline materials through internal friction spectrum. It makes it possible to identify defect related dynamic phenomena associated to the different material phases. The characteristic spectrum of WC-6wt.%Co measured in the 700-1400 K temperature range at 1 Hz exhibits three peaks (hereinafter referred to as peak P1, P2 and P3)(see Fig. 1(a) ). In this frequency range, peaks P1 and P2 appear respectively at 920K and 1125K, while the peak P3 appear at 1350K. Previous studies [1], [2] showed similar characteristic internal friction spectra for WC-Co materials. The two first relaxation peaks P1 and P2 were attributed to the cobalt phase. The third peak P3 appears at about 1350 K at 1 Hz and it is associated with grain boundary sliding of the hard phase [1]. The crystallographic structure at room temperature of cobalt in WC-Co was usually reported to be f.c.c, with a large number of h.c.p. stacking faults bordered by partial dislocation [3], [4]. Mari [1] has proposed that the Co relaxation peak P2 could be influenced by a para-ferromagnetic transition. According to [5] such magnetic transition would also be responsible for a spinodal decomposition in the tungsten rich cobalt phase. The peaks P1 and P2 were both associated with the dragging of W atoms by dislocations. The shift in temperature observed between those peaks was explained by a change in the associated dislocation free length. At low temperature, the W-rich zones in the cobalt would act like strong pinners and reduce the mean free length of the dislocations. At higher temperatures, the W zones dissolve and the greater dislocation mean free length would correspond to the cobalt mean free path in f.c.c. structures. In a new study [6] on submicron grain size WC-Co, a new microstructure of the cobalt phase has been found. It showed nanotwins in polycrystalline Co twinned nanodomains. The long-range order f.c.c. structure observed up to now in WC-Co materials was replaced by a harder and more brittle structure, where the twins enhance hardening and block dislocations. For WC-6wt.%Co with submicron carbide grains specimens, the activation energy as well as the limit relaxation time corresponding to the peak P2 are measured in this work. Fig. 1(b) presents the Arrhenius plot of the IF peak P2 measured in isothermal condition between 3mHz and 4Hz in a high temperature inverted torsion pendulum from 1300K to 1000K. This figure reveals an anomaly between two temperature ranges: above 1140K, the limit relaxation time  $\tau_0$  is found to be  $10^{-12}$  s, while below this temperature limit the latter is equal to  $10^{-13}$  s. In order to verify or refute the magnetic origin of this anomaly, several experiments were

conducted. First of all, the magnetic transition of WC-10wt.%Co specimens was measured and a Curie temperature of approximately 1130K was found. A second set of experiments was then carried out on magnetically polarized samples to test the magnetic effects on the relaxation peak P2. These results were also compared with measurements made under a permanent magnetic field. The authors are convinced that these last observations, added to research published in previous works [6], allow a reconsideration of the microstructure defect model related to P2 relaxation peaks in WC-Co. The latest observations do not refute the model combining dislocation dynamics and W-rich zone dissolution; nonetheless, the variation of the relaxation time depending on temperature ranges may suggest a second interpretation based on point defects. The relaxation could be interpreted as a stress-induced reorientation of solute W-atoms clusters, and therefore correspond to a Zener relaxation mechanism.

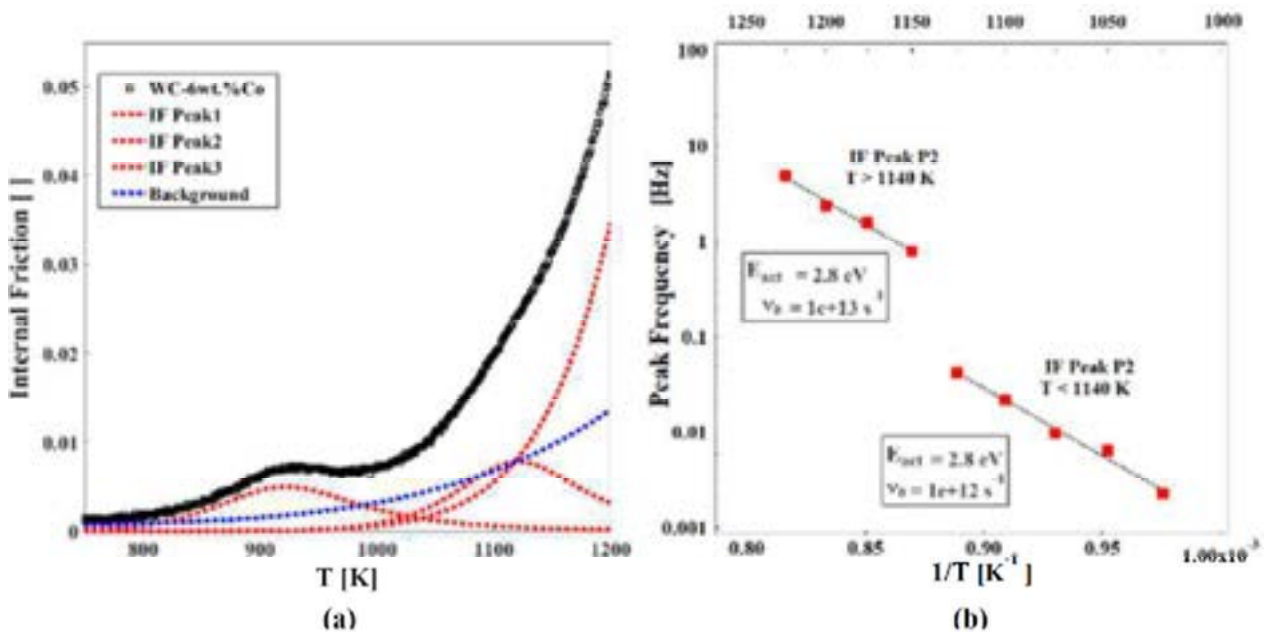


Fig. 1 – (a) WC-6wt.%Co Internal Friction spectrum as function of the temperature  
 (b) Arrhenius plots for the Relaxation peak P2, measured in isothermal mode on WC-6wt.%Co

- [1] D. Mari, “Understanding the mechanical properties of hardmetals through mechanical spectroscopy,” *Mater. Sci. Eng. A*, vol. 521–522, pp. 322–328, 2009.
- [2] R. Schaller, J. J. Ammann, and C. Bonjour, “Internal friction in WC-Co hard metals,” *Mater. Sci. Eng.*, vol. 105–106, no. PART 2, pp. 313–321, 1988.
- [3] R. Schaller, J. J. Ammann, D. Mari, and M. Maamouri, “Mechanical properties of tungsten carbide-11cobalt (WC-11Co) studied by internal friction,” *ASTM Spec. Tech. Publ.*, no. 1169, pp. 510–524, 1992.
- [4] D. Mari, S. Bolognini, G. Feusier, T. Viatte, and W. Benoit, “Experimental strategy to study the mechanical behaviour of hardmetals for cutting tools,” *Int. J. Refract. Met. Hard Mater.*, vol. 17, no. 1, pp. 209–225, 1999.
- [5] G. Östberg, B. Jansson, and H. O. Andrén, “On spinodal decomposition in the Co-W system,” *Scr. Mater.*, vol. 54, no. 4

SPEC. ISS., pp. 595–598, 2006.

- [6] S. Adjam, D. Mari, and T. La Grange, “Strain glass transition of cobalt phase in a cemented carbide,” *Int. J. Refract. Met. Hard Mater.*, vol. 87, no. 105161, 2020.

# Analysis of the recrystallization peak of Ti 5553 using torsion pendulum

L. Favre, D. Mari

(LQM EPFL, Lausanne, Switzerland) loic.favre@epfl.ch

## Abstract:

Titanium is a material of special interest because of the combination of low density, high mechanical properties and high resistance to corrosion.  $\beta$ -Metastable titanium alloys are used in many domains and especially landing gear assembly of aircraft [1]. This type of alloy typically is heat treated at 950°C for one hour (50°C above the  $\beta$ -transus) followed by quenching to have a homogeneous  $\beta$  structure. The alloy can undergo different heat treatments after homogenisation depending on the aimed microstructure. A typical heat treatment is a 3 hours dwell at 600°C to grow a thin  $\alpha$  microstructure in the  $\beta$  grain [2-3]. Mechanical spectroscopy is an interesting method to analyse the change in microstructure, allowing dynamic measurement. A periodic stress is applied to the sample and the shift between the signal and the response is related to the dissipated energy. Changes in microstructure typically shows change in internal friction. Samples of Ti5553 ( $\beta$ -transus 850°C) produced by TIMET have been cut to 1x4x30 mm and homogenised at 1000°C for 2 hours under argon atmosphere. They were then cold rolled to a thickness of 0.6 mm. The mechanical loss was measured in a forced torsion pendulum at a frequency of 1 Hz. The samples were heated above the  $\beta$ -transus (927 °C) and cooled down at the rate of 1°C/min. This cycle was repeated four times in total. We can see on figure 1 that two peaks are observed. The first at 740 K (467°C) is attributed dislocation movement in the  $\alpha$  phase probably controlled by vanadium diffusion. This peak cannot be observed during the first heating because the  $\alpha$  phase is not present. There is a sharp peak at 1137 K (864°C) that is attributed to recrystallisation. In fact, this peak only appears in samples that have been cold-worked. The temperature of this peak is only 10 K above the  $\beta$ -transus. It is possible that the fine  $\alpha$  microstructure that should appear during the heating restrains the movement of dislocations. When the  $\alpha$  phase dissolve, the mobility of dislocations increases leading to a fast recrystallisation and a sharp internal friction peak. After the second cycle only a background seems to remain at high temperature. The lowering level attained can be explained by some grain growth: the internal friction decreases until it reaches saturation in cycle three and four.

This research is promising as a way to control the recrystallization in Ti5553.

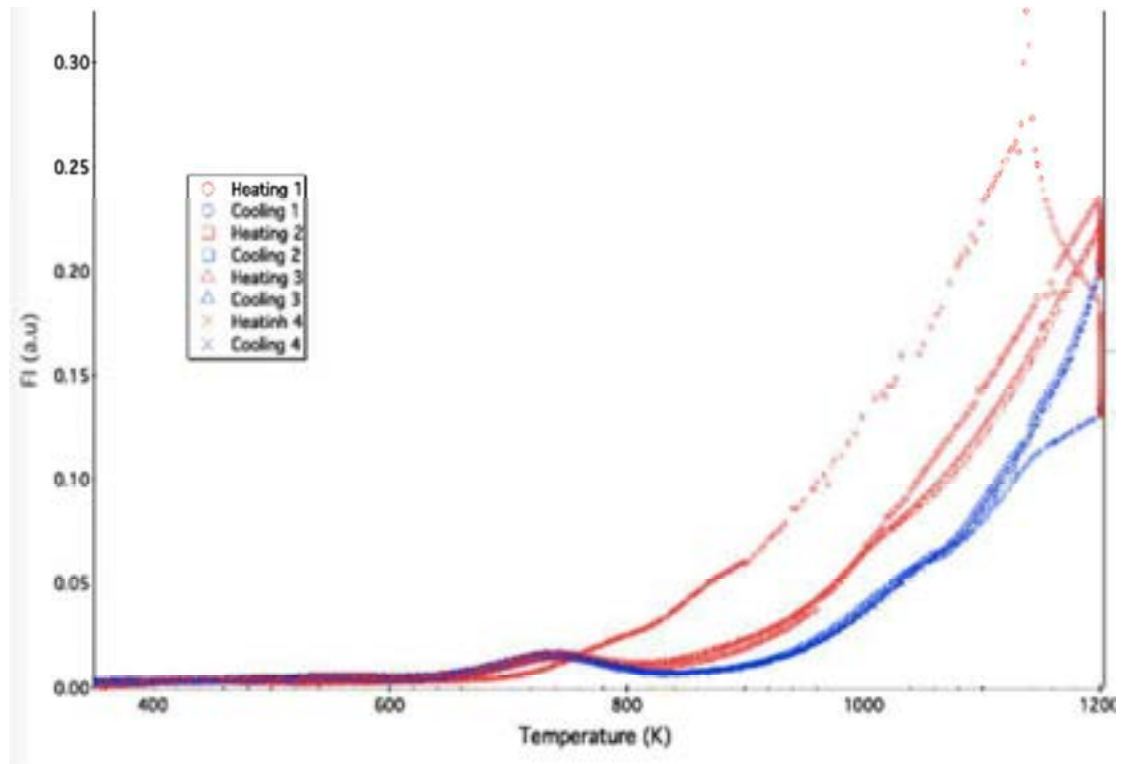


Figure 2: Internal friction spectra over four thermal cycles

[1] R.R. Boyer, R.D. Briggs, The use of  $\beta$  titanium alloys in the aerospace industry, *J. Mater. Eng. Perform.* 14 (2005) 681–685.

[2] P.J. Arrazola, A. Garay, L.M. Iriarte, M. Armendia, S. Marya, F. LeMaitre, Machinability of titanium alloys (Ti6Al4V and Ti555.3), *J. Mater. Process. Technol.* 209 (2009) 2223–2230.

[3] J.C. Fanning, R.R. Boyer, Properties of TIMETAL 555-a new near-beta titanium alloy, in: G. Luetjering, J. Albrecht (Eds.), *Titanium 2003: Science and Technology, IV*, Wiley-VCH, Hamburg, Germany 2003, pp. 2643–2650.

# ANALYSIS OF THE DAMPING CAPACITY IN A WELTKLANG SAXOPHONE MANUFACTURED IN 1969

B. Weidenfeller<sup>1\*</sup>, O.A. Lambri<sup>2</sup>, F.G. Bonifacich<sup>2</sup>, M.L. Lambri<sup>2</sup>, L. Weidenfeller<sup>3</sup>, A. Sover<sup>4</sup>

<sup>1</sup>*Department of Materials Science – Institute of Electrochemistry, Clausthal University of Technology, D-38678, Clausthal-Zellerfeld, Germany*

<sup>2</sup>*CONICET-UNR - Laboratorio de Materiales, Escuela de Ingeniería Eléctrica, Centro de Tecnología e Investigación Eléctrica, Facultad de Ciencias Exactas, Ingeniería y Agrimensura, Avda. Pellegrini 250, 2000 Rosario, Argentina*

<sup>3</sup>*Department of Mechanical Engineering, Ilmenau University of Technology, Max-Planck-Ring 12, 98693 Ilmenau*

<sup>4</sup>*Applied Polymer Technology, Ansbach University of Applied Science, Residenzstr. 8, 91522 Ansbach*

\*bernd.weidenfeller@tu-clausthal.de

The behaviour of the damping response as a function of temperature, frequency and strain, is studied in samples taken from a “Weltklang” Tenor saxophone, manufactured in 1969 in German Democratic Republic and used until 2018. The saxophone is constructed in brass and covered by a silver layer. According to X-ray fluorescence (XRF) studies the composition of the brass is 67wt. % Cu - 33 wt. % Zn. Samples were taken from the column, the bow and the bell of the saxophone. Each kind of sample was studied in the as-received state and after removing the Ag cover.

Figure 1 shows the behavior of damping and square frequency as a function of the temperature measured during the warming and its subsequent cooling down - one thermal cycle - for samples taken from the bell in the as-received state and after removing the Ag cover. The solvent grain boundary peak (SP) for the copper and the solute grain boundary peak (STP) of the zinc were recorded at around 530 K and 700 K, respectively [1,2]; during the warming. In addition, a damping peak at higher temperatures than the STP also develops, for both kinds of samples, whose peak temperature is close to 800 K. The appearance of the overlapping process was determined through the deconvolution of the spectra in single peaks. It was done by means of Peak Fit [3] using the second-derivative method with Gaussian functions.

For the sample without Ag cover, during the cooling after having reached 810 K, the peak at around 800 K markedly decreases its height and the peak height for STP increases. In contrast, the damping behaviour for a sample in the as-received state during the cooling, after the warming up to 1000 K, exhibits a decrease in the peak heights both for the STP and the peak at higher temperature. Besides, the peak height for the SP is also decreased during the cooling.

The changes in the damping spectra for each kind of sample will be explained considering the appearance, dissolution and reorganization of particles at the grain boundaries depending on the annealing temperature during the mechanical spectroscopy tests. In fact, it will be shown that the peak which appears at around 800 K is promoted by the appearance of particles at the grain boundaries [1,2].

In both thermal cycles shown in Figure 1, heating up to 1000 K led to a strong increase of pressure in the measurement system due to outgassing of samples which was higher for the silver-plated sample than for the samples without silver. Vapor could be related to the evaporation of  $\text{CO}_2$  and  $\text{CO}$ , from the transformation of the  $\text{ZnCO}_3$  at around 573 K and from the boiling of  $\text{Ag}_2\text{CO}_3$  at 823 K; as determined from Fourier transform infrared spectroscopy (FTIR) studies as a function of temperature.  $\text{ZnCO}_3$  and  $\text{Ag}_2\text{CO}_3$  would be by products remnants from the silver plating process.

The evaporation related processes from the above compounds would be controlling the arrangement of the particles at the grain boundaries and then, their mobility.

In addition, the changes in the damping spectra for the sample with the Ag cover, which was heated up to 1000K, could have also the contribution of Cu-Ag precipitates at the Ag rich interface. These precipitates can block the movement of the grain boundaries. Moreover, the contribution of melting processes at the interfaces from Zn-Ag and Cu-Ag could be also occurring.

On the other hand, amplitude dependent damping measurements performed at room temperature (RT) exhibit a decrease in damping as the oscillating strain increases. This might be explained by an instability in the dislocation's arrangement in the samples, as it is for example promoted by the vibrations while the instrument is played with increasing loudness. This instability would agree with the decrease in the damping values as a function of time which was measured in an ageing treatment of the samples under vibration at RT for 48 hours. These ageing mechanisms are discussed in the present work. In addition, complementary studies of thermogravimetry, FTIR as a function of temperature, XRF, scanning electron and laser light microscopy, and energy dispersive X-Ray spectroscopy were also performed.

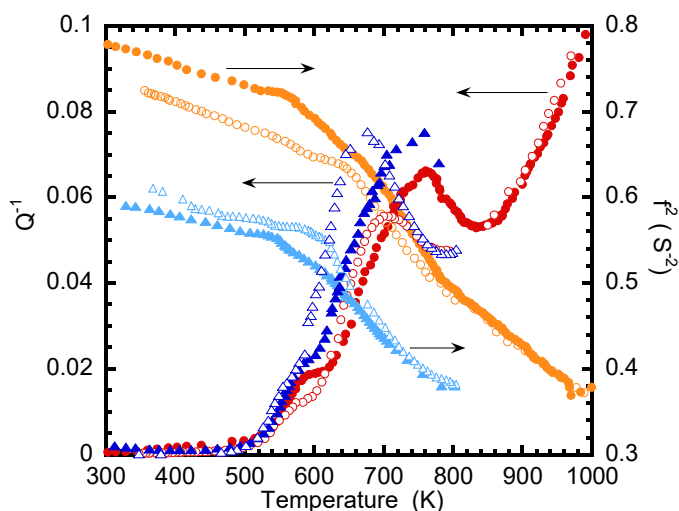


Fig. 1. Damping ( $Q^{-1}$ ) and square frequency ( $f^2$ ) measured during warming (full symbols) and cooling (empty symbols). In each curve only one of every three measured points was plotted for clarity. Samples taken from the saxophone bell. Circles: samples in the as-received state. Triangles: samples after removing the Ag cover by mechanical polishing.

- [1] R. Schaller, G. Fantozzi, G. Gremaud (Eds.), Mechanical Spectroscopy, Trans Tech, Switzerland, 2001.
- [2] M.S. Blanter, I.S. Golovin, H. Neuhäuser, H.-R. Sinning, Internal Friction in Metallic Materials. A handbook, Springer, Berlin, 2007.
- [3] PeakFit. V. 4., Jandel Scientific Software, Germany, 1995.

# STUDY OF THE DAMPING BEHAVIOUR ON IRON-ELECTRODEPOSITED COPPER SAMPLES FROM AN IONIC LIQUID

O.A. Lambri<sup>1</sup>, B. Weidenfeller<sup>2</sup>, F.G. Bonifacich<sup>1</sup>, L. Weidenfeller<sup>3\*</sup>,  
F.D.Lambri<sup>1</sup>, J. Xu<sup>4</sup>, G.I. Zelada<sup>1</sup>, G. Pulletikurthi<sup>4</sup>, F. Endres<sup>4</sup>

<sup>1</sup>*CONICET-UNR - Laboratorio de Materiales, Escuela de Ingeniería Eléctrica, Centro de Tecnología e Investigación Eléctrica, Facultad de Ciencias Exactas, Ingeniería y Agrimensura, Avda. Pellegrini 250, 2000 Rosario, Argentina*

<sup>2</sup>*Department of Materials Science – Institute of Electrochemistry Clausthal University of Technology D-38678, Clausthal-Zellerfeld, Germany*

<sup>3</sup>*Ilmenau University of Technology, Department of Microsystems Technology, Max-Planck-Ring 12, 98693, Ilmenau, Germany*

<sup>4</sup>*Institute of Electrochemistry, Clausthal University of Technology, D-38678 Clausthal-Zellerfeld, Germany*

\*laura.weidenfeller@tu-ilmenau.de

Recently, a new method of obtaining nanocrystalline iron by means of its electrodeposition on a given substrate material, which involves the use of an ionic liquid, was reported [1].

In the present work for the electro-deposition of iron on a copper substrate, an ionic liquid of 1-butyl-1-methylpyrrolidinium trifluoromethylsulfonate, (Py1,4)TfO, with a purity of 99% (IOLITEC GmbH, Germany) was used. The water content of the as received (Py1,4)TfO was measured to be 341 ppm by using Karl-Fischer titration. In addition, Iron(II) chloride, FeCl<sub>2</sub>, with a concentration 0.2 mol/L (from ALFA, Germany) was used as the salt. The electrodeposition on the copper substrate (working electrode) was performed at 363 K with a voltage of -1.7 V. Copper substrate was annealed under high vacuum at 800 K during 120 minutes prior the electrodeposition process. Platinum and iron were used as reference and counter electrodes, respectively. For more details about the electrodeposition process see Ref. [1]. Samples were electrodeposited during different periods of time, 10, 20, 30, 40 and 50 minutes. Mechanical spectroscopy (MS) measurements [2] (damping,  $Q^{-1}$ , and natural frequency,  $f$ ;  $f^2$  being proportional to the elastic shear modulus) were performed in an inverted torsion pendulum, as a function of temperature,  $T$ , frequency and strain. MS studies were performed also as a function of temperature under the application of a direct magnetic field,  $H_{DC}$ , of 30 kA m<sup>-1</sup>. The magnetic properties and structure characteristics of the electrodeposited samples have been determined by magnetic hysteresis loops and X-ray diffraction (XRD) studies performed on the samples both in the as-electrodeposited state and after the annealing during the MS studies. Magnetic hysteresis loops were recorded through a computer-controlled A.C. digital hysteresis recorder based on a Rigol DG1022 (China) synthesized wave function generator and Rigol DS1052E (China) high speed digital oscilloscope; at 20 Hz and at room temperature (RT). XRD studies were performed in a LD-554800 (Hürth, Germany), with high resolution module, using Mo-K $\alpha$  as incident radiation.

Figure 1 shows the damping spectra for an electrodeposited sample during 50 minutes measured during different heating runs, without  $H_{DC}$ . These heating

runs correspond to three successive thermal cycles which involve heating runs up to 973 K and their corresponding cooling down to RT. The first heating run (circles) exhibits the solvent grain boundary damping peak (SP) and the intermediate temperature grain boundary damping peak (ITP) at around 590 K and 630 K, respectively; corresponding to copper substrate [3]. In fact, in a copper sample without electrodeposition these two peaks were recorded only.

It should be noticed that at around 790 K the solvent grain boundary peak for the iron electrodeposited layer was found.

During the second heating run, which was performed without annealing after having reached the maximum temperature during the first heating run, a marked decrease in the peak height of SP of the Cu occurs and a new peak seems to arise at around 670 K. Moreover, during the third heating run, which was performed after an “in situ” annealing at 973 K during 20 minutes after having reached the maximum temperature of heating run #2, the peak height of this new peak increases markedly. This new peak could be related to the diffusion of copper along the Fe particles in agreement with previous works [4]. Fe particles could develop in the copper matrix due to the annealing during the MS tests as a result of the promotion of the Cu+ $\alpha$ -Fe intermediate phase, accordingly to the phase diagram [5]. Therefore, in the present work, for the Cu samples with a layer of electrodeposited Fe, the driving force controlling both the damping behavior as a function of the thermal cycles and this new peak will be studied through coupling the results of the above mentioned experimental techniques.

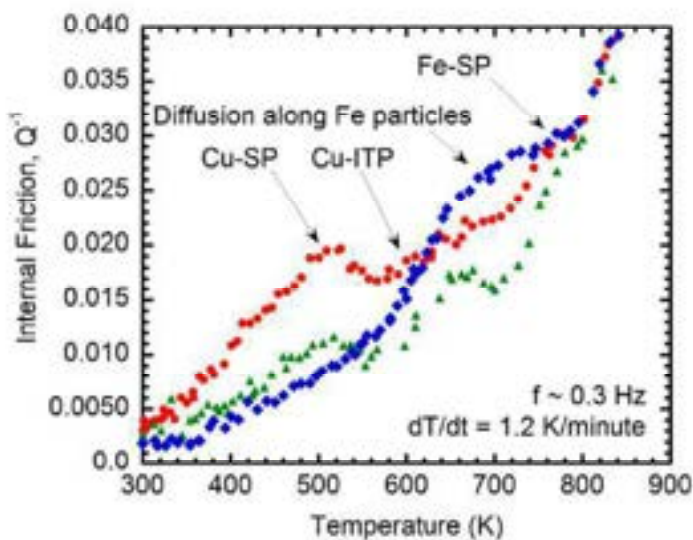


Fig.1: Damping spectra measured during heating for an electrodeposited sample. The maximum temperature for each heating run was 973 K. Circles denote the first heating run. The second heating run (triangles) was performed without annealing after having reached 973 K. The third heating run (diamonds) was performed after an “in situ” annealing at 973 K during 20 minutes.

- [1] P. Giridhar, B. Weidenfeller, S.Z. El Abedin, F. Endres, *Physical Chemistry Chemical Physics*, 16 (2014) 9317.
- [2] R. Schaller, G. Fantozzi, G. Gremaud (Eds.), *Mechanical Spectroscopy*, Trans Tech, Switzerland, 2001
- [3] F. Povolo, B. Molinas, *Il Nuovo Cim. D*, 14 (1992) 287
- [4] R. Monzen, K. Suzuki, A. Sato, T. Mori, *Acta Metall*, 31 (1983) 519.
- [5] W. Gale, T. Totemeir, *Smithells Metals Reference Book*, eighth ed, Elsevier Butterworth-Heinemann, Massachusetts, USA, 2004.

# Mechanical relaxation due to grain boundary diffusion and grain boundary viscous flow

Chuangchuang Duan<sup>1\*</sup>, Yujie Wei<sup>2,3</sup>

<sup>1</sup>*College of Mechanical Engineering and Automation, Huaqiao University, Xiamen, Fujian, 361021, China*

<sup>2</sup>*State Key Laboratory of Nonlinear Mechanics, Institute of Mechanics, Chinese Academy of Sciences, Beijing 100190, China*

<sup>3</sup>*School of Engineering Sciences, University of Chinese Academy of Sciences, Beijing 100049, China*

\* Presenter, [duanchuangch@lnm.imech.ac.cn](mailto:duanchuangch@lnm.imech.ac.cn)

Grain boundary (GB) diffusion and GB viscous flow play dominant roles in the mechanical relaxation of polycrystalline materials. The pioneering analyses of Zener and Kê reveal an internal friction peak resulting from GB viscous shearing. Later on investigations further account for relaxation associated with GB diffusion.

In this talk, we highlight the significance of the coupling between GB diffusion and viscous flow in governing the relaxation of polycrystalline materials at high temperatures or low frequencies. We establish a continuum model coupled viscous flow and diffusion in GBs and calculate the loss modulus spectra of polycrystalline solids with varying grain sizes  $d$  and different relative rates of diffusion and viscous flow  $R$ . The characteristic relaxation times can be extracted from the positions of peaks in the loss modulus spectra. By analyzing the variations of the characteristic relaxation times with grain size  $d$  and relative diffusion rate  $R$ , the characteristic deformation modes in polycrystalline materials are identified. We illustrate that competitive viscous flow and diffusion for normal stress relaxation give rise to distinct dependence of relaxation time on grain size. The essential features of internal friction spectrum of polycrystalline materials from our analysis are consistent with available experimental observations. These findings may also be applicable to study relaxation dynamics of other material systems such as metallic glasses and porous materials.

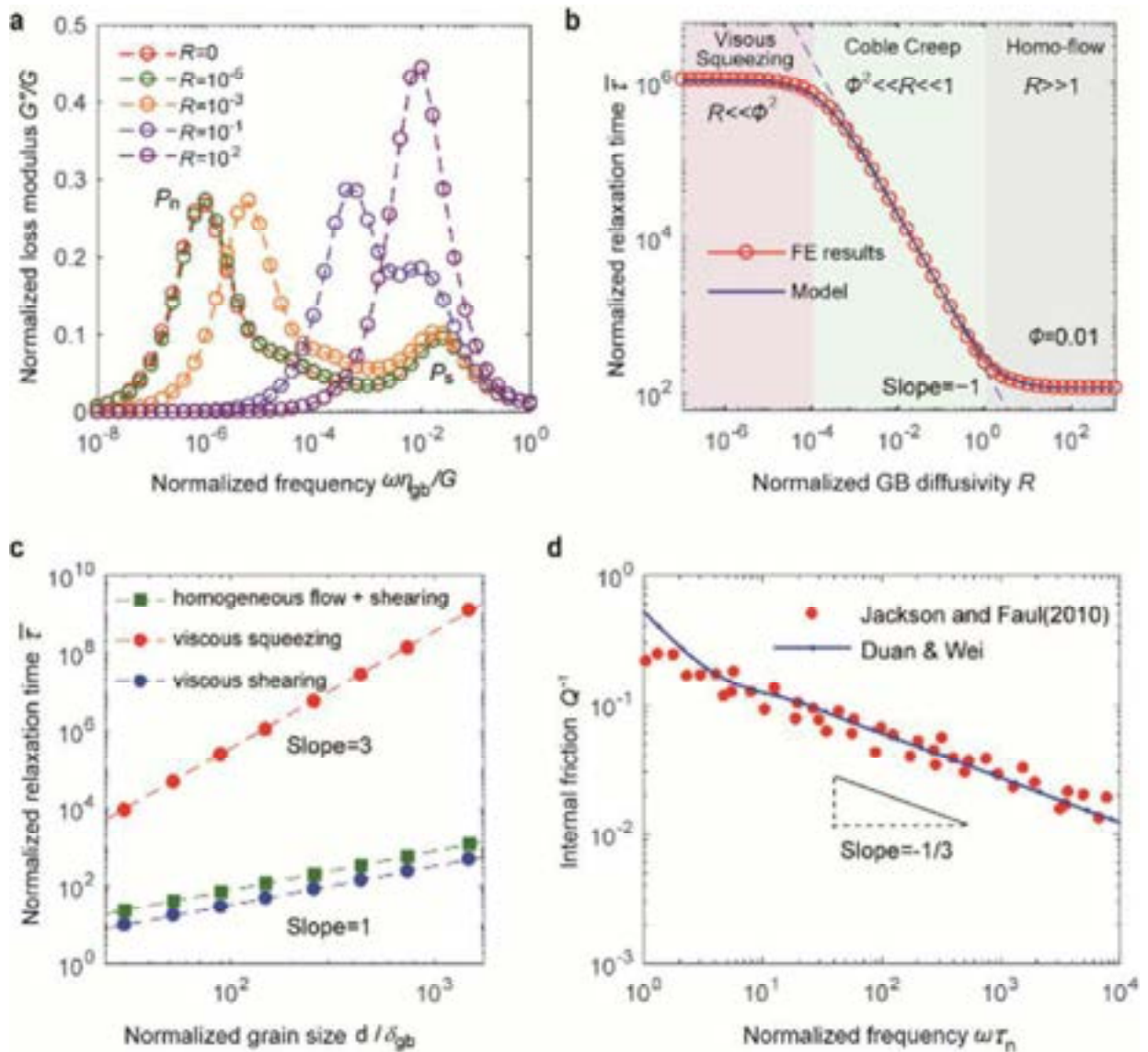


Fig. 1. Mechanical relaxation due to GB diffusion and GB viscous flow. (a) Normalized loss modulus spectra of polycrystalline samples with GB diffusivities denoted by  $R$ . The relaxation times at the loss modulus peaks in (b) as functions of normalized GB diffusivity  $R$  and in (c) as functions of normalized grain size. (d) Internal friction as a function of frequency normalized by the relaxation time of GB normal stress. The red dots represent experimental results and the blue line comes from our FE calculation.

[1] Duan C, Wei Y., *Science China Materials*, **65**(2022) 1403-1412.

<https://doi.org/10.1007/s40843-021-1837-9>

[2] Duan C, Wei Y., *Acta Materialia*, **201**(2020) 350-363.

<https://doi.org/10.1016/j.actamat.2020.10.004>

# **Shape memory alloys and phase transition**

# DETERMINATION OF THE CLAUSIUS-CLAPEYRON COEFFICIENT IN SMA THROUGH MECHANICAL SPECTROSCOPY

M. Pérez-Cerrato<sup>1\*</sup>, B. Maass<sup>2</sup>, M.L. Nó<sup>3</sup>, J.M. San Juan<sup>1</sup>

<sup>1</sup> *Dpt. Física de la Materia Condensada, Facultad de Ciencia y Tecnología, University of the Basque Country, UPV/EHU, Bilbao, Spain*

<sup>2</sup> *INGPULS GmbH, Bochum, Germany*

<sup>3</sup> *Dpt. Física Aplicada II, Facultad de Ciencia y Tecnología, University of the Basque Country, UPV/EHU, Bilbao, Spain*

\*mikel.perez@ehu.eus

The unique properties of Shape Memory Alloys (SMAs) can be of great interest in a wide variety of fields, and all of that comes from the microscopic mechanisms that are responsible for the reversible martensitic transformation. SMAs are considered as high damping materials due to the motion of martensitic interfaces and there are previous works that study the way of developing high damping SMAs [1], and to this end, mechanical spectroscopy is a powerful tool to study the mechanisms responsible for the dissipation of mechanical energy. However, the damping behavior of SMAs is rather complex, and the internal friction spectrum during a thermoelastic martensitic transformation can be explained as the addition of three contributions [1,2]: the transitory or kinetic term, which is strongly dependant on the temperature rate ( $\dot{T}$ ), the oscillation frequency ( $\omega$ ) and the applied stress amplitude ( $\sigma_0$ ); the isothermal term, associated to the transformation itself; and the intrinsic term due to the contribution of each phase (austenite and martensite). From the theoretical models explaining this behavior, a lot of information can be obtained about the thermo-mechanical properties of the SMA, and in the present work our interest is focused on the Clausius-Clapeyron (C-C) coefficient, which in the first-order phase transitions depicts the change of the transformation temperature with the applied stress. This parameter is critical in SMAs because determines the stress-induced transformation controlling many of their applications. In the present work we demonstrate that the C-C coefficient can be determined by mechanical spectroscopy and the corresponding methodology is developed.

The experimental study is focused on the NiTiHf High-Temperature SMA, and we profit from the advantage of the non-destructive nature of the internal friction measurements, which is especially relevant in the case of NiTiHf alloys because the high cost of production. In addition, this HTSMA transforms at 550K, making the direct measurements of C-C coefficient challenging, and determining this coefficient through mechanical spectroscopy is really helpful.

The material used within this work was a  $\text{Ni}_{49.5}\text{Ti}_{35.5}\text{Hf}_{15}$  (at.%) alloy produced by induction melting at INGPULS GmbH. Samples for mechanical spectroscopy measurements were cut into rectangular cross section rods ( $0.9 \times 5 \times 50 \text{ mm}^3$ ). The experiments were performed in a sub-resonant torsion pendulum designed to work in a range of temperatures between 90K and 1150K, with frequencies between  $10^{-4}$  and 10Hz as described in reference [3].

From the internal friction measurements it is possible to obtain the transformed volume fraction of martensite  $n(T)$ , the start and finish temperatures of the direct and reverse transformation ( $M_s$ ,  $M_f$ ,  $A_s$  and  $A_f$ ), as well as the softening of the dynamic modulus, as it is depicted in Figure 1. The transformation peaks were analysed and the transitory term was isolated in order to obtain the C-C coefficient through the model for martensitic transformation [4].

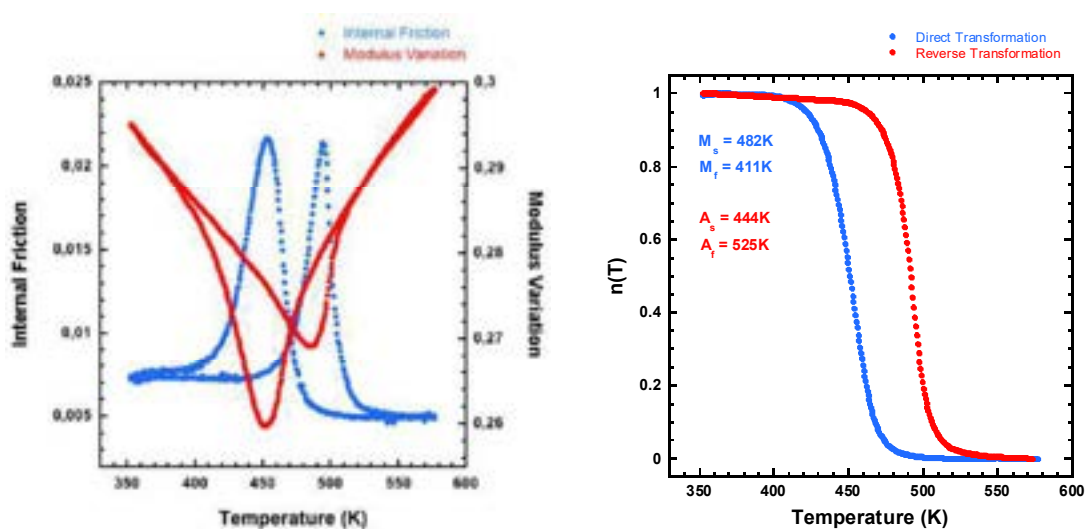


Fig. 1. Internal friction spectra and dynamic modulus variation curve, showing the martensitic transformation. This particular measurement was done with a heating/cooling rate of 2 K/min and a frequency of 3 Hz. Nevertheless, these parameters were changed in a large range, in order to analyze the spectra through the theoretical model of Gremaud et al. [4]. From the series of spectra, the Clausius-Clapeyron coefficient was determined.

- [1] J. San Juan, M.L. Nó, *J. Alloys & Compounds* **355** (2003) 65-71.
- [2] J. San Juan, R.B. Pérez-Sáez, *Mater. Sci. Forum*, **366-368** (2001), 416-437.
- [3] I. Gutierrez-Urrutia, M.L. Nó, E. Carreño-Morelli, B. Guisolan, R. Schaller, J. San Juan, *Mater. Sci. Eng. A*, **370** (2004), 435-439.
- [4] G. Gremaud, J.E. Bidaux, W. Benoit, *Helv. Phys. Acta*, **60** (1987), 947-958.

# SUPERELASTIC DAMPING IN Cu-BASED SHAPE MEMORY ALLOYS BY NANO-COMPRESSION TESTS

J.F. Gómez-Cortés<sup>1\*</sup>, V. Fuster<sup>1,2</sup>, M. Pérez-Cerrato<sup>1</sup>, P. Lorenzo<sup>1</sup>, I. Ruiz-Larrea<sup>3</sup>,  
T. Breczewski<sup>3</sup>, M.L. Nó<sup>3</sup>, J.M. San Juan<sup>1</sup>

<sup>1</sup>*Dpt. Física de la Materia Condensada, Facultad de Ciencia y Tecnología, Universidad del País Vasco UPV/EHU, Bilbao, Spain*

<sup>2</sup>*Instituto de Física Rosario, Consejo Nacional de Investigaciones Científicas y Técnicas (CONICET) □ Universidad Nacional de Rosario, 2000 Rosario, Argentina*

<sup>3</sup>*Dpt. Física Aplicada II, Facultad de Ciencia y Tecnología, Universidad del País Vasco UPV/EHU, Bilbao, Spain*

\* josefernando.gomez@ehu.es

Shape memory alloys (SMA) are considered as High-Damping Materials (HDM) due to the martensite interface mobility [1]. The superelastic effect (SE) is a thermomechanical property distinctive of SMA, and results from the stress-induced martensitic transformation on the austenite phase, being completely reversible when the stress is released. The output signal during one SE cycle draws a hysteresis loop on the stress-strain field, and this loop area offers a quantitative way to measure the dissipated energy per cycle, using the loss factor  $\eta$ , as the index ratio between dissipated energy (hysteresis cycle area) and the total applied energy (load area). The damping behavior at macroscopic scale was widely measured in many different families of SMA. However, damping applications in micro and nano technologies, for instance in Micro Electro-Mechanical Systems (MEMS), represent a new challenge for the use of SMA as HDM. The mechanical damping capacity was studied in Cu-Al-Ni SMA at the nano-scale using nano-compression tests on micro-pillars, getting outstanding results in terms of a superlative damping capacity (ultrahigh damping  $\eta > 0.2$ ) [2], exhibiting long-term reliability ( $> 5000$  cycles) [3,4]. In addition, new size-effects appear when decreasing the dimension of the samples [2,5].

In this work, we used an instrumented nano-indenter to perform nano-compression tests in micro and nano pillars of SMA, in order to study the superelastic damping capacity at very small scale. Several series of pillars were milled, in previously growth single crystals, by Focused Ion Beam (FIB) technique from 2  $\mu\text{m}$  down to 250 nm. The study was carried out on different ternary and quaternary SMA, not explored yet in this field of damping at micro/nano scale, such as Cu-Al-Be, Cu-Al-Ni-Be, and Cu-Al-Ni-Ga. We compare loss factor results at the nano-scale with previous findings in the Cu-Al-Ni alloy, as well as with its macroscopic counterparts. The influence of the other incorporated elements in the Cu-based SMA is analyzed and discussed.

As an example of the FIB milled pillars, Figure 1a exposes a Cu-Al-Ni pillar of 900 nm in diameter and its superelastic response under a nano-compression test. The superelastic cycle is plotted in Figure 1b in both kind of axis, stress-strain and load-displacement. Thus, it can be appreciated the small critical load to provoke the stress-induced transformation as well as the small displacement of about 160 nm involved in the fully closed cycle. The enclosed area inside the cycle evidences an ultra-high damping, which is analyzed along the present work for the different SMA studied at micro and nano scale.

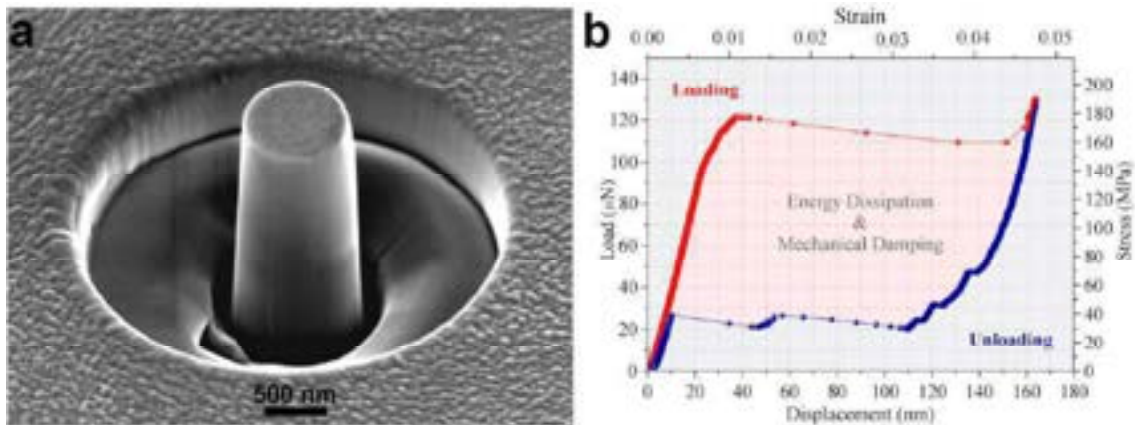


Fig. 1. (a) Single crystal [100] oriented pillar with 900 nm in diameter. (b) Superelastic response on the load-displacement and strain-stress axis, measured on the showed pillar.

- [1] J. San Juan, M.L. Nó, *J. Alloys & Compounds* **355** (2003) 65-71.
- [2] J.M. San Juan, M.L. Nó, C.A. Schuh, *Nat. Nanotechnology* **4** (2009) 415-419.
- [3] J. San Juan, J.F. Gómez-Cortés, G.A. López, C. Jiao, M.L. Nó, *Appl. Phys. Lett.* **104** (2014) 011901.
- [4] J.F. Gómez-Cortés, M.L. Nó, I.R. Ruíz-Larrea, T. Breczewski, A. López-Echarri, C.A. Schuh, J.M. San Juan, *Acta Mater.* **166** (2019) 346-356.
- [5] J. San Juan, M.L. Nó, *J. Alloys & Compounds* **577S** (2013) S25-S29.

# INTERNAL FRICTION ASSOCIATED WITH $\epsilon$ MARTENSITE IN SHAPE MEMORY STEELS

L. Del-Río<sup>1</sup>, M.L. Nó<sup>1</sup>, A. Sota<sup>2,3</sup>, I. Perez-Casero<sup>2</sup>, J.F. Gómez-Cortés<sup>1</sup>, M. Pérez-Cerrato<sup>1</sup>, A. Veiga<sup>2,3</sup>, S. Ausejo<sup>2,3</sup>, N. Burgos<sup>2,3</sup>, J.M. San Juan<sup>1\*</sup>

<sup>1</sup> *Dpt. Física, Facultad de Ciencia y Tecnología, Universidad del País Vasco, UPV/EHU, Apdo 644, 48080-Bilbao, Spain.*

<sup>2</sup> *CEIT-Basque Research and Technology Alliance, BRTA, Manuel de Lardizabal 15, 20018 Donostia/San Sebastian, Spain*

<sup>3</sup> *Universidad de Navarra, Tecnun, Manuel de Lardizabal 13, 20018 Donostia/San Sebastian, Spain.*

\* [jose.sanjuan@ehu.es](mailto:jose.sanjuan@ehu.es)

Different families of shape memory alloys (SMA) were developed because the high number of applications related to shape memory and superelastic properties. The more known SMA are those of the Ti-Ni system and the Cu-Al-based, but several alternative SMA families were also investigated, and among them the Fe-Mn-Si-Cr-Ni family attracted the interest because of their low cost. In this iron-based SMA, the shape memory effect is associated with the martensitic transformation between the austenite (FCC) and the  $\epsilon$ -martensite (HC), which can be well identified by internal friction measurements [1]. Although the  $\epsilon$  martensitic transformation is non-thermoelastic and do not exhibit superelastic effect, these alloys found several applications based on the shape memory effect [2, 3] and the research was focused on obtaining large recovery strain [4, 5]. In addition, the convergence of the composition of these SMA with the Fe-Mn steels, exhibiting TRIP (Transformed Induced Plasticity) and TWIP (Twinning Induced Plasticity) behavior [6], gave place to a renewed interest in this shape memory steels. At present, the new paradigm of Additive Manufacturing [7], has also irrputed in SMA, being mainly focused on the Ti-Ni system [8] and particularly using the powder bed technologies [9]. However, in this Fe-M-Si-Cr-Ni SMA, only a partial  $\epsilon$ -martensitic transformation, with a low latent heat, takes place, making difficult its investigation by conventional techniques like differential scanning calorimetry (DSC), which is widely used in many studies of SMA. On the contrary, mechanical spectroscopy offers a powerful tool to study the  $\epsilon$ -martensitic transformation in this shape memory steels.

In this work, the study of the  $\epsilon$ -martensitic transformation was approached, by mechanical spectroscopy, in two alloys with different chemical composition of Mn and Si wt%, Fe-20Mn-5Ni-8.5Cr-5Ni and Fe-16Mn-6Si-9.2Cr-5Ni, produced by conventional casting and rolling, in comparison with another third alloy with a balanced intermediate composition, Fe-19Mn-6Si-9.2Cr-5Ni, produced by additive manufacturing using the Laser Metal Deposition (LMD) technique.

The presence of the  $\epsilon$ -martensitic transformation and its evolution of cycling were followed through internal friction and dynamic modulus measurements. An internal friction peak is associated with the forward and reverse  $\epsilon$ -martensitic transformation during cooling and heating respectively, as well as a change of the dynamic modulus, as it is shown in Fig. 1a. In parallel, the microstructure of the sample, as well as the apparition and evolution on cycling of the  $\epsilon$ -martensite, was observed by scanning electron microscopy (SEM) in back scatter mode as well as through in-situ cooling and heating experiments inside the SEM. As an example, a SEM image of the  $\epsilon$ -martensite is shown in Fig. 1b.

Finally, the correlation between the internal friction peak strength associated to the  $\epsilon$ -martensite, with the electron microscopy observations was analyzed and discussed.

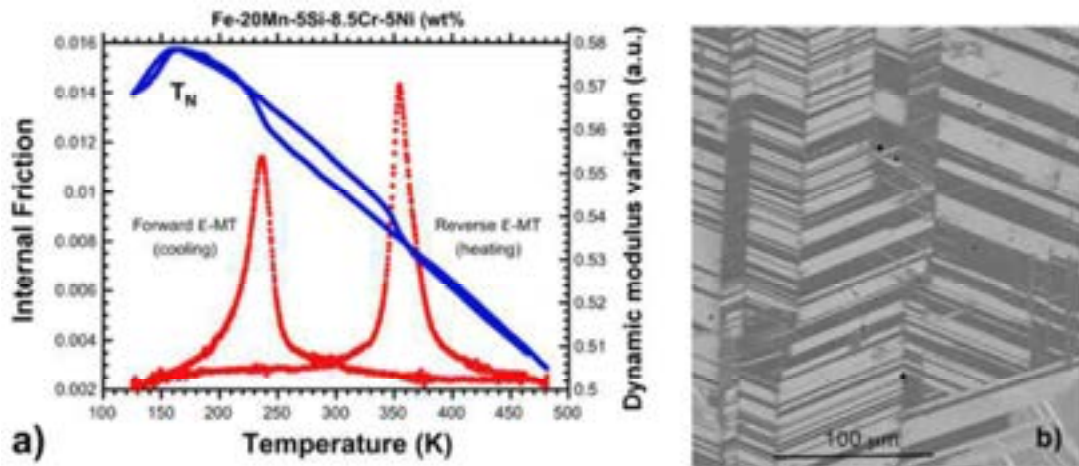


Fig. 1. (a) Internal friction spectra and dynamic modulus, measured during cooling and heating, showing the peaks associated to the forward and reverse  $\epsilon$ -martensitic transformation. (b) Back scatter SEM image of the  $\epsilon$ -martensite variants produced during cooling.

- [1] R.B. Pérez-Sáez, M.L. Nó, J. San Juan, *J. Alloys & Comp.* **211/212** (1994) 212.
- [2] A. Druker, A. Perotti, I. Esquivel, J. Malarria, *Mater & Design* 56 (2014) 878.
- [3] A. Cladera, B. Weber, C. Leinenbach, C. Czaderski, M. Shahverdi, M. Motavalli, *Const. & Building Mater.* 63 (2014) 281.
- [4] Y.H. Wen, H.B. Peng, D. Raabe, I. Gutierrez-Urrutia, J. Chen, Y.Y. Du, *Nature Communications* 5 (2014) 5964.
- [5] H. Peng, J. Chen, Y. Wang, Y. Wen, *Adv. Eng. Mater.* 20 (2018) 1700741.
- [6] P. Chowdhury, D. Canadinc, H. Sehitoglu, *Mater. Sci. Eng. R* 122 (2017) 1-28.
- [7] J.O. Milewski, *Additive Manufacturing of Metals*, Springer (2017).
- [8] M. Elainia et al. *Progress in Materials Science* 83 (2016) 630-663.
- [9] A.N. Alagha, S. Hussain, W. Zaki, *Mater. & Design* 204 (2021) 109654.

## Effect of stabilization and destabilization by prestrain on acoustic properties and resistivity of Ni-Ti-Nb shape memory alloy

A. Ojeda\*, C. Picornell, J. Pons, S. Kustov

*Universitat de les Illes Balears, Cra Valldemosa km. 7.5, Palma de Mallorca 07122, Spain*

\*alex.ojedasanchez@gmail.com

Ni-Ti-Nb shape memory alloys are famous for their wide hysteresis of the martensitic transformation, ca. 50-70 K, compared with 30 K in binary alloys [1]. The difference between the temperature of the first reverse on heating and consequent direct transformation can be further increased by prestrain of Ni-Ti-Nb alloys up to 150 K [2]. This one-time increase of the reverse transformation is usually referred to as stabilization of martensite. The origin of the prestrain-induced stabilization of Ni-Ti-Nb alloys remains a subject of intense discussions due to a complex microstructure of hypoeutectic alloys. In the present work we use commercial Ni<sub>45.2</sub> Ti<sub>45.9</sub> Nb<sub>3.9</sub> ( $\pm 0.3\text{at}\%$ ) alloy (Memry Corporation, USA), prestrained by drawing. In the present work we apply an acoustic technique and resistivity measurements to characterize structural modifications of the alloy induced by prestrain. We use the samples in as received stabilized state and tensile stabilized samples prestrained by compression. We show first that the stabilization effect can be removed by compressive strain. Measurements of the temperature spectra of elastic (Young's modulus) and anelastic properties (linear and non-linear damping) between 15 and 300 K show a dramatic suppression of anelasticity and increase of the modulus induced by stabilization over the entire temperature range studied. On the other hand, the prestrain that induces stabilization of the samples reduces substantially (by ca. 20%) their resistivity. This effect stems from the decrease of the residual low-temperature resistivity. Acoustic properties and resistivity data do not agree with the most popular hypothesis of stabilization effect in Ni-Ti-Nb as due to the plastic prestrain of Nb particles.

[1] X.M. He, D.S. Yan, L.J. Rong, YY. Li, AIP Conf. Proc. 711 (2004) 18-25.

[2] K.N. Melton, J. Simpson, T.W. Duering, in: Proc. Of the International Conference on Martensitic Transformations, The Japan Inst. Of Metals, 1986, pp. 1053-1058

# Effect of Ni and Mn additions on the damping characteristics of Cu-Al-Fe based High Temperature Shape Memory Alloys

S.Santosh\*, Kevin Thomas. J, Rajkumar. K, Sabareesh. A

Department of Mechanical Engineering, Sri Sivasubramaniya Nadar College of Engineering,

Kalavakkam – 603110. Tamilnadu, India.

*\*Corresponding author email: santoshs@ssn.edu.in*

## Abstract

Shape Memory Alloys (SMAs) are smart materials which involves a transition from martensitic phase to austenitic phase when it is induced by a change in temperature or stress. SMAs have proved to possess damping properties which is caused by the internal friction that occurs in the martensitic phase. This work focuses on exploring the damping properties of the copper-based ternary and quaternary SMAs using Dynamic Mechanical Thermal Analysis by calculating internal friction. The results show that the peak value of damping lies near to the martensitic start temperature of the respective alloys. Addition of quaternary element to the existing ternary alloy decreases the transformation temperatures thereby decreasing the temperature at which the peak damping value occurs. Ni - Ti alloy attains its peak value of damping at temperatures lower than the temperatures at which peak value is attained for these alloys. Therefore the results proves that the damping can be done using SMAs for a wide range of temperatures.

Keywords: Cu-Al-Fe, internal friction, damping, High temperature shape memory alloy, characterization

## Defect relaxation and phase transition behavior in manganese-containing microalloyed steels

M. Sun<sup>1\*</sup>, X.Q. Liu<sup>1</sup>, W.B. Jiang<sup>1,2</sup>, X.P. Wang<sup>1</sup>, Q.F. Fang<sup>1</sup>

<sup>1</sup>Key Laboratory of Materials Physics, Institute of Solid State Physics, HFIPS, Chinese Academy of Sciences, Hefei 230031, China

\*mengsun@issp.ac.cn

As one of the third-generation advanced high strength steels (3G-AHSS), medium Mn steels have been widely applied in transportation vehicles such as high-speed railways and ships, owing to the advantages such as lightweight, low cost, and elevated product of strength and elongation (PSE, usually up to 20–50 GPa%). The elevated PSE in the medium Mn steels can be attributed to the co-existence of retained austenite ( $\gamma_R$ ) and martensite ( $\alpha'$ ) phases. On the one hand, the transformation of  $\gamma_R$  into  $\alpha'$  under external stress can induce plasticity (TRIP), while the  $\alpha'$  phase with high dislocation density can ensure the high strength of the material. On the other hand, the interfaces between  $\gamma_R$  and  $\alpha'$  phases can significantly hinder the crack spreading and improve the plasticity of the material. Therefore, an in-depth and comprehensive understanding of the reverse austenitic transformation (RAT) and martensitic transformation (MT) is necessary for the design of medium Mn steels with high performance. In our work, the IF behavior of a Fe-7Mn-0.1C medium Mn steel with different heat-treatment states were systematically investigated in the range from room temperature (RT) to 800 °C. Two IF peaks corresponding to the RAT and MT were observed, and the mechanisms of the IF peaks were carefully discussed. Also, a design concept of heat-treatment parameters based on phase transition IF peaks was suggested to significantly improve the PSE of the medium Mn steel. This study can not only deepen the understanding of phase transitions but also has a reference value for performance optimization of medium Mn steels.

# **Composites and inhomogeneous materials**

## Comparison of Internal friction measurements on Ni-Ti reinforced smart composites prepared by Additive Manufacturing

S. Santosh<sup>1\*</sup>, G. Nithyanandh<sup>1</sup>, J. Ashwath<sup>1</sup>, K. Lalith Kishore<sup>1</sup>

<sup>1</sup>Department of Mechanical Engineering, Sri Sivasubramaniya Nadar College of Engineering, Kalavakkam, Chennai-603110, India

\*Email: [santoshs@ssn.edu.in](mailto:santoshs@ssn.edu.in), [santosh13011@mech.ssn.edu.in](mailto:santosh13011@mech.ssn.edu.in)

Polymer 3D printing has been utilized in aerospace to produce complex lightweight structures, in medical fields to print tissues and organs [1], and in a number of other industries to combat the rising demand for weight-saving engineering solutions. Pure polymer goods created through 3D printing, on the other hand, lack strength and functionality. Therefore, by combining matrix and reinforcing materials, 3D printing of polymer composites can overcome these problems. Also various researchers have used matrix system either epoxy resin or vinyl ester resin. Despite its wide usage, resins have few drawbacks like microleakage and high curing time which could be eliminated by 3D printing. In this work, we have focused on using 3D printed polymer matrix system. To enhance the property, shape memory alloys (SMAs) are introduced in the structure as a reinforcement. Shape memory alloys are a class of smart material that, when heated over a certain temperature, can recover deformation. SMAs exhibit two main characteristics i.e., shape memory effect (SME) and superelasticity (SE) [2]. SMAs are available in a variety of shapes, including wires, springs, sheets, and tubes. The SMA wires can be embedded in the composites for a variety of reasons, such as enhancing mechanical properties, shape morphing of structures and for use as actuators. Damping is one such mechanical property which can be enhanced by reinforcing SMA wires. In this research work, the samples were fabricated using 3D printing of PLA and PETG with SMA wires embedded in two different forms i.e., continuous and discontinuous. The samples were then examined under a dynamic mechanical analyzer to study the damping (internal friction) behavior of the smart composites. It has been found that the incorporation of SMA wires into the matrix had a significant influence on the dynamic mechanical properties. Also, the samples with SMA reinforced in continuous manner had the higher value of  $\tan \delta$  i.e., it had good damping properties in comparison to short fibre reinforced composites.

[1] N.B. Morgan, Medical shape memory alloy applications - The market and its products, *Mater. Sci. Eng. A*, **378** (2004) 16-23.

[2] C.M. Wayman, Shape Memory Alloys, *MRS. Bull.*, **18** (1993) 49-56.

# EVALUATION OF THE DIAGENESIS DEGREE IN ARCHAEOLOGICAL BONES THROUGH THE HAVRILIAK—NEGAMI EXPRESSION

M.L. Lambri<sup>1,2</sup>, O.A. Lambri<sup>1,2</sup>, M. Weidenfeller<sup>3\*</sup>, B. Weidenfeller<sup>4</sup>, F.G. Bonifacich<sup>1,2</sup>, G.I. Zelada<sup>1,2</sup>, R.R. Mocellini<sup>1,2</sup>, A.M. Rocchietti<sup>2</sup>

<sup>1</sup>CONICET-UNR – Lab. de Materiales, Esc. de Ing. Eléctrica, CETIE, Fac. de Cs. Exactas, Ingeniería y Agrimensura, Avda. Pellegrini 250, 2000 Rosario, Argentina

<sup>2</sup>Center for the Studies in Historical Archaeology, Faculty of Humanities and Arts, National University of Rosario, Entre Ríos 758, 2000 Rosario, Argentina

<sup>3</sup>Friedrich Alexander-Universität Erlangen-Nürnberg, Fakultät für Medizin, Krankenhausstr. 12, 91054 Erlangen, Germany

<sup>4</sup>Department of Materials Science – Institute of Electrochemistry, Clausthal University of Technology, D-38678, Clausthal-Zellerfeld, Germany

\*martin.weidenfeller@fau.de

The damping behaviour recorded in three archaeological bones recovered from the Archaeological Site (AS) from “Boca de Lega” in Santa Fe, Argentina, is studied. The damping peak related to the viscous movement of the collagen fibrils due to the triple helix to random coil transition (TH→RC) from the collagen, is studied from the behaviour of the parameters of the Havriliak-Negami (HN) expression for dynamical modulus (eq.1). HN is fitted to the damping spectra from the archaeological bones, exhibiting different degree of diagenesis, and then, the different mesostructures in the bones promoted by the diagenetic processes can be inferred.

$$G^*(T, \omega) = G_u(T) - (\delta G(T) / \left[ 1 + (i\omega \tau(T))^\alpha(T) \right]^{\beta(T)}) \quad (1)$$

where  $G^* = G' + i G''$  is the complex modulus.  $T$ ,  $\omega$ ,  $G_u(T)$  and  $\delta G(T)$  are the absolute temperature, the circular frequency, the unrelaxed modulus and the relaxation magnitude, respectively.  $\tau(T) = \tau_0 e^{(H/kT)}$  is the relaxation time, with  $\tau_0$  the pre-exponential factor and  $H$  the activation energy, respectively. Besides,  $\alpha$  and  $\beta$  are phenomenological parameters that described the symmetrical and asymmetrical broadening of the relaxation peak, respectively.

Indeed, the behaviour of the parameters calculated from the HN expression are considered as a function of the Ca content and the amount of substitution of Na and K, related to the  $Ca^{2+}$ , in the dahllite. Therefore, the behaviour of  $\alpha$ ,  $\beta$  and  $\tau_0$  calculated from the damping spectra can be related to different stages of diagenesis in the remnant collagen in the archaeological bone.  $H$  in the relaxation time and the relaxation strength for the HN expression was calculated following the procedure described in Ref. [1]. Ca and their substitutions were evaluated from a wide study of scanning electron microscopy (SEM) plus energy dispersive X-ray spectroscopy (EDS). In addition, the extra porosity in archaeological bones, due to the diagenetic processes during the burial at the AS, was determined from 2D image analysis from SEM micrographs.

In order to take a reference state for the HN-parameters, additional MS measurements both as a function of temperature and strain were also performed in fresh bones and fresh bones after controlled ageing treatments. Figure 1 shows the  $\tan(\phi)$  spectra measured for fresh and two archaeological bones, with different

degree of diagenesis, in the temperature range from the TH→RC onwards.  $P_A$  peak is related to the viscous movement of the collagen fibrils promoted by the TH→RC due to the break of the hydrogen bridges.  $P_B$  peak was only recorded in fresh bones, and it is related to a subsequent stage of massive bulk deterioration of the collagen, involving firstly an additional shrinkage from the mesostructure and finally the loss of the mechanical integrity of the bulk collagen [1]. The maximum temperature for the measurement of archaeological bones has depended on the kind of sample. However, often these samples cannot reach describing the  $P_B$  peak, since the subsequent contraction from the mesostructure cannot be supported by the bone, due to the large deterioration in the remnant collagen fibrils. It explains the high brittleness from the archaeological samples.

Dotted lines in Figure 1 represent  $P_A$  peak, for the bone samples, reconstructed by means of the HN expression after determining their parameters from the experimental data. As it can be seen from the Figure, the numerical fits to the experimental data are reasonably good for all the cases. It was found that a decrease in the calcium content due to diagenetic processes in around 100%, leads to an increase both in  $\beta$  and in  $\tau_0$  in around 11% and in more of one order of magnitude, respectively. In contrast,  $\alpha$  only increases in around 4%.

The values for HN parameters for a fresh bone for  $\beta$  and  $\tau_0$  are smaller than in archaeological bones in around 30% and in more than three orders, respectively. In fact, in fresh bone the  $P_A$  peak is described with a  $\tau_0$  in the range of  $10^{-15}$ . This behaviour is related to the fast frictional movement of the fibrils after the loss of the triple helix superstructure, and it is in agreement with a decrease in the damping values as a function of the increasing strain amplitude; in a narrow temperature interval between the 490 K and the peak temperature for  $P_A$ . In contrast, for fresh bones  $\alpha$  is around 6% higher than for archaeological bones, indicating a less damaged mesostructure than in archaeological bones.

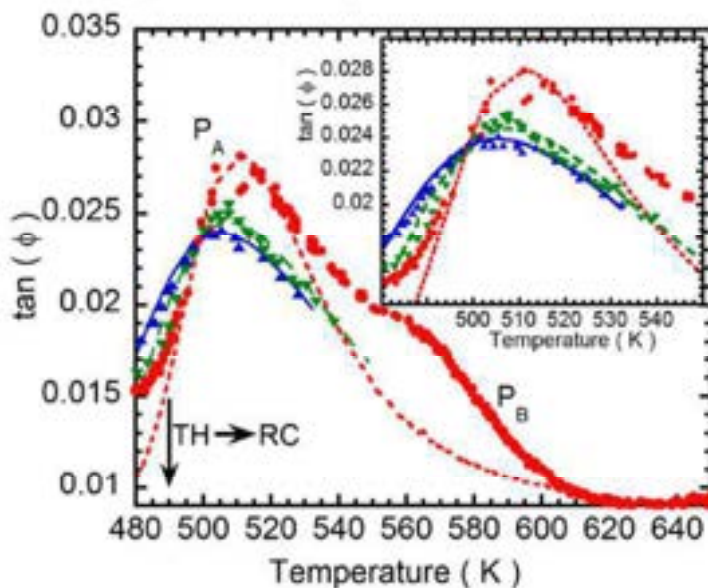


Figure 1: Damping spectra for different bone samples. Circles: Fresh bone. Inverted triangles: Archaeological bone with 2.1 wt.% Ca. Triangles: Archaeological bone with non-detected Ca. Dotted lines: Damping peaks calculated from the HN expression for temperatures higher than the TH→RC transition, whose temperature is shown by the vertical arrow. Inset: Magnification for the temperatures zone near the peak temperature.  $P_A$  and  $P_B$  see explanation in the text.

1) M.L. Lambri, E.D. Giordano, P.B. Bozzano, F.G. Bonifacich, J.I. Pérez-Landazábal, G.I. Zelada, D. Gargicevich, V. Recarte, O.A. Lambri, *J. Renew. Mater.*, **4** (2016), 251-257.

## Mechanical properties of the metal/polymer composites membranes for hydrogen separation

V. Zadorozhnyy<sup>1,\*</sup>, S. Klyamkin<sup>2</sup>, M. Zadorozhnyy<sup>1</sup>, A. Stepashkin<sup>1</sup> and S.D. Kaloshkin<sup>1</sup>

<sup>1</sup>National University of Science and Technology (MISIS), Moscow, Russia

<sup>2</sup>Department of Chemistry, Lomonosov Moscow State University, Moscow, Russia

\*zadorozhnyyvlad@gmail.com

Membrane gas separation is one of the most actively developing areas of science and technology in recent years. In hydrogen production, palladium-based membranes are conventionally employed in spite of their serious disadvantages. Besides the high cost, these materials are subjected to hydrogen embrittlement and coking that significantly limits their life cycle. The above alloys can be replaced by palladium-free hydride-forming intermetallic compounds (IMCs), but new solutions are needed to adjust them to membrane separation processes.

In the present work, the composite membranes based on polyethylene and IMC LaNi<sub>5</sub> were prepared through mechanical activation processing with subsequent compression [1]. The physical features of the produced composites were investigated before and after the hydrogenation process, including dynamical mechanical analysis (DMA) experiments.

The static tests demonstrated that tensile strength of the composite is of 26 MPa, and it slightly decreases after hydrogen activation procedure. Additional brittleness of the intermetallic particles after interaction with hydrogen can be considered as the main reason for this effect. In course of DMA experiments, gradual changes in the storage modulus with corresponding peaks in loss modulus were observed for all samples in the plastic transition region. The peak position changes with frequency in a systematic way that allows us to calculate the activation energy of the phase transition. It was found that hydrogen processing leads to a sharp drop of the activation energy from  $144 \pm 31$  kJ/mol to  $138 \pm 19$  kJ/mol due to weakening of polymer chain bonding. The mechanical spectroscopy study evidenced additional influence of hydrogen processing which manifest itself in a significant shift of the internal friction peaks to lower temperature for activated membranes [2].

The authors gratefully acknowledge the financial support of the Russian Science Foundation, project no. 19-13-00207.

[1] D.V. Strugova, et al., *Int. J. Hydrogen Energy*, **43** (2018) 12146-12152.

[2] V. Zadorozhnyy, et al., *J. Alloys Compd.*, **866** (2021), 159014.

# Mechanical spectroscopy study of quaternary cation ionic liquids: effects of different conformational flexibility

A. Paolone<sup>1,\*</sup>, O. Palumbo<sup>1</sup>, D. Rauber<sup>2</sup>, F. Philippi<sup>3</sup> and T. Welton<sup>3</sup>

<sup>1</sup> *Consiglio Nazionale delle Ricerche, Istituto dei Sistemi Complessi, Piazzale Aldo Moro 5, 00185 Rome, Italy*

<sup>2</sup> *Department of Chemistry, Saarland University, 66123 Saarbrücken, Germany*

<sup>3</sup> *Department of Chemistry, Molecular Sciences Research Hub, Imperial College London, White City Campus, London W12 0BZ, United Kingdom*

\*annalisa.paolone@roma1.infn.it

Ionic liquids (ILs) present interesting properties which make them attractive for several applications and that can be tailored according to the different applicative requirements, by means of a proper choice of the cation and/or the anion. Despite the large amount of research carried out in recent years on ILs, there are still some challenges to be tackled to foster their widespread use. One of the central issues is their high viscosity, which limits liquid handling and transport properties [1, 2].

We present a mechanical spectroscopy study of several ILs composed by quaternary cations and various anions having different conformational flexibility. Indeed flexible ions are capable of a fast structural reorganization on a local level, which weakens the charge network and promotes fluidity, while rigid ions have fewer degrees of freedom for relaxation [1, 2]. The experiments are performed by means of an innovative method which allows the measure of the mechanical modulus of the ILs and of its variation during the main phase transitions occurring by varying the temperature, in both the liquid and the solid states [3-5].

The obtained results evidence the occurrence of a relaxation process in the liquid phase of the ILs with flexible anions and the analysis of the data provides information about the possible involvement of nonequivalent configurations as well as their energy separation. For ILs having rigid anions instead, a fast dynamic at local level in the liquid phase is not observed since the transition to a solid state is favored. For these liquids, the measurements can also suggest the formation of aggregates, whose organization can result in aggregation and domain formation.

[1] F. Philippi, D. Rauber, B. Kuttich, T. Kraus, C.W.M. Kay, R. Hempelmann, P.A.Hunt and T. Welton, *Phys. Chem. Chem. Phys.* **22** (2020) 23038-23056.

[2] F. Philippi, D. Rauber, J. Zapp, C. Präsang, D. Scheschkewitz and R. Hempelmann, *Chem. Phys. Chem.* **20** (2019) 443–455.

[3] O. Palumbo, F. Trequattrini, F. M. Vitucci, A. Paolone, *J. Phys. Chem. B* **119**, (2015) 12905-12911.

[4] A. Paolone, O. Palumbo, F. Trequattrini, G. B. Appetecchi, *Mat. Res.* **21**

(2018)e20170870.

[5] F. Trequattrini, A. Paolone, O. Palumbo, F.M. Vitucci, M. A. Navarra, S. Panero,  
*Arch. Met. Mat.* **60** (2015) 385-390.

# TEMPERATURE-DEPENDENT DAMPING OF THE TONEWOOD SPRUCE

J. Göken

*University of Applied Sciences Emden/Leer, Faculty of Maritime Sciences, Bergmannstr. 36,  
26789 Leer, Germany*

e-mail: [juergen.goeken@hs-emden-leer.de](mailto:juergen.goeken@hs-emden-leer.de)

## ABSTRACT

The material wood is sustainable, resource- and energy-efficient and recyclable. Its low density which ranges between 0.5 and 0.8 g/cm<sup>3</sup> makes from it an important material in the transport sector, in which weight reduction is a key factor against the background of energy savings and the associated reduction in CO<sub>2</sub> emissions.

Wood can be regarded as a low-damping material, due to its molecular structure and its relatively high modulus of elasticity. This characteristic is well known to musical instrument makers. For musical instruments with a resonance body (e.g. piano, harpsichord, viola, cello, double bass, cymbal, harp, zither and certain organ pipes) spruce is the first choice of wood. Since the parameters time, temperature and moisture content influence the mechanical properties of wood, it is considered to be viscoelastic. Especially, the moisture content of the wood can significantly alter its sound quality and, thus, its damping behaviour.

In order to study that moisture influence, the individual drying behaviour of nearly 130 years old spruce and new spruce wood was investigated by damping measurements as a function of the temperature. The material damping of new spruce wood was found to be generally higher than that of old spruce wood. Furthermore, former results showed that the damping of new wood is less sensitive to moisture content changes, which corresponds to a stable tone colour. Activation energies for damping mechanisms were calculated based on data from the Arrhenius plot of both woods. These results suggest that further or stronger damping mechanisms are active in new spruce wood.

Keywords: spruce wood, moisture influence, drying behaviour, damping measurement

# Temperature dependence of internal mechanical losses of gypsum stone with complex composition and structure

A.S. Voznesenskii<sup>1\*</sup>, E.I. Ushakov<sup>1</sup>

<sup>1</sup>National University of Science and Technology, Moscow, Russian Federation

\*asvozesenskii@misis.ru

Key words: gypsum stone, loss factor, temperature, dehydration, resonance method

## 1. Introduction

The peculiarities of materials structure and composition determine internal friction in them. It affects the elastic and strength properties, and reflects the damage of the material. Scientists studied the internal friction of materials [1] in metals [2], composites [3], rocks [4], natural materials [5], geopolymers [6]. The aim of the work is to establish the dependences of the loss coefficient of gypsum-containing rocks of complex structure on temperature.

## 2. Materials and methods

Experimental studies used specimens of gypsum stone from the Novomoskovskoye deposit. The samples were cylinders 40 mm in diameter and 70–80 mm in length, and they had piezoelectric transducers at their ends. The samples included three groups: without silicon layers, two-layer with a flint layer located in the end part of the sample, and three-layer with a flint layer in the middle part of the sample. Some specimens contained interlayers of carbonaceous clays, which had a reduced strength and burned out on heating.

The  $Q^{-1}$  resonant measurements used an experimental laboratory-scale setup consisting of a GW Instek SFG-2110 digital generator and the GW Instek GDS-71022 oscilloscope.

## 3. Results

The figures below show examples of temperature dependences of inverse quality factors  $Q^{-1}$  and resonant frequencies  $f_0$ .

The specimen GK-11-2

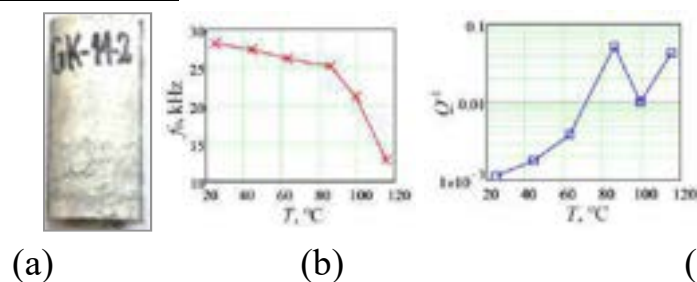


Fig. 1. Photo (a), dependencies  $f_0(T)$  (b) and  $Q^{-1}(T)$  (c) for specimen GK-11-

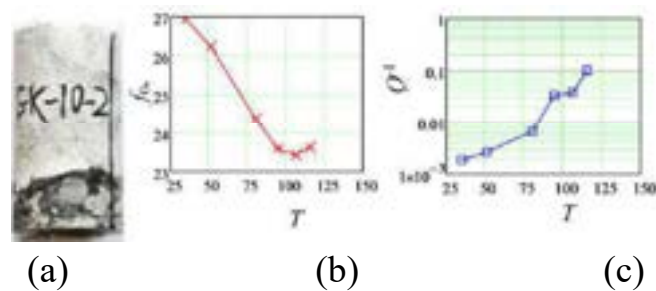


Fig. 2. Photo (a), dependencies  $f_0(T)$  (b) and  $Q^{-1}(T)$  (c) for specimen GK-10-1

### 3. Discussion and conclusions

Studies have shown that with an increase in the temperature of gypsum stone samples, mechanical losses increase, and resonance frequencies decrease. At the same time,  $Q^{-1}$  maximum was at temperatures of about 95°C and above 110°C. The increase in  $Q^{-1}$  is associated with the evaporation of physically bound water and mechanical losses during resonant oscillations. The reason for the first maximum of  $Q^{-1}$  was the dehydration of gypsum and its transition to hemihydrate gypsum  $\text{CaSO}_4 \cdot 2\text{H}_2\text{O} \rightarrow \text{CaSO}_4 \cdot 0.5\text{H}_2\text{O} + 1.5\text{H}_2\text{O}$ . The reason for the second maximum of  $Q^{-1}$  was the transition to anhydrous gypsum with the complete removal of chemically bound water.

This work was carried out with the financial support of the RFBR grant (project No. 20-05-00341).

### References

- [1] A.L. Kimball, D.E. Lovell, Internal friction in solids, *Phys. Rev.* 30 (1927) 948–959. <https://doi.org/10.1103/PhysRev.30.948>.
- [2] W. Duffy, Acoustic quality factor of aluminum alloys from 50 mK to 300 K, *J. Appl. Phys.* 68 (1990) 5601–5609. <https://doi.org/10.1063/1.346971>.
- [3] G. Zhou, H. Jiang, C. Liu, H. Huang, L. Wei, Z. Meng, Effect of porous particle layer on damping capacity and storage modulus of AlSi30p/5052Al composites, *Mater. Lett.* 300 (2021). <https://doi.org/10.1016/j.matlet.2021.130162>.
- [4] B. Tittmann, M. Abdel-Gawad, R. Housley, Elastic velocity and Q factor measurements on Apollo 12, 14, and 15 rocks, *Lunar Planet. Sci. Conf. Proc.* 3 (1972) 2565–2575. [https://www.researchgate.net/publication/23846358\\_Elastic\\_velocity\\_and\\_Q\\_factor\\_measurements\\_on\\_Apollo\\_12\\_14\\_and\\_15\\_rocks](https://www.researchgate.net/publication/23846358_Elastic_velocity_and_Q_factor_measurements_on_Apollo_12_14_and_15_rocks) (accessed July 10, 2021).
- [5] V. Bucur, Traditional and new materials for the reeds of woodwind musical instruments, *Wood Sci. Technol.* 53 (2019) 1157–1187. <https://doi.org/10.1007/s00226-019-01117-9>.
- [6] S. Zhou, Z. Yang, R. Zhang, F. Li, Preparation, characterization and rheological analysis of eco-friendly road geopolymer grouting materials based on volcanic ash and metakaolin, *J. Clean. Prod.* 312 (2021). <https://doi.org/10.1016/j.jclepro.2021.127822>.